A New Stethoscope for Reduction of Heart Sounds from Lung Sound Recordings

YIP Lung

A Thesis Submitted in Partial Fulfillment

of the Requirements for the Degree of

Master of Philosophy

in

Electronic Engineering

June 2001

Acknowledgements

I would like to express my deepest gratitude to my supervisor, Prof. Y. T. Zhang, for his enlightening and insightful advice throughout this study. Warmest thanks to my colleagues, Mr. K. F. Hung, Ms. J. Yao, Ms. X. L. Wu, and Mr. K. W. Chan for providing many valuable suggestions on my research work. The technical assistance of Mr. S. M. Chiu in BME lab is much appreciated.

My friend, Ms. Ellna Yu, is a source of inspiration and encouragement not only for this work but also for my entire life. Ms. Shirley Lau, is also an invaluable friend and advisor, I learn a lot by writing papers with her. It is great to have these people as friends.

I would like to thank the Department of Electronic Engineering, CUHK, for its support. Finally, I would like to express my love to my dearest parents for their never-ending encouragement and constant support.

Abstract

Auscultation is a simple, non-invasive and effective method for diagnosing pulmonary-related diseases. Lung sound analysis, which involves the use of time and frequency domain techniques, is a widely accepted approach in Western medicines for diagnosis of the diseases. Stethoscope, a tool for conducting auscultation, collects both lung sounds and heart sounds simultaneously. However, the design poses a problem in that lung sounds recordings are often disturbed by the unwanted heart sounds, making accurate analysis of lung sounds almost impossible. One method commonly used to minimize heart sounds involves filtering the sounds with the use of linear high pass filters. However, the technique is far from effective in separating the two sounds due to overlapping of their spectra.

Adaptive filtering may be considered the most suitable method to effectively reduce the unwanted heart sounds. It requires a "noise only" reference signal. In the past studies, electrocardiographic (ECG) signal acted as a reference signal, and the heart sounds were reduced by 65 percent on average. However, this technique requires at least two extra sensors to pick up the reference signal, such as the lead II ECG. This makes diagnosis inconvenient and time-consuming. Another approach involves extracting the "noise only" reference signal by a delayed version of the original signal. After some complex signal processing techniques, such as heart sound reformation and forth-order statistics calculation, satisfactory results could be obtained. However, this scheme calls for a huge amount of computation and it is difficult to be implemented in a hardware standalone device for the real time applications.

In this thesis, a new approach -- Laplacian ECG (LECG) for the "noise only" reference signal has been developed. Both the electronic signal -- Laplacian ECG, and the acoustic signal -- lung sounds mixed with heart sounds, can be picked up simultaneously by a specially designed electronic stethoscope. This is a product we have developed by combining a mechanical stethoscope's

head, conductive rubber, silver epoxy, and an acoustic-electric transducer. An integrated platform, which consists of a stethoscope's head, a signal pre-processing circuit, the least-mean-square (LMS) adaptive filtering algorithm, and an automated gain control (AGC) scheme, has been developed to process the signal in real time. Using this LECG-based adaptive approach, over 75% of heart sounds can be eliminated while the auscultation can be kept simple. The approach has led us to develop a brand new electronic stethoscope scheme, which encompasses several functions. They include heart sounds reduction from lung sound recordings, LECG visualization, and acoustic waveform graphical display.

論文摘要

對於有關肺部的疾病，聽診是一種簡單、非侵入性而有效的診斷方法，而在肺音診斷的領域中，時域及頻域分析又是廣泛被西方醫學界所接納。作為聽診的工具 —— 聽診器，則能夠同時收集由人體所產生的肺音及心音。可惜的是，聽診器的設計令到肺音的診斷受到心音的干擾，從而令醫護人員未能對肺音作出準確的判斷。現今的解決辦法是利用高通濾波器去將心音剔除，可是，由於兩種聲音的頻譜是重疊的，從而令到以上的技術不能有效地發揮。

自適應濾波器可能是一種最有效的儀器去把不必要的心音減少，但要運用到這種儀器，我們必須找到“純噪音”信號作為相關信號。在過去的研究當中，曾經有人利用心電圖信號，結果發現大概有百份之六十五的心音由原音中給壓下。但是，這種設計需要外加兩個感應器去收集由人體所產生的二導連心電圖信號，從而令到診斷過程變得大費週章及費時失事。另外一項研究指出，“純噪音”信號可由延遲版的原音中提取，經一輪複雜的信號處理，正如心音重整及四階統計計算，便獲得了一個不俗的結果。但奈何，這套設計用到了大量的運算程序，從而另到實時儀器的開發變得困難重重。

而這篇論文則指出了一項嶄新的方案，就是用 Laplacian 心電圖信號作為“純噪音”信號。我們設計了一種特別的聽診器，能同時間獲取電信號 —— Laplacian 心電圖信號跟聲音信號 —— 肺音加上心音的原音信號。而這種聽診器的設計，是結合了機械式聽診器的聽頭、導電性橡膠、導電性接合劑以及聲電傳感器。結果一個包含了特別設計的聽診器、信號預處理線路、LMS 自適應濾波器和自動增益控制算法的雜成平台終被開發成功。利用上述方案，不單保留了聽診的簡單性，而且將最少百份之七十五的心音會由原音中實時地剔除。此外，是次方案啟發了我們去發展出一個全新的多功能電子聽診器，它的功能除了有最重要的心音抑壓功能外，還有 Laplacian 心電圖信號視象化及原音圖像顯視。

Contents

3 Signal Pre-processing Unit

4 Central Platform

5 Conclusion and Further Development

List of Tables

List of Figures

Chapter 1

Introduction

This chapter presents the statistical data related to the heart and lung diseases in different areas and indicates the need of the stethoscope in diagnosis. A brief history of stethoscope is introduced. It highlights the disadvantages of a number of stethoscopes in the market that drive us to develop a new electronic stethoscope. This is followed by an overview of the major achievements of the new electronic stethoscope we have developed. Finally, in the last section of this chapter the overall organization of this thesis is outlined.

1.1 Heart and Lung Diseases

Both heart and lung diseases are common in the world. Every year, over 100 million people died from hypertensive heart disease, pneumonia, and chronic obstructive pulmonary diseases. The following section is an analysis of their threat in, three areas, namely Hong Kong, China, and the USA.

1.1.1 Hong Kong

Nowadays, heart disease is the second killer in Hong Kong [1]. It is taking its toll on an increasing number of people due to long time working stress, and a lack of exercise. In 1998, over 5,000 people died from heart related diseases (Fig. 1.1). Pneumonia, a kind of lung disease, is another deadly disease that kills more than 3,000 people annually [1].

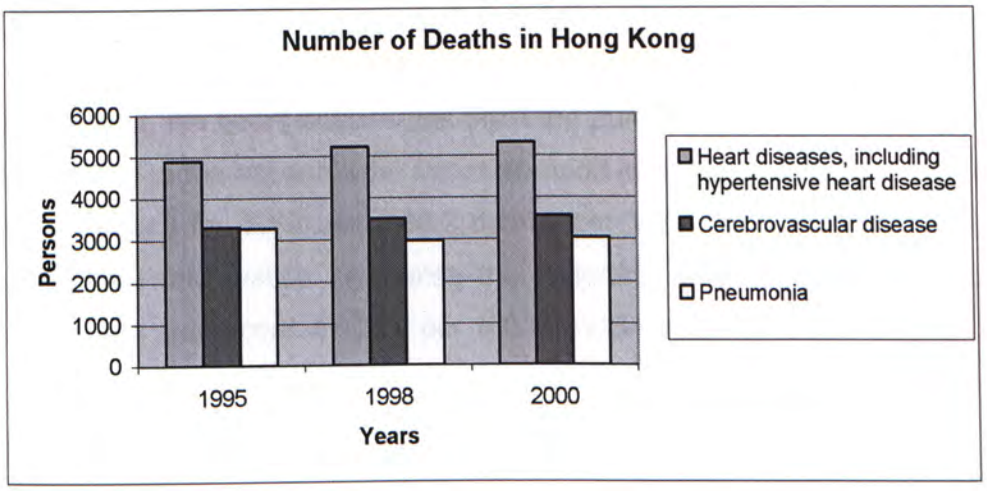

Fig. 1.1. Number of deaths in Hong Kong

1.1.2 China

While heart and lung disorders are not the major killers in China [2] (Fig. 1.2), unfortunately, over 24 million people (4 times the population of Hong Kong) died from these diseases in recent years. Factors including the change of diet habit and an increase in the consumption of high cholesterol food have increased the threat of heart diseases [2]. Another common problem in China is air pollution as a result of the rapid economic growth in last ten years. The polluted air emitted from factories and dust from construction sites cause millions of people to suffer from pulmonary system disorder [2].

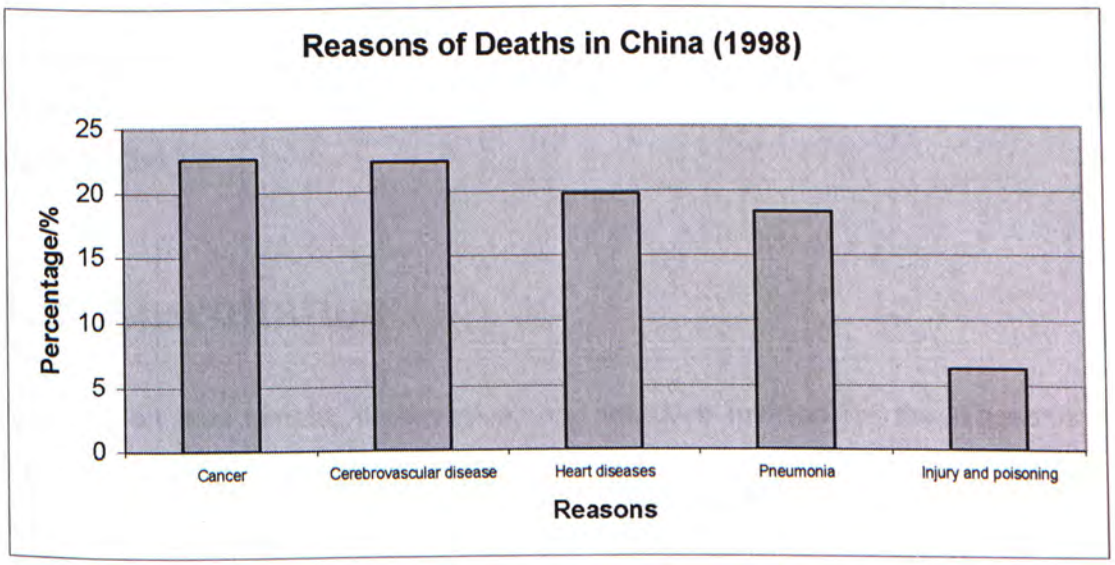

Fig. 1.2. Reasons of deaths in China (1998)

1.1.3 The United States of America (USA)

For many years, the heart disease has been the number one killer in the USA (Fig. 1.3). According to the national vital statistics report in 2000 [3], the crude death rate of heart diseases for 1998 was 268.2 deaths per 100,000 populations. The age-adjusted death rate, which eliminates the distorting effects of the aging of the population, was at a record of 128.6 per 100,000 USA populations.

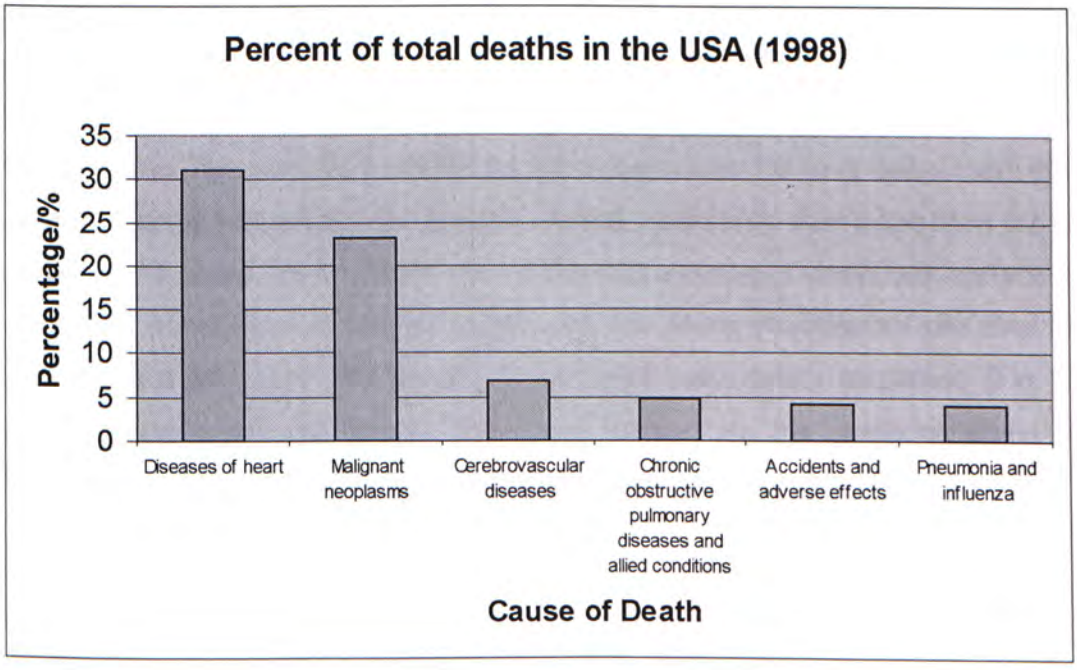

Fig. 1.3. Percentage of total deaths in the USA (1998)

Fortunately, heart related-diseases in the USA are under control now [3], decreasing by 36.5% compared to 1979; however, a rising trend of lung related diseases, which has increased by 45.9% compared to 1979, is another warning signal to give us.

1.2 Auscultation

Auscultation is a simple, noninvasive, and effective method for the diagnosis of cardiovascular and pulmonary disorders. A stethoscope as an auscultation tool can collect both lung sounds and heart sounds at the same time. Thus, auscultation is an important method for preliminary diagnosis. This session introduces auscultation and compares it with ultrasound.

1.2.1 Introduction of Auscultation

Auscultation [4] allows people to detect breath sounds and heart sounds transmitted through the chest wall. Most stethoscopes have a diaphragm and a bell, with one or two tubes leading to the binaural headpiece and earpieces. The diaphragm is for listening high-pitched sounds and the bell for low-pitched sounds.

Applying the stethoscope firmly to the chest wall will amplify high frequency sounds. However, if too much pressure is applied when using the bell, the stretched skin will function as a diaphragm and filter out low-pitched sounds. The lung sounds auscultatory sequence [5] for the posterior chest wall surface (Fig. 1.4) includes 10 different sites. The first site is above the left scapula over the lung apex. From there, the auscultatory sequence follows a pattern that progresses downward from the lung apices to the bases. This pattern covers the entire posterior chest wall surface and includes a comparison of sounds heard over the same auscultatory site over both the right and left lungs. The anterior chest wall auscultatory sequence (Fig. 1.5) includes nine sites and follows the same pattern as the posterior chest wall sequence. The pattern also includes sites over the lateral chest wall surfaces.

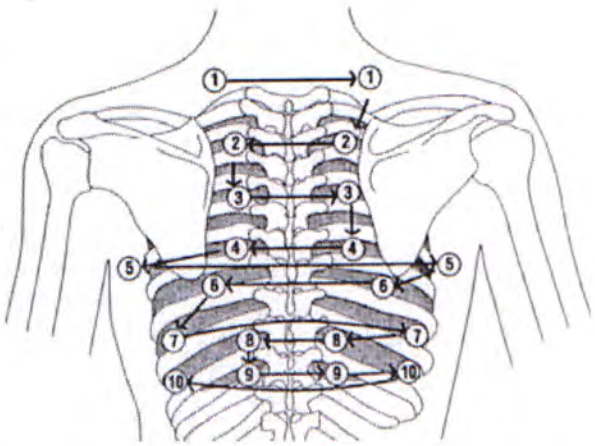

Fig. 1.4. Lung sounds auscultatory sequence in posterior chest

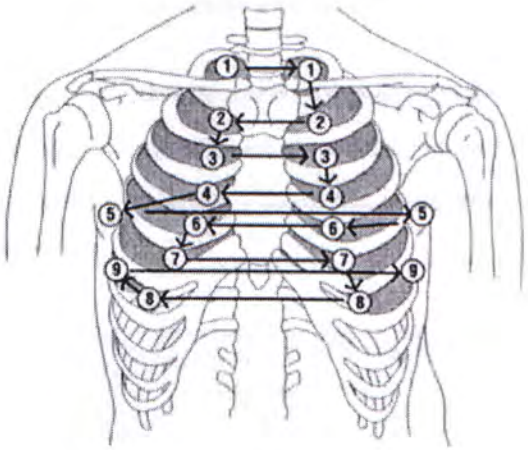

Fig. 1.5. Lung sounds auscultatory sequence in anterior chest

Heart sounds [6] travel through the body from the heart and major blood vessels to the body surface. Because of the acoustical properties of the transmission path, sound waves are attenuated and not reflected. The largest attenuation of the wave-like motion occurs in the most compressible tissues, such as the lungs and fat layers. There are optimal recording sites for the various heart sounds (Fig. 1.6), sites at which the intensity of sound is the highest because the sound is being transmitted through solid tissues or through a minimal thickness of inflated lung. There are five basic chest locations for auscultation [6], first with the diaphragm mode and then with the bell mode. Aortic area is the first area. After listening through several cycles, the diaphragm is moved toward the pulmonic area. Then we listen over the Erb's point and the tricuspid area. Finally, the sequence should end at the mitral area.

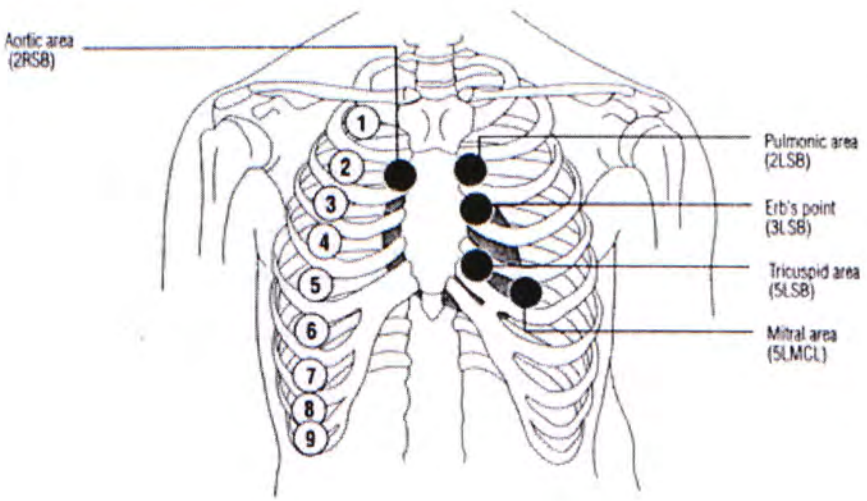

Fig. 1.6. Heart sounds auscultatory locations

1.2.2 Comparison between Auscultation and Ultrasound

Ultrasound (Fig. 1.7) is one of the most popular and productive non-invasive diagnostic tools in medicine. The ability of an ultrasonic wave to traverse soft tissue and to be partially reflected from tissue interfaces is applied to probe virtually every organ and region of the body.

Fig. 1.7. Example of ultrasound image

Ultrasound is created by an extremely short (1-2μs) voltage pulse applied to the electrodes of a piezo-electric transducer crystal. After 'ring down' time, when vibration of the crystal has stopped, the transducer detects the returning echoes over around 1000μs. The returning echoes result from acoustic impedance differences inside the body. They are used to form an ultrasound image on the screen. The pulse sequence is repeated 1000 to 5000 times per second.

Some people believe that the ultrasound will replace the stethoscope in the near future; however, both methods involve different approaches. Technically, a stethoscope, which is a passive device, collects the acoustic auscultation signals generated from patients. Ultrasound machine is an active device (needs power to drive it), and needs to generate ultrasound signals and receive the echo signals to form a Doppler sound or image for diagnosis. Also, the ultrasound machine needs complex designed circuit, heavy processing power Micro-controller (MCU), imaging device, special probe and sensor. All these make the system quite expensive. Besides, it needs heavy power to drive it. So it is inconvenient for physicians to carry such a heavy device for out-door work.

Besides, the ultrasound technique is used for detecting body soft tissues movement and blood flow. Nevertheless, stethoscope auscultation is used to detect acoustic signals formed by our heart and lung tissues. Clinically, echo ultrasound is mainly used for heart diseases (blood flow detection). For some lung diseases such as fibrosis and consolidation, it is hard for them to be detected. Increasing the transmitted ultrasound power will improve the signal to noise ratio of the image. However ultrasound absorption in the body can cause heating up of body tissues, which may be harmful if overheated. Therefore, it is important to keep the overall power to a minimum yet sufficient level to produce an accurate diagnosis. Monitoring output power levels also provides a means to monitor the performance of scanning equipment. To sum up, it is hard to say that the ultrasound treatment method can replace the function of the stethoscope in the near future.

1.3 Stethoscope

In this session, a brief history of the stethoscope is introduced. Meanwhile, the disadvantages of the stethoscope in the market and the comparison with the new electronic stethoscope are discussed.

1.3.1 History of Stethoscope

The stethoscope was not invented until in 1816 when a French physician named Rene Theophile Hyacinthe Laennec was examining a young woman [7]. He was having trouble hearing her heart by the standard method of placing his ear to her chest and did not want to embarrass her. He then rolled up 24 sheets of paper into a tight roll and placed one end to the woman's chest and the other to his ear. To his delight, he found that the sound was transmitted clearly and loudly, and that was the first generation of stethoscope, named paper stethoscope.

a) Monaural Stethoscope

Laennec then took the idea further [7], and made a stethoscope out of a hollow tube of wood (Fig. 1.8). At one end was a small hole, and at the other, a conical hollow. A

fir was inserted into the hollow. It was used for listening to the sounds of the heart. With the insert removed, the physician could listen to the sounds of the lungs.

Fig. 1.8. Laennec's Stethoscope

In 1820, Piorry took Laennec's model and shortened it [7]. He made a flat ear piece of ivory and gave it a flaring chest piece. This became the model of the monaural stethoscope for the rest of its tenure. The monaural stethoscope was made in many different shapes and sizes (Fig. 1.9 and Fig. 1.10)

Fig. 1.9. Aluminum monaural stethoscope since 1890

Fig. 1.10. Unusual French monaural, since 1890

The monaural stethoscope was used up to the late 19th and into the early 20th century and is still used today in some parts of the world, such as the former Soviet Union. However, monaural stethoscope had a single tube for auscultation only, there was a drive to invent a better instrument that would convey sound more clearly, loudly and be more comfortable and convenient for both physicians and patients. Thus, the binaural stethoscope was invented.

b) Binaural Stethoscope

The Binaural stethoscope originated in the early 1850's [7]. The first commercially marketed model was that of Dr. Marsh of Cincinnati who, in 1851, patented a

binaural stethoscope with a diaphragm type chest piece and bulky metal ear pieces. In 1855, Dr. George Cammann of New York patented the first practical binaural model (Fig. 1.11). It was constructed of a bell piece made of wood, which had a ball on top of it, designed to resonate and enhance sound. To this were attached two tubes, about 3 inches long, made of flexible tubing and covered with woven fabric. These connected to the metal ear pieces which were held together by a simple hinge joint. Tension holding the ear pieces together was established by an elastic spring.

Fig. 1.11. Cammann's Binaural Stethoscope, since 1860

At the beginning of the 20th century [7], the stethoscope remained relatively the same. The invention of the diaphragm chest piece in the early 1920's started the stethoscope on the road to its modern look. Below is one typical model (Fig. 1.12) that was invented in the mid 1900's, and is still in use today.

Fig. 1.12. Rieger-Bowles Stethoscope circa 1940, still in using today

Binaural stethoscope provided a good model structure to the modern stethoscope. As the technology advanced, the modern stethoscope had better acoustic performance, and was comfortable for physicians to diagnosis for a long period of time. However, the basic structure and theory between binaural stethoscope and modern stethoscope remain unchanged.

c) Modern Mechanical Stethoscope

The modern mechanical stethoscope [8] operates by two modes - bell and diaphragm. Normally, the head of stethoscope has two pieces of device for bell mode in the backside and diaphragm mode in the front side respectively. Some modern stethoscopes (Fig. 1.13) have tunable diaphragms allowing the physician to monitor both high and low frequencies without having to turn over the chest piece. There are some new advanced features such as solid stainless steel chest piece, two-tubes-in-one design, non-chill rim, and double-leaf binaural spring. They provide better acoustics performance, which is significant improvement in terms of low-frequency response (Fig. 1.14 & Fig. 1.15). Their operating frequencies [8] range from 30Hz to 1kHz.

Fig. 1.13. Master Cardiology Stethoscope

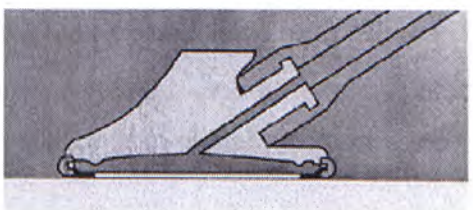

Fig. 1.14. **Bell Mode (low-frequency)**
Use light contact with tunable chestpiece to hear low frequency sounds.

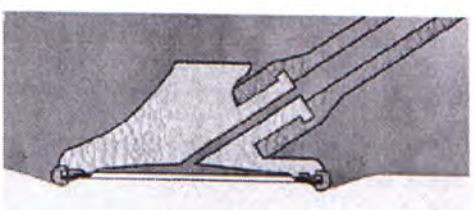

Fig. 1.15. **Diaphragm Mode (high-frequency)**
Without turning the chestpiece over, use firm pressure to hear high frequency sounds.

The modern mechanical stethoscope provides a convenient medium for diagnosis; however, it is difficult to add more features in the modern stethoscope such as adjustable volume control, noise reduction, and wireless transmission. Thus, many researchers try to develop more advanced electronic stethoscope.

d) Electronic Stethoscope

In the 20th century, the advance in technology made the electronic medical devices. Electronic stethoscope [9] [10] can solve many inherent problems embedded in the mechanical stethoscope. For example, electronic stethoscope has adjustable volume control to let physicians hear a clear signal at a comfortable level. Analog or digital filter was introduced to reduce the background noise to improve the diagnostic accuracy.

The following electronic stethoscope (Fig. 1.16) amplifies heart sounds and other biological sounds by up to 14 times more than mechanical stethoscopes. Through its microelectronic design, it eliminates sound loss and resonance effects associated with mechanical stethoscopes.

Fig. 1.16. Hewlett-Packard "Stethos" Electronic Stethoscope

The electronic stethoscope analyzer (Fig. 1.17) enhances the system by incorporating the visual ability of personal computer (PC) [11]. People can observe the waveform graphically, and the data can be stored, called up at a later date, and even be e-mailed. Sound files can also be viewed as charts and graphs, allowing the practitioner to visually compare the patient's condition and progress over time.

Fig. 1.17. Welch Allyn Meditron Analyzer – Model 5079-402

The following stethoscope (Fig. 1.18) is an example of wireless electronic stethoscope. The system uses infrared for the wireless transmission because a

wireless device operating at a normal radio frequency is usually prohibited in hospital. The system also has the distribution ability for teaching purpose.

Fig. 1.18. SimulScope® Auscultation System

e) Disadvantages of Stethoscopes on the Market

The modern mechanical stethoscope still carries the advantages of auscultation. However, there is still environmental noise that disturbs medical diagnosis. For example, in an ambulance, it is difficult to hear a clear heart and lung sound due to the high pitch noise of the ambulance alarm. Moreover, the modern stethoscope has a fix acoustic amplification only. If a patient, especially a child, has weak signal, some useful information will be blurred.

The present electronic stethoscopes use several digital or analog filters to filter out the unwanted noise. This noise is mainly white noise. The concept is based on the frequency band of the patient's heart and lung sounds. By applying suitable band pass filter, the noise-suppressed signal will be obtained. However, the primary noise in the signals during auscultation is not a white noise. During heart sounds auscultation, lung sounds are the main source of distributing noise, or vice versa. For an experienced physician, it is not a big problem to listen lung sounds that are contaminated by heart sounds. However, it is difficult to train a medical student about auscultation using polluted lung sounds. Heart signal mainly comprises two heart sounds, namely the first heart sound and the second heart sound. The second heart sound is relatively low compared with the first heart sound, and is affected by lung sounds easily. As a result, useful medical information is lost in the second heart sound auscultation [6]. Therefore, a proper method to separate those sounds is needed for diagnosis.

Unfortunately, the frequency band of heart sounds and lung sounds are overlapped [12] (normal lung sounds range from 75Hz to 500Hz and heart sounds

range from 50Hz to 150Hz). If we use a digital filter to suppress heart sounds, two possible results will occur. The first is that lung sounds will be embedded in the heart sounds. The second is that the patient's heart sounds will be distorted. An experiment of separation of heart sounds and lung sounds by using digital filter is presented in chapter 4.

f) Previous Other Works

Adaptive filters [13] are widely accepted to be the most suitable method to reduce intelligently the unwanted heart sounds in lung sound recordings. The underlying idea is to design an adaptive filter based on some assumptions about correlation between LECG signal and heart sounds. An estimate of lung sounds is obtained as the system adapts; there are usually two phases of operation: 1) training the system to arrive at the filter coefficients, and 2) operation with the deduced coefficients to approximate the desired response. However, in situations where the mechanism in producing interference is time varying, it is mandatory to dynamically update the coefficients to adapt to the dynamics of the time varying process. Besides, training and operation become simultaneous.

In as early as 1986, some researches pointed out the relationship between the ECG and heart sounds. Using this relationship, the adaptive filter is developed to estimate the heart sounds from the ECG signal (reference signal). After constructing an appropriate circuit, heart sounds were reduced in the lung sound recordings. Heart sound energy reduction (HSER) is around 50-80 percent [14]. Other researchers [15] had proved that the adaptive filter was useful to reduce heart sound without significantly affecting breath sounds. However, this technique requires at least two extra sensors to pick up the reference signal such as the lead II ECG. It is inconvenient for physicians in auscultation.

In 1992, another approach was developed to estimate the heart peak location from the original acoustic sounds [16]. After several signal processing, a smooth waveform signal corresponding to the heart peak location was formed for adaptive filtering reference. That means the whole platform needs only a single microphone signal. This algorithm uses adaptive filtering as in the past. Therefore it still preserves the entire spectrum of lung sounds. However, in the case of breathing

normally, it is difficult to estimate the heart sound location. Therefore, the HSER of this approach is 24% to 49%.

In 1997, another heart sound location estimated scheme was indicated by a new algorithm, so-called LOGREE algorithm [17]. Based on fourth-order statistics (FOS) of the recorded signal -- without requiring recorded "noise-only" reference signal -- was presented. This algorithm used adaptive filtering again to preserve the entire spectrum. Furthermore, the proposed filter was independent of Gaussian uncorrelated noise and insensitive to the step size parameter. It converged fast with small excess errors. Experimental results showed that the HSER was around 85%.

Unfortunately, this complicated processing requires enormous computation power. Assuming that 3 multiplications (3 taps) are needed in least-mean-square (LMS) algorithm, over 457 multiplications (3 taps) are needed in FOS adaptive filtering. A huge calculation demand means that FOS filtering is possible in offline processing only. For signal analysis, it is good enough. However, it is difficult to implement such kind of algorithm in a standalone stethoscope for physicians in auscultation diagnosis.

1.3.2 New Electronic Stethoscope

In order to overcome the disadvantages of existing stethoscopes and other previous approaches, a new electronic stethoscope are proposed in this thesis. The main function of the newly designed stethoscope is to reduce heart sounds so as to better detect lung sound recording. Also, add-on functions, such as waveform visualization, adjustable volume control and automated gain control, have been developed. All hardware and software designs have been integrated in a single platform to process the signal in real time (Fig. 1.19). Both the electronic signal – Laplacian ECG [18], and the acoustic signal – Lung sounds mixed with heart sounds can be picked up by a new electronic stethoscope. After several signal processing algorithm, lung sounds with depressed heart sounds are formed.

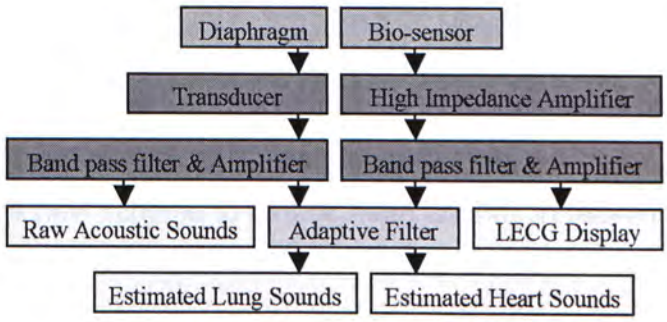

Fig. 1.19. Block diagram of a new electronic stethoscope

A comparison of the new stethoscope to others is given in Table 1.1 [7], [8], [9], [10], [11]. It is clear that the new electronic stethoscope has many useful functions, which are absent in others. Those functions can help physicians in diagnosis.

Table 1.1. Comparison among typical stethoscopes

Items	Freq. Range (Hz)	Amp. 1	ECG or LECG signal	Graphical Display	Auto-mated Gain Control 2	Reduction of Heart sounds from Lung sounds
Monaural Stethoscope						
Laennec's	NA	No	No	No	No	No
Ebony 2-piece	NA	<1	No	No	No	No
Aluminum	NA	<1	No	No	No	No
French monaural	NA	<1	No	No	No	No
Binaural Stethoscope						
Cammann's	NA	<1	No	No	No	No
Rieger-Bowles	NA	1	No	No	No	No
Modern Mechanical Stethoscope						
Master Cardiology	30-1k	1	No	No	No	No
Welch Allyn Tycos	30-1k	1	No	No	No	No
Electronic Stethoscope						
Hewlett-Packard	45-20k	1~14	No	No	**Yes**	No
Welch Analyzer	30-1k	1~5	No	**Yes**	No	No
SimulScope	30-2k	1~5	No	No	No	No
New Electronic Stethoscope	25-1k	1~10	**Yes**	**Yes**	**Yes**	**Yes**

1 Amplification level of acoustic signal compared to neutral diaphragm amplification
2 Adjust the signal amplitude automatically

1.4 Main Purpose of the Study

The original motivation of this work was triggered by observations of the reduction of heart from lung sound recordings in past studies. We wondered whether it was possible to invent a new scheme to reduce heart sounds in real-time while keeping auscultation simple. The main purposes of our study are as follows:

- To develop a new scheme, which can effectively reduce the heart sounds so as to better detect lung sound recordings without heavy distortion.
- To compare the new scheme with past studies, trying to find the advantages of our scheme over others.
- To invent a new electronic stethoscope based on our scheme.

1.5 Organization of Thesis

This thesis is divided into several parts based on different modules of stethoscope. Each part contains the information of the related hardware design, software design, simulation, and experimental results.

Chapter 1 provides the background information on the statistical data of heart and lung diseases, the basic information of auscultation and stethoscope, the overall structure of a new electronic stethoscope and an overview of the thesis.

Chapter 2 presents the hardware design of a new electronic stethoscope's head. Related experimental results in an acoustic-electric transducer are discussed.

Chapter 3 presents the circuit design of the signal pre-processing unit. Several IC components are used to amplify and band pass the extremely weak Laplacian ECG signal in our human body. Several experimental results in the pre-processing unit are explained.

Chapter 4 presents the software design in the central platform, which is an integrated design to fulfill the requirement of the function to reduce heart sounds Several algorithms have been developed to adjust the proper level of LECG and

acoustic mixed signal due to the human body imbalance impedance and chest curvature.

Chapter 5 concludes an overall design of the new electronic stethoscope. The proposed hardware standalone device, wireless transmission, slow play-back, and feature extraction are discussed in the same chapter.

References

[1] Hong Kong Government home page, "http://www.info.gov.hk/"

[2] China Government home page, "http://www.gov.cn/index.html"

[3] National Vital Statistics Report, volume 48, number 11, July 24, 2000.

[4] J. W.Clark, M. R. Neuman, W. H. Olson, R. A. Peura, F. P. Primiano, M. P. Siedband, J. G. Webster, and L. A. Wheeler, *Medical Instrumentation: Application and Design*. New York, Chichester, Weihheim: John Wiley & Sons, INC., 1998.

[5] J. V. Gray, V. S. Kothare, and D. Weinstock, "Introduction to breath sounds," in *Auscultation Skills: Breath & Heart Sounds*. Pennsylvania: Springhouse Coproration, 1998.

[6] J. V. Gray, V. S. Kothare, and D. Weinstock, "The heart and auscultation," in *Auscultation Skills: Breath & Heart Sounds*. Pennsylvania: Springhouse Coproration, 1998.

[7] Stethoscope page, "http://www.cybernurse.com/antiques/MONAURAL.html"

[8] Stethoscope page, "http://www.allheart.com/littmannstethoscopes.html"

[9] Stethoscope page, "http://www.allheart.com/digitalscopes.html"

[10] L. A. Dowell, G. E. Fant, and W. D. Watkins, "Design and construction of an electronic stethoscope," *Journal of Clinical Engineering*, vol. 13, pp. 355-7, 1988.

[11] H. Boom, C. Robinson, W. Rutten, M. Neuman, and H. Wijkstra, "Digital recording and computer-based analysis of lung sounds," in Proc. 18th Annu, Int, Conf, IEEE,, 2301-2, 1996.

[12] J. Xu, Q. Chen, Y. Zhang, and S. Liu, "Spectrum analysis of lung sounds," in Proc. 11th Annual Int. Conf. Med. Bio. Society, pp. 1676-7, 1989.

[13] B. Widrow, J. R. Glover, J. M. McGool, J. Kaunitz, C. S. Williams, R. H. Hearn, J. R. Zeidler, E. Dong, and R. C. Goodlin, "Adaptive Noise Canceling: Principles and Applications," in Proc. IEEE, 1692-716, 1975.

[14] V. K. IYER, P. A. Ramamoorthy, H. Fan, and Y. Ploysongsang, "Reduction of Heart Sounds from Lung Sounds by Adaptive Filtering," *IEEE Trans. on BME*, vol. 33, pp. 1141-8, 1986.

[15] Y. Ploysongsang, V. K. Iyer, and P. A. Ramamoorthy, "Characteristics of normal lung sounds after adaptive filtering," *Amer. Rev. Respir. Dis.*, pp. 951-6, 1989.

[16] M. Kompis and E. Russi, "Adaptive Heart-noise Reduction of Lung Sounds Recorded by a Single Microhphone," in Proc. 14th Annu. Int. Conf. IEEE. Eng. Med. Biol. Soc., 691-2, 1992.

[17] L. J. Hadjileontiadis and S. M. Panas, "Adaptive Reduction of Heart Sounds from Lung Sounds Using Fourth-Order Statistics," *IEEE Trans. on BME*, vol. 44, pp. 642-8, 1997.

[18] B. He and R. J. Cohen, "Body Surface Laplacian ECG Mapping," *IEEE Trans. on BME*, vol. 39, pp. 1179-91, 1992

Chapter 2

A New Electronic Stethoscope's Head

2.1 Introduction

Usually, stethoscope can acquire acoustic signal from the human body. The collected signal is a medical indicator for physicians to determine patients' conditions. In modern mechanical stethoscope, acoustic signal is amplified by the air chamber allocated behind the diaphragm. Electronic stethoscope transforms acoustic signal to electronic signal through an acoustic-electric device, and then amplified by several integrated circuits (IC). However, both types of stethoscopes collect raw acoustic signals (sounds) only.

In this thesis, a special type of stethoscope has been invented. It collects both acoustic signal (raw heart sounds and lung sounds) and electronic signal (LECG) at the same time. The acoustic signal would be pre-amplified naturally by an air chamber by a principle of standing wave, and then transformed to electronic signal by a transducer. Electronic signal is collected by two concentric ring biopotential electrodes. The voltage difference between both electrodes represents the LECG signal.

In this chapter, the characteristics of biosensor are introduced followed by the discussion of acoustic-electric transducer. The hardware design of the stethoscope's head is analyzed after both sections. An experiment of the stethoscope's head is used to analyze and determine a suitable bias voltage applied to a stethoscope's head. Moreover, another experiment proves that there is no significant acoustic waveform distortion after adding two concentric ring sensor in front of stethoscope's diaphragm followed by the section of discussion. Finally, a summary of the stethoscope's design is given in the last session.

2.2 Biopotential Electrode

In order to measure and record potentials and, hence, currents in the body, it is necessary to provide an interface between the body and the electronic measuring apparatus. This interface function is carried out by Biopotential electrodes [1]. In any practical measurement of potential, current flow in the measuring circuit for at least a function of the period of time over which the measurement is made. Ideally this current should be very small. However, in practical situations, it is never zero. Biopotential electrodes must therefore have the capability of conducting a current across the interface between the body and the electronic measuring circuit. Actually, the electrode also acts a transducer, because current is carried in the body by ions, whereas it is carried in the electrode and its lead wire is carried by electrons. Thus the electrode serves as a transducer to convent an ionic current to an electronic current.

2.2.1 Flexible Electrode

Usually, the electrode is solid and is either flat or has a fixed curvature, such as platinum and silver/silver chloride electrode. The body surface, on the other hand, is irregularly shaped and can change its local curvature with movement. Solid electrodes cannot conform to this change in body-surface topography, which can result in additional motion artifact. To avoid such problems, a flexible electrode has been developed [1].

A carbon-filled silicone rubber (conductive rubber) compound in the form of a thin strip or disk has been used as the active element of an electrode [1]. They require some type of adhesive component to hold them in place against the conducting wire. New electrolytic hydrogel material (silver epoxy) has been developed, which is in the form of a thin, flexible slab of gelatinous material. This substance has a sticky surface that is similar to the adhesive tack on the tape and can be used to hold the electrode in place. By virtue of the mobile ions that contains, it is also electrically conductive. Because the electrode and this interface material are both flexible, a good, mechanically secure electric contact can be made between the electrode and the skin.

One drawback of this material is its relatively high electrical resistance, compared to that of the electrolyte gel routinely used with electrodes; however, because the amplifiers used with these electrodes now have input impedance of the order of 10MΩ or higher, which is greater than the resistance of the electrolytic material. Often there is less motion artifact when these electrodes are used.

2.2.2 Laplacian Electrocardiogram

In as early as 1988, Waller described the ways in which the laws of physics could be applied to heart and theoretically assumed that the heart could be represented by a bipolar electrical source [2]. Numerous investigators had utilized the body surface potential map (BSPM) and shown that the BSPM could provide additional information to that contained in the conventional electrocardiogram (ECG) [3]. The BSPM had been shown by a number of investigators to reliably identify major single cardiac event. In a number of experimental studies [4], correlation of surface potential patterns with experimental interventions such as ectopic pacing, epicardial burns as well as myocardial infarction, had been reported. While the BSPM may be useful in characterizing a single cardiac event, experimental evidence indicates that the BSPM is quite limited in its ability to resolve multiple simultaneous bioelectrical event in the heart. This limitation of the BSPM is caused by the smoothing effect of the volume conductor. Thus, it becomes difficult to identify and localize multiple spatially distributed cardiac electrical events.

To improve the spatial resolution of body surface mapping, a new approach of bioelectrical sources associated with normal and abnormal cardiac activities by measuring the surface Laplacian of the body surface potential [4], [5], [6], [7], [8] has been developed. The body surface Laplacian map (BSLM) may be interpreted as an image of a two dimensional charge density distribution, or as a map of the normal derivate of the normal component of the current density at the body surface. The surface Laplacian recording of bioelectrical activity was first applied by Hjorth in 1975 to the electroencephalogram (EEG) [9]. In his first implementation, Hjorth used five unipolar surface EEG electrodes to estimate the surface Laplacian of the EEG on the scalp.

Considering a set of five unipolar electrodes ($\phi_0, \phi_1, \phi_2, \phi_3, and \phi_4$) on the body surface, the two-dimensional Laplacian of the potential at center point 0 can be given by [9]

$$\begin{aligned}\nabla^2{}_{xy}\phi &= \partial^2\phi/\partial x^2 + \partial^2\phi/\partial y^2 \\ &= \partial(\partial\phi/\partial x)/\partial x + \partial(\partial\phi/\partial y)/\partial y \\ &\approx [(\phi_1 - \phi_0)/b - (\phi_0 - \phi_3)/b]/b + [(\phi_2 - \phi_0)/b - (\phi_0 - \phi_4)/b]/b \\ &\approx (4/b^2)\left[(1/4)\sum_{i=1}^{4}\phi_i - \phi_0\right] \end{aligned} \tag{2.1}$$

where $\{x, y\}$ is a local Cartesian coordinate system with an origin at the observation point 0 on the body surface. ϕ_i represents the electrical potential at electrode i as shown in Fig. 2.2 and b is the inter-electrode distance. Equation (2.1) shows that the two-dimensional Laplacian of the potential at the center point 0 is approximately proportional to the difference of the average potential of four neighboring points with the potential at the center point. As long as the inter-electrode distance b is sufficiently short, the approximation in (2.1) will yield a good approximation of the two-dimensional Laplacian.

Since the two-dimensional Laplacian of the potential should be independent of the coordinate system selected, the relationship established in (2.1) should hold for another coordinate system $x'-y'$, which can be obtained by rotating the coordinate $x-y$ around the center point 0. That is, the two-dimensional Laplacian of the potential at point 0 can also be approximated by

$$\nabla^2_{x'y'}\phi \approx (4/b^2)\left[(1/4)\sum_{i=1'}^{4'}\phi_i - \phi_0\right] \tag{2.2}$$

The surface Laplacian of the potential at the center point 0 can be estimated from the potential difference between the potential at the center 0 and the averaged potential over four neighboring points 1-4 (Fig. 2.1). The same result can be obtained from the potential difference between the center potential and averaged potential difference over another four neighboring points 1'-4' which can be obtained by rotating the four neighboring points 1-4 around the center 0. The potential

difference between the center point 0 and the average potential over the ring, is the ensemble average of the five-point estimation of the surface Laplacian taken over all rotations.

By averaging the estimate of the two-dimensional Laplacian over a complete circular rotation of the coordinate system, we obtain

$$\nabla_{xy}^2 \phi \approx \left(4/b^2\right)\left[(2\pi b)\int_0^{2\pi b} \phi \; dl - \phi_0\right] \qquad (2.3)$$

where the integral is taken around a circle of radius b. Based on the formula (2.3), an integrated bipolar Laplacian electrode was developed to measure directly the surface Laplacian of the potential, or the equivalent charge density, on the body surface [4].

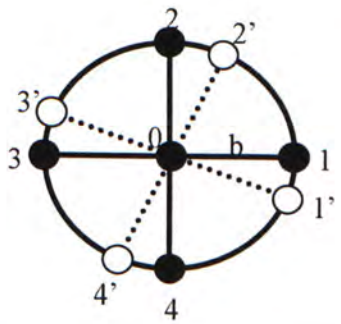

Fig. 2.1. Schematic diagram of circular realization of surface Laplacian recording.

Figure 2.2 depicts the basic schematic diagram of the bipolar Laplacian electrode [10]. The electrode consists of two parts: a central conductive disk and a concentric circular conductive ring. The intermediate area between them is an electric insulator. The output of the bipolar Laplacian electrode is the potential difference at the center and the averaged potential over the outer ring. The surface area of the central disk was set to be the same as that the outer ring [10].

Fig. 2.2. Schematic diagram of the circular bipolar Laplacian electrode structure

2.3 Transducer

A transducer [11], [12] is defined as a device that receives energy from one system and retransmits it, often in a different form, to another system. The energy transmitted by these systems may be of any form, such as electrical, mechanical, or acoustical. It may be of the same or different forms in the various input and output systems. Transducers in industry and medicine are used to measure pressure, force, velocity and acceleration, flow, sound, temperature, chemical parameters such as partial pressures, pH, electrical impedance, and many more. The signals produced by transducers, sensors, or bioelectronic electrodes are small and amplification is required for an analog or digital readout. This concept applies in general to electronic, mechanical, and especially the medical events.

In this thesis, one type of acoustic-electrical transducer, named condenser microphone [13], is discussed briefly. Put simply, a microphone is a device, which converts acoustic energy (received as vibratory motion of air particles) into electrical energy (sent along the microphone cable as vibratory motion of elementary electrical particles called 'electrons'). Sound waves are inherently short lived and can travel only a relatively brief distance before they sink below the limits of audibility. Electric currents, by contrast, can be amplified and sent along any required length of wire or they can be modulated onto high-frequency radio waves for 'wireless' transmission all round the world. They can also be recorded on a variety of different media for subsequent playback at a later date.

A condenser microphone, originally proposed by Edison but eventually introduced around 1971 by Wente, relies on electrostatic charges. Basically, it consists of a thin conductive diaphragm separated by a narrow air gap from a solid back plate to form a capacitor [13]. A polarizing voltage is connected across the two plates through a resistance so that a quasi-constant electrical charge is established. Motion of the diaphragm causes the charge-carrying ability (capacitance) of the structure to alternate above and below its stationary value and the resulting voltage gives rise to the desired AC signals.

2.4 Design of the Head of Stethoscope

A new stethoscope's head has the basic structure of mechanical stethoscope [14]. In this section, the structure of the stethoscope's head design [15], [16] is discussed, including the component of stethoscope's head, cement material, and dimension. Schematic diagrams of a new stethoscope's head are shown in Figure 2.3 and 2.4.

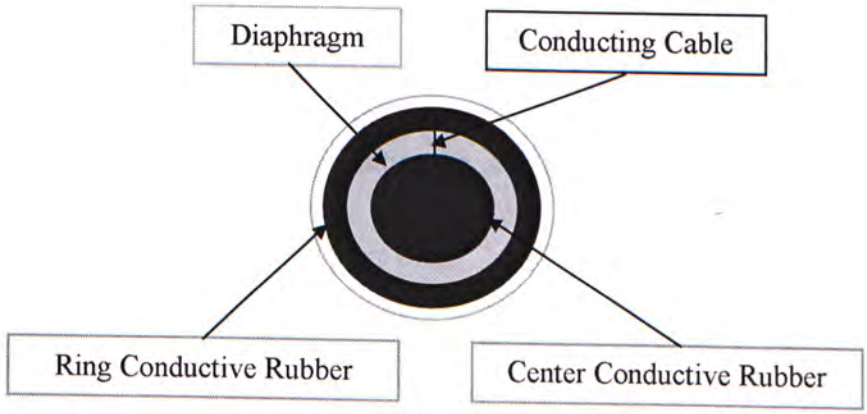

Fig. 2.3. Front view schematic diagram of a stethoscope's head

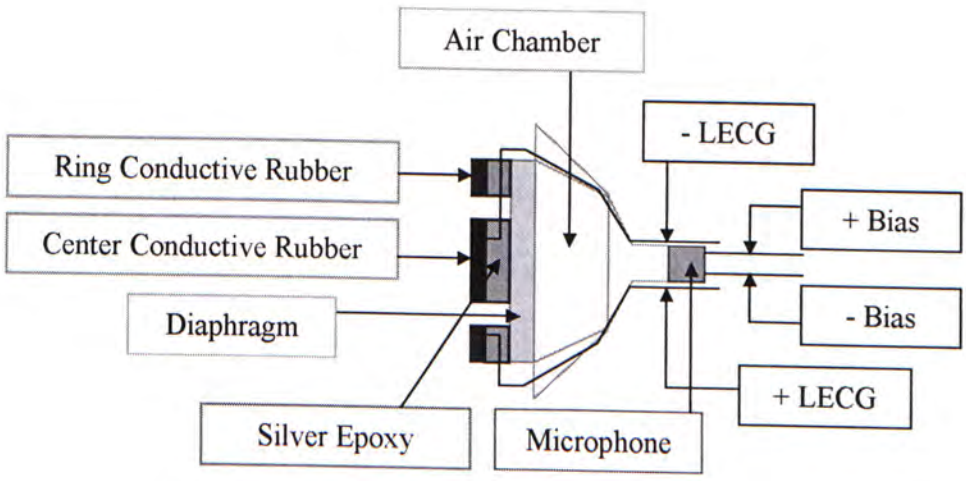

Fig. 2.4. Side view schematic diagram of a stethoscope's head

Because it is necessary to give a bias potential to the condenser microphone for proper function, a circuit design is needed. The related design is discussed in the next chapter.

2.5 Experimental Results

2.5.1 Bias Voltage of Condenser Microphone

The reason of transducer property inside condenser microphone is that the changeable impedance value (capacitance and resistance) due to the different acoustic level received. In this experiment (Fig. 2.5.), the proper value of bias voltage of a condenser microphone is determined. Different DC voltage levels were applied to a condenser microphone. The current values were received corresponding to different DC voltages in static state. Experimental results are summarized in Table 2.1.

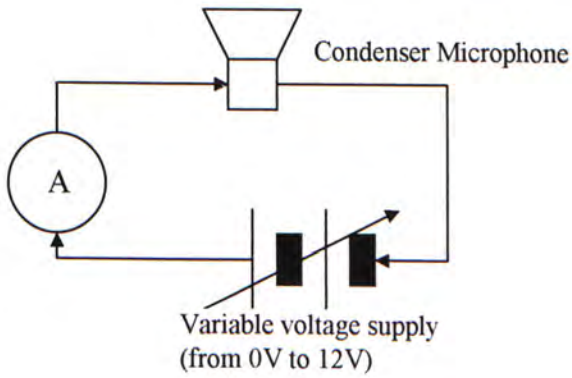

Fig. 2.5. Experimental testing of bias voltage of condenser microphone

Table 2.1. Voltage and current relationship of condenser microphone

Voltage/V	0.0	0.5	1.0	1.5	2.0	2.5	3.0	3.5	4.0	4.5	5.0	5.5	6.0
Current/mA	0.00	0.21	0.22	0.22	0.22	0.23	0.23	0.23	0.24	0.24	0.24	0.25	0.25

Voltage/V	6.5	7.0	7.5	8.0	8.5	9.0	9.5	10.0	10.5	11.0	11.5	12.0
Current/mA	0.25	0.26	0.26	0.26	0.27	0.27	0.28	0.29	0.30	0.35	0.45	0.93

Therefore, the I-V characteristic graph and impedance versus voltage graph (by ohm's law) are formed (Fig. 2.6 and Fig. 2.7).

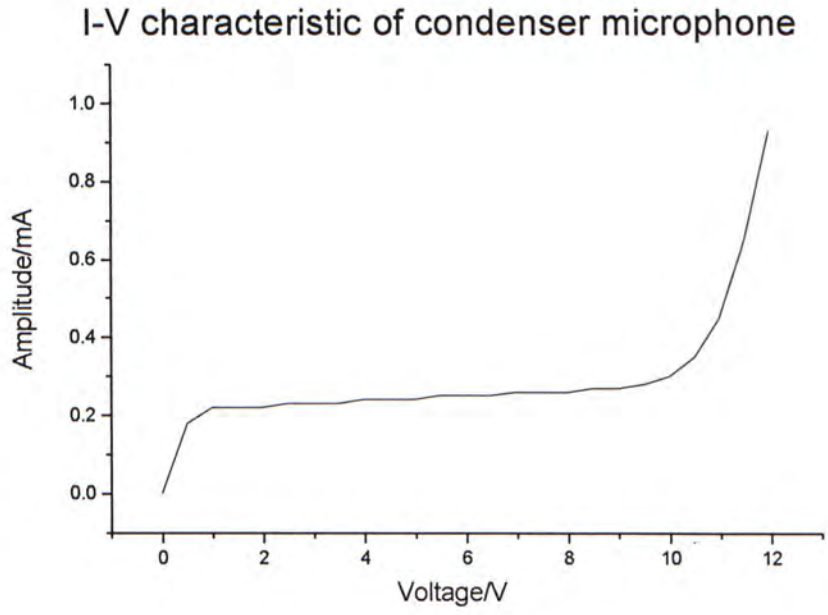

Fig. 2.6. Current-voltage relationship in a condenser microphone

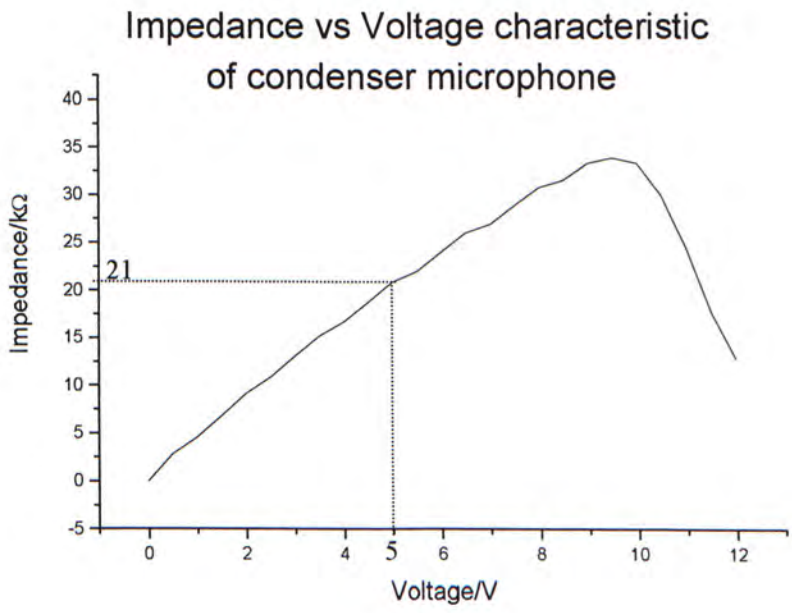

Fig. 2.7. Impedance-voltage relationship in a condenser microphone

2.5.2 Frequency Response of New Stethoscope's Head

Because of two concentric ring sensors attached in front of stethoscope's diaphragm, a thin layer of silver epoxy is used for a cement material. In this experiment, the acoustic performance between our newly designed stethoscope and a market product, named SimulScope, were compared (Fig. 2.8). Different sounds with monotonic frequency, input output was set to 100mVrms, Vin, were applied to both products. Electronic signals, Vout, were received corresponding to different monotonic frequency in different products. Experimental results are summarized in Table 2.2.

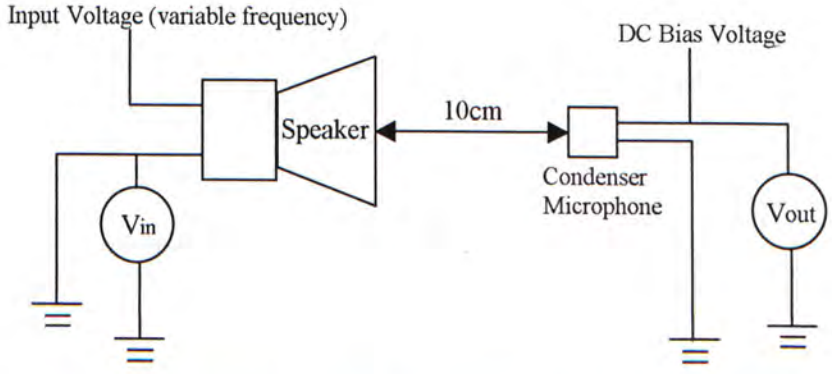

Fig. 2.8. Experimental testing of frequency response of condenser microphone

Table 2.2. Frequency response of condenser microphone

Frequency/Hz	50	75	100	150	200	300	400	500	600	700	800	900
New Product/mVrms	49	100	175	191	183	171	195	233	269	281	281	346
SimulScoope/mVrms	240	473	740	855	843	821	963	1050	1370	1320	1390	1710

Frequency/Hz	1000	1100	1200	1300	14000	1500	1600	1700	1800	1900	2000
New Product/mVrms	358	378	1160	936	540	407	423	390	414	586	896
SimulScope/mVrms	2160	4340	3590	2400	1400	963	728	579	462	344	208

After a simple calculation, dividing Vout by Vin, the frequency-response curve versus gain value in both testing products is formed (Fig. 2.9).

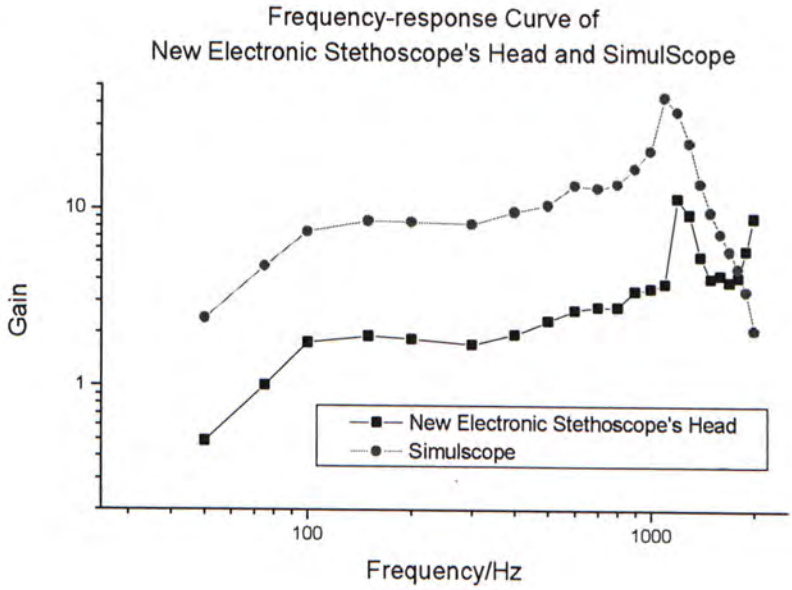

Fig. 2.9. Frequency-response curve of new electronic stethoscope's head and SimulScope

2.6 Discussion

In the head design of stethoscope (Fig. 2.3 and Fig. 2.4), the function of conductive rubber is used to acquire the biopotential signal. The difference between both electrodes (+LECG and –LECG) is the LECG signal. Silver epoxy is conductive cement to hold the conductive rubber in place against the diaphragm. The thickness of conductive rubber is less than 1mm to minimize the acoustic signal distortion before entering the diaphragm. Diaphragm is a normal diaphragm of mechanical stethoscope. The acoustic raw signals are pre-amplified by the air chamber behind the diaphragm and then transformed to electronic signal by the condenser microphone.

In an experiment of microphone bias voltage determination, as shown in Figure 2.7, the impedance values of a condenser microphone were changed due to different applied voltages. By observation, the linear region located within the applied voltage around from 0V to 10V. The middle value, 5V, was chosen in the circuit design for proper usage in a microphone (corresponding to 21kΩ impedance).

After determining a DC bias voltage, a condenser microphone can work for a transducer to convert the acoustic waveform to electrical signal (AC signal).

In the frequency response experiment, the new electronic stethoscope's head and SimulScope were tested and compared. We found that they both had similar frequency-response curve under 1700Hz. Be reminded that the bandwidth of acoustic channel of the new electronic stethoscope is from 25Hz to 1kHz. Thus, a similar acoustic performance, compared with SimulScope, was obtained even though two concentric ring electrodes were added in front of diaphragm. However, a higher gain value in SimulScope was obtained due to the signal amplifying circuit embedded in SimulScope. Thus, a signal amplification circuit is needed in the new electronic stethoscope. Details of signal pre-processing circuit is discussed in the following chapter.

2.7 Section Summary

In this chapter, the details of a new stethoscope's head have been discussed. In the section of biopotential, the material of flexible electrode and the principle of LECG have been introduced. One type of transducer, named condenser microphone, was chosen in a new stethoscope's head for acoustic-electronic signal conversion. The schematic diagram of a new stethoscope's head was sketched to present its overall structure design. After that, due to the need of bias voltage on condenser microphone, the related experiment was done to determine that value to make a transducer working properly. Another experiment pointed out that the adding concentric ring sensor in front of stethoscope's diaphragm would have only slight distortion to the acoustic waveform. To sum up, the function of a new stethoscope's head (Fig. 2.10) is used to collect the acoustic signal (heart sound and lung sound) together with the electronic signal at the same time. Due to the effect of the human body imbalance impedance and the curve shape of the chest, a further signal processing circuit is needed to filter out the unwanted noise and to amplify the inherent human body week signal. The analysis of the circuit is discussed in the following chapter.

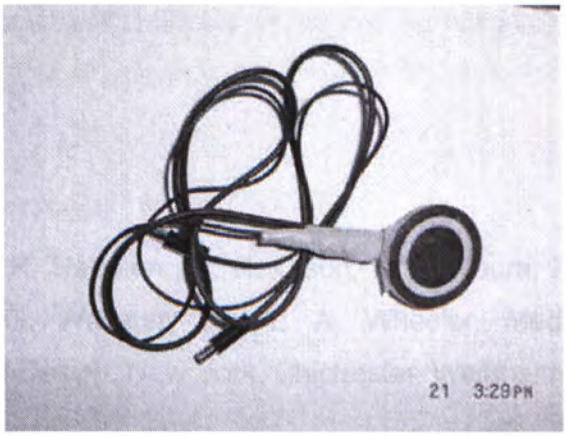

Fig. 2.10. Hardware of a new electronic stethoscope's head

References

[1] J. W.Clark, M. R. Neuman, W. H. Olson, R. A. Peura, F. P. Primiano, M. P. Siedband, J. G. Webster, and L. A. Wheeler, *Medical Instrumentation: Application and Design*. New York, Chichester, Weihheim: John Wiley & Sons, INC., 1998.

[2] A. D. Waller, "The Electromotive Properties of the Human Heart," *brit. Med. J.*, vol. 2, pp. 751-4, 1988.

[3] S. D. M. Mirvis, *Body Surface Electrocardiographic Mapping*. Boston: Kluwer Academic, 1988.

[4] C. C. Lu, R. Plourde, W.Y.Fang, S.Uhborn, and P. P. Tarjan, "Laplacian Electrocardiograms with Active Electrodes," in Proc. Annual. IEEE, pp. 121-4, 1997.

[5] D. B. Geselowitz and J. Ferrara, "Is Accurate Recording of the Surface Laplacian Feasible?," in Proc. 2nd Int. Conf. on Bioelectromagnetism, Melbourne, Australia, pp. 3-4, 1998.

[6] B. He, "Theory and Applications of Body-Surface Laplacian ECG Mapping," *IEEE EMBS*, pp. 102-9, 1998.

[7] I. Benitez and C.-C. Lu, "Portable Real-Time Body Surface Laplacian ECG Mapping," in Proc. The First Joint BMES/EMBS, Atlanta, GA, USA, 301, 1999.

[8] J. Lian, S. Srinivasan, H. C. Tsai, and B. He, "Comments on "Is Accurate Recording of the ECG Surface Laplacian Feasible?"," *IEEE Trans. on BME*, vol. 48, pp. 610-3, 2001.

[9] B. Hjorth, "An On-line Transformation of EEG Scalp Potentials into Orthogonal Source Derivations," *Electroencepth. clin. Neurophysiol*, vol. 39, pp. 526-30, 1975.

[10] M. Kaufer, L. Rasquinha, and P. Tarjan, "Optimization of Multi-ring Sensing Electrode Set," in Proc. Annual, Int. Conf. IEEE. MBS, pp. 612-3, 1990.

[11] J. A. Allocca and A. Stuart, "General Operation of Transducers," in *Transducers: Theory & Applications*. Reston, Virginia, USA: Reston Publishing, 1984.

[12] F. P. Branca, F. Mastrantonio, G. Calcagnini, and S. Cerutti, "A simple low-cost transducer for breath detection over 24H in clinical cardiology," in Proc. IEEE and CMBEC, pp. 1575-6, 1995.

[13] J. Borwick, "Basic acoustics," in *Microphones: Technology and Techniques*. London and Boston: Focal Press, 1990.

[14] A. Jones, D. Jones, K. Kwong, and S. SC, "Acoustic Performance of Three Stethoscope Chest Pieces," in Proc. 20th Annual Int. Conf. IEEE. MBS, pp. 3219-22, 1998.

[15] C.-C. Lu and P. P. Tarjan, "Pasteless, Active, Concentric Ring Sensors for Directly Obtained Laplacian Cardiac Electrograms," in Proc. of BSI99, pp. 280-3, 1999.

[16] M. Talero and C. C. Lu, "Active Bipolar Concentric Ring Sensor for Surface Laplacian ECG," in Proc. The First Joint BMES/EMBS, Atlanta, GA, USA, 789, 1999.

Chapter 3

Signal Pre-processing Unit

3.1 Introduction

Amplifiers are an important part of modern instrumentation systems for measuring biopotentials. The essential function of a biopotential amplifier is to take a weak electric signal, especially LECG, of biological origin and increase its amplitude so that it can be further processed, recorded, or displayed. Usually such amplifiers are in the form of voltage amplifiers, because they are capable of increasing the voltage level of a signal. Moreover, voltage amplifiers also serve to increase power levels, so they can be considered power amplifiers as well.

Signal pre-processing unit must operate in that portion of the frequency spectrum in which the biopotentials and the mixed sounds that they amplify exist. Because of the low level of such signals, it is important to limit the bandwidth of the amplifier so that it is just great enough to process the signal adequately. In this way, the optimal signal-to-noise ratio is obtained.

In this chapter, a signal pre-process unit to pre-process signal before entering the central platform is introduced. The operational principle of high input impedance is discussed followed by a voltage control voltage source filtering circuit [1]. Moreover, the overall circuit diagram [2], [3] of a signal pre-processing unit is displayed after introducing a multiple feedback filtering circuit. After that, an experiment is used to test the function and stability of the signal pre-processing unit. Finally, the whole design is concluded in the section of summary.

3.2 High Input Impedance IC Amplifier

To be useful biologically, all biopotential amplifiers must meet certain basic requirements. They must have high input impedance, so that they provide minimal loading of the signal being measured. The characteristics of biopotential electrodes can be affected by the electric load they see, which, combined with excessive loading can result in distortion of the signal. Loading effects are minimized by making the amplifier input impedance as high as possible, thereby reducing this distortion. Usually, biopotential amplifiers have input impedance of at least 10MΩ. To fulfill the entire requirement, extremely high input impedance IC, INA118, produced by BURR-BROWN is needed.

The INA118 is a low-powered instrumentation amplifier used for general purposes. Its versatile 3-op amplifier design and small size make it ideal for a wide range of applications. Current-feedback input circuitry provides wide bandwidth even at high gain (70kHz at Gain = 100). The INA118 provides a convenient variable gain control (from 1 to 10,000) by a resistance value of a single resistor. A low offset voltage and high common-mode rejection ration (110dB at Gain = 1000) make it a suitable device for biopotential amplifier.

In the signal pre-processing unit, the INA118 (Fig. 3.1) is used to amplify the LECG signal acquired from the chest primary. The overall gain factor is set to 1000 to amplify the LECG signal. The gain factor of INA 118 is set to 50 because it is a low noise amplifier. A large value of gain factor in low noise amplifier will depress the noise figure in the whole unit. For the specification provided by BURR BROWN, a single resistor-capacitor set (a 1KΩ resistor and a 33μF capacitor), connected in series, serves as a voltage amplifier and a high-pass filter for both input leads, with a gain factor of 10 and a corner frequency of 5Hz. Therefore, no common signal can be converted into a differential signal.

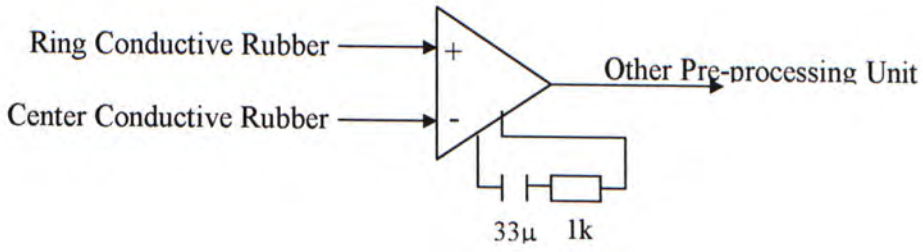

Fig. 3.1. Circuit diagram of the high impedance IC circuit

3.3 Voltage Control Voltage Source High Pass Filter Circuit

Continuoususly active filters are active networks (circuits) with characteristics that make them useful in today's system design. Their response can be predetermined once their excitation is known, provided that their characteristic function is known or can be derived from their circuit diagram.

A number of popular circuits is considered using the non-inverting (positive gain) and inverting (negative gain) operational amplifier configurations. In both cases, the open-loop gain of the amplifier is taken to be high and in the first class of circuits to be considered, the so-called voltage-controlled-voltage-source (VCVS) [4], it will be seen that the circuit gain may be adjusted by means of a resistor ratio. It has good circuit isolation properties (high input impedance and low output impedance), which means that they may be cascaded to form higher-order filters without the need for additional isolation amplifiers. In the signal pre-processing unit, the second order VCVS Butterworth active high pass filters (Fig. 3.2) are used to filter out the dc noise of the signal in LECG and raw sounds:

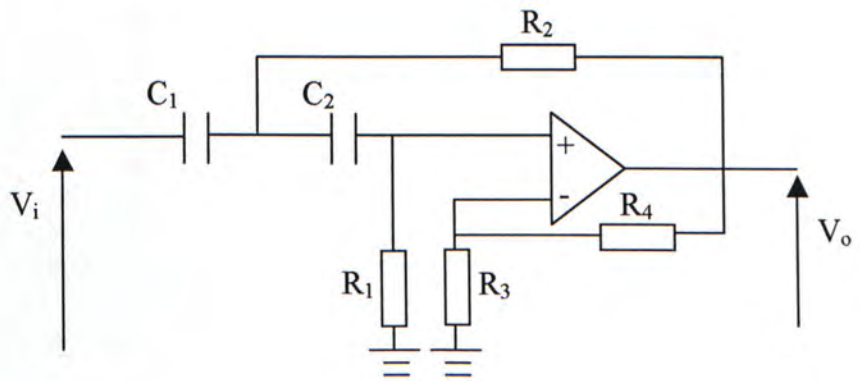

Fig. 3.2. Circuit diagram of VCVS second order high pass filter

where V_i and V_o represent the input voltage and output voltage respectively, R_1 to R_4 indicate the resistors in the circuit. C_1 and C_2 represent the capacitors. This type of circuit was first proposed by Sallen and Key [4]. Calculation procedure is discussed in the section of Appendix A.1. Finally, All necessary parameters are summarized in Table 3.1 and Table 3.2:

Table 3.1. Scaled values of component in VCVS LECG channel

Components	Values
R_1	$28.85k\Omega$
R_2	$8.79k\Omega$
R_3	$75.27k\Omega$
R_4	$75.27k\Omega$
C_1	$2\mu F$
C_2	$2\mu F$

Table 3.2. Scaled values of component in VCVS raw acoustic sound channel

Components	Values
R_1	$28.85k\Omega$
R_2	$8.79k\Omega$
R_3	$75.27k\Omega$
R_4	$75.27k\Omega$
C_1	$0.4\mu F$
C_2	$0.4\mu F$
K	2
f_0	24.956Hz

3.4 Multiple Feed Back Low Pass Filter Circuit

Multiple feedback (MFB) circuit [4] is an alternative to the previously considered VCVS circuit, which has a relatively low closed-loop gain, insofar as the operational amplifier is deemed to be working as an ideal VCVS with an infinite gain. The overall circuit gain is finite and fixed by the circuit components. The expression multiple feedbacks refer to the two feedback paths. Also, the output has 180° phase shift in addition to the phase shift through the network.

This circuit possesses much smaller sensitivities than the VCVS circuit previously considered, especially that the Q-factor associated with the closed-loop gain. With this configuration it is possible to realize reasonably large values of Q-factor at low frequencies, although the trade-off is a narrower bandwidth and a much higher open-loop gain requirement. In signal pre-processing unit, the second order MFB Butterworth low pass filters (Fig. 3.3) are used to filter out the high frequency white noise of the signal in LECG and raw sounds:

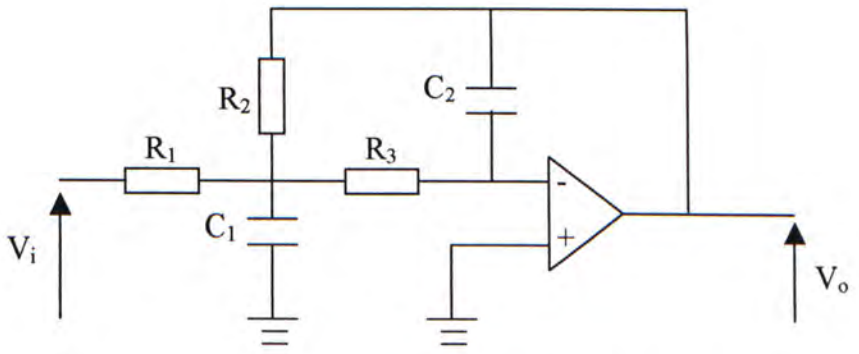

Fig. 3.3. Circuit diagram of MFB second order low pass filter

where V_i and V_o represent the input voltage and output voltage respectively, R_1 to R_3 indicate the resistors in the circuit. C_1 and C_2 represent the capacitors. Calculation procedure is discussed in the section of Appendix A.2. Finally, All necessary parameters are summarized in Table 3.3 and Table 3.4:

Table 3.3. Scaled values of component in MFB LECG channel

Components	Values
R_1	$13.21k\Omega$
R_2	$132.14k\Omega$
R_3	$192.95k\Omega$
C_1	$2\eta F$
C_2	$200\rho F$

Table 3.4. Scaled values of component in MFB raw acoustic sound channel

Components	Values
R_1	$134.13k\Omega$
R_2	$268.25k\Omega$
R_3	$94.48k\Omega$
C_1	$10\eta F$
C_2	$100\rho F$
K	20
f_0	999.72Hz

3.5 Overall Circuit

In section 3.2 to 3.4, all theoretical parameters have been figured out. In this section, the whole circuit diagram of the single pre-processing unit (Fig. 3.4 and Fig. 3.5) would be discussed together with the hardware implantation details.

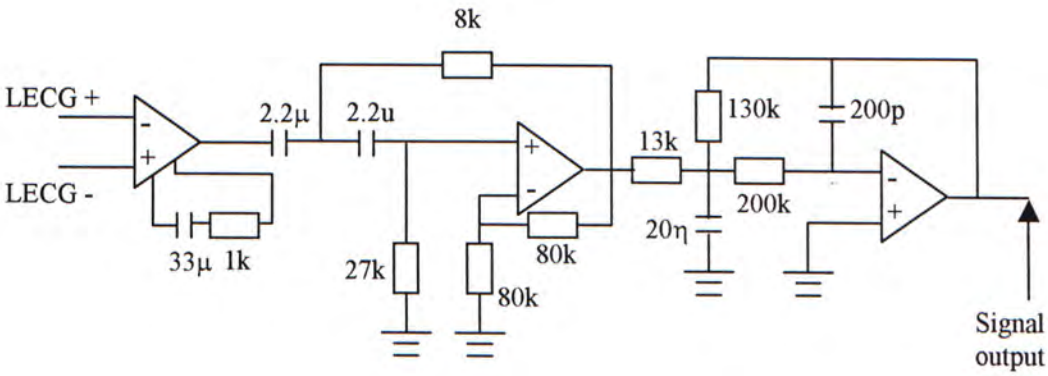

Fig. 3.4. Overall circuit diagram of LECG channel

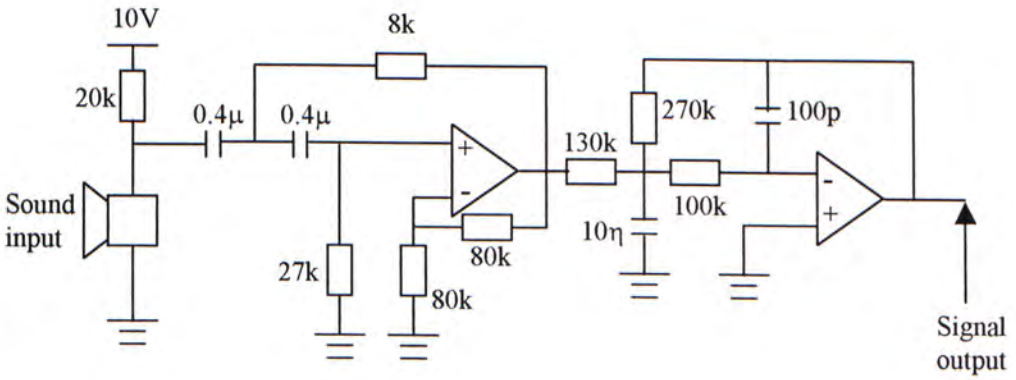

Fig. 3.5. Overall circuit diagram of raw acoustic sound channel

As shown in Figure 3.4 and Figure 3.5, the resistors and capacitors value have some differences from calculation because it is difficult to find such kinds of device with the exact values. However, the overall distortions have been adjusted so that the gain factors and cutoff frequencies would not deviate too much from the theoretical value. All parameters are summarized in Table 3.5

Table 3.5. Parameters of devices setting in signal pre-processing circuit

	Channels	
	LECG	Acoustic Sound
High Input Impedance Circuit		
Gain	50	Nil
High pass cutoff frequency	5Hz	Nil
Order	1st order	Nil
Inverting or non-inverting	Inverting	Nil
VCVS circuit		
Gain	2	2
High pass cutoff frequency	5Hz	25Hz
Order	2nd order	2nd order
Inverting or non-inverting	Non-inverting	Non-inverting
MFB circuit		
Gain	10	20
Low pass cutoff frequency	500Hz	1000Hz
Order	2nd order	2nd order
Inverting or non-inverting	inverting	inverting
Overall circuit		
Total gain	1000	40
bandwidth	5Hz to 500Hz	25Hz to 1000Hz
Order	3rd order	2nd order
Inverting or non-inverting	Non-inverting	Inverting

3.6 Experimental Results

In this experiment, both channels, LECG and raw acoustic sounds, were tested to observe whether the performance of a real hardware matched the theoretical results. In the experiment (Fig. 3.6), different frequency signals with the same voltage levels were applied to the circuits. Then, the output voltage levels were received.

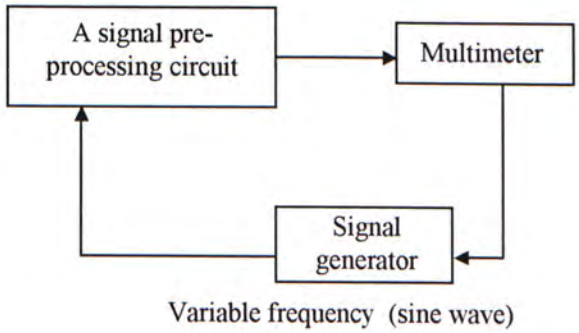

Fig. 3.6. Block diagram of experimental testing of signal pre-processing unit

In LECG channel, 1mv/rms was applied to the input, frequency ranged from 0.01Hz to 1000Hz with an appropriate step. In raw acoustic sound channel, 25mV/rms was applied to the input, frequency ranged from 0.01Hz to 1500Hz. All experimental results are summarized in Table 3.6 and Table 3.7.

Table 3.6. Frequency and voltage relationship of LECG channel

Frequency (Hz)	0.01	1.0	2.0	3.0	4.0	5.0	6.0	7.0	8.0	9.0	10.0	20
Output voltage (Vrms)	0.00	0.01	0.07	0.23	0.48	0.67	0.78	0.84	0.87	0.90	0.91	1.00

Frequency (Hz)	50	100	200	300	400	500	600	700	800	900	1000
Output voltage (Vrms)	1.02	1.04	1.05	1.00	0.93	0.73	0.60	0.51	0.43	0.39	0.35

Table 3.7. Frequency and voltage relationship of raw acoustic sound channel

Frequency (Hz)	0.01	5.0	10	15	20	25	30	35	40	45	50	100
Output voltage (Vrms)	0.19	0.23	0.38	0.60	0.95	1.11	1.16	1.20	1.21	1.22	1.23	1.24

Frequency (Hz)	200	300	400	500	600	700	800	900	1000	1100	1200
Output voltage (Vrms)	1.24	1.25	1.25	1.25	1.24	1.24	1.21	1.14	1.03	0.94	0.83

Frequency (Hz)	1300	1400	1500
Output voltage (Vrms)	0.74	0.69	0.63

According to the figures of Table 3.6 and table 3.7, the corresponding frequency spectrums are formed as shown in Figure 3.7 and Figure 3.8:

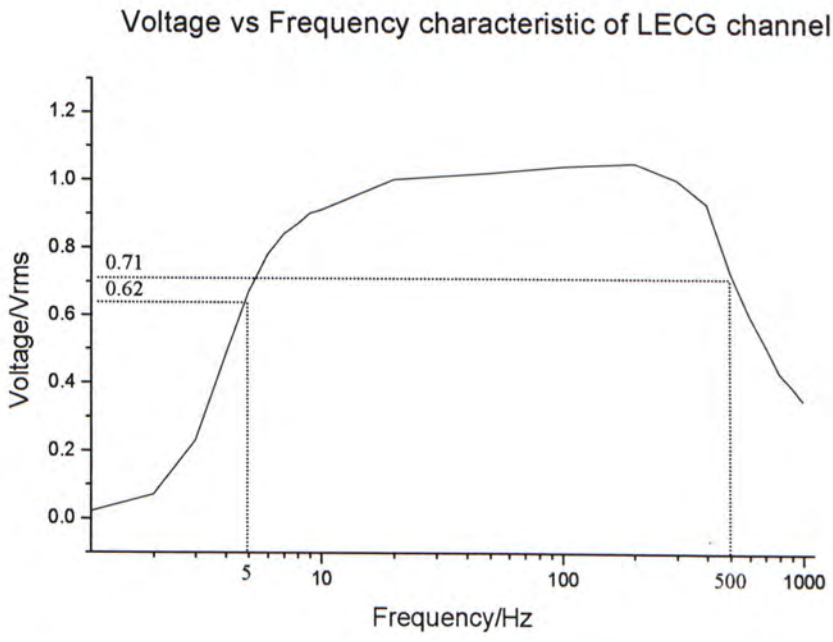

Fig. 3.7. Frequency spectrum of LECG channel

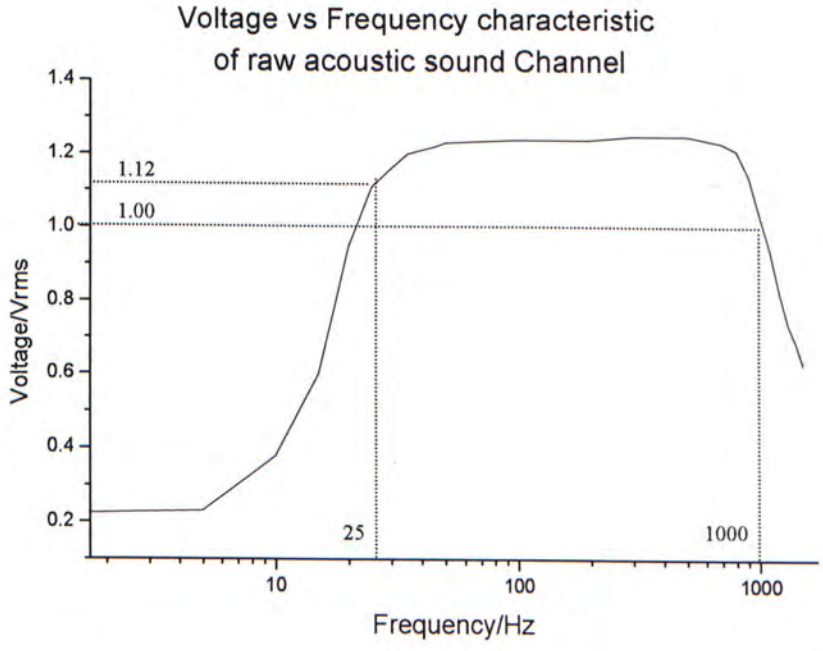

Fig. 3.8. Frequency spectrum of raw acoustic sound channel

3.7 Discussion

In signal pre-processing unit, a high input-impedance circuit amplifier is the first device to collect the electronic biosignal from the chest. The differential DC potential appears at the non-inverting input of the amplifier. The differential DC voltage also appears at the inverting input end of the instrumental amplifier (IA). A single resistor-capacitor set, connected in series, serves as a high pass filter for both input leads, with a cutoff frequency of 5Hz. Therefore, no common signal can be converted into a differential signal, in other words, there is no CMRR degradation. Again, the LECG signals are amplified by the gain factor of 50 in this preliminary stage. After that, the signal is processed by a VCVS circuit with a gain factor of 2 and a high pass cutoff frequency of 5Hz. Finally, a MFB circuit enhances a further 10 times of voltage amplitude, with a low pass cutoff frequency of 500Hz, to process the LECG signal.

In raw mixed sounds channel, it is not necessary to use high input impedance amplifier to collect the signal. Thus, a high pass VCVS circuit with 25 Hz cutoff frequency is the first unit in signal pre-processing unit with the gain factor of 2. It is followed by a low pass MFB circuit with a cutoff frequency of 1kHz and a gain factor of 20.

The amplifiers we used in VCVS and MFB circuits are produced by Linear Technology. Their product (LT1013) is a precision dual op amp in the 8-pin industry standard configuration. Moreover, as shown in Table 3.5, the overall performance of acoustic channel is inverting because in acoustic signal, it is not necessary to provide a non-inverting media. The inverting form does not affect the quality of sounds. Thus, an inverting circuit design was constructed to keep the circuit with fewer electronic components.

In the graph of LECG channel frequency spectrum (Fig. 3.7), the flat band frequency response is almost located within the predicted bandwidth from (5Hz to 500Hz). The average voltage amplitude within flat band is around 1Vrms. Thus, the gain factor should be 1Vrms/1mVrms = 1000, which matches the theoretical result predicted in the previous section. In the graph of acoustic channel frequency spectrum (Fig. 3.8), the flat band response is still located within the bandwidth from (25Hz to 1000Hz). The gain factor in the experimental result is around 50 rather

than 40 in the theoretical result. However, this over-gain effect does not distort the shape of waveform of acoustic sound.

3.8 Section Summary

Bio-signal measurements involve voltages that often are at low levels. The amplitude of the human signal may be lower than 1mV especially the raw LECG. Amplifiers are required to increase signal strength while maintaining high fidelity. In a new electronic stethoscope, both LECG and raw mixed sounds are processed by several amplification circuits to enlarge their amplitudes. Also, they need several filter techniques to reduce the influence of the white noise. As a result, the signals with enhanced signal-to-noise ratio have been received.

Three signal pre-processing units (Fig. 3.9) have been introduced in this chapter, including high input impedance amplifier, VCVS high pass filter circuit, and MFB low pass filter circuit. The corresponding theoretical and experimental results in LECG channel and in raw acoustic sound channel have shown that it is successful to pre-process those signals collected by a new stethoscope's head. As a result, the pre-processed signal can reach the central platform for further advanced signal processing. Details of main platform are discussed in the following chapter.

Fig. 3.9. Hardware of signal pre-processing unit

References

[1] T. Deliyannis, Y. Sun, and K. F. J, "Realization of First- and Second-Order Functions Using Opamps," in *Continuous-Time Active Filter Design*. Boca Rato London New York Washington, D.C.: CRC Press, 1999.

[2] C.-C. Lu and P. P. Tarjan, "Pasteless, Active, Concentric Ring Sensors for Directly Obtained Laplacian Cardiac Electrograms," in Proc. of BSI99, pp. 280-3, 1999.

[3] M. Talero and C. C. Lu, "Active Bipolar Concentric Ring Sensor for Surface Laplacian ECG," in Proc. The First Joint BMES/EMBS, Atlanta, GA, USA, 789, 1999.

[4] A. Waters, "Basic Filter Circuits," in *Active Filter Design*. Hampshire, England: Macmillan New Electronics, 1991.

Chapter 4

Central Platform

4.1 Introduction

In this chapter, we introduce a central platform that has been developed to reduce heart sounds from lung sound recordings by adaptive filtering. The principle of adaptive filtering technique and least-mean-square (LMS) algorithm are also introduced. Then, the determination of parameters in adaptive filter and two-offline approaches are discussed. It is followed by a real-time platform, composed by LABVIEW, to process the signal simultaneously. Several experiments in subjects indicate the effectiveness of the new approach. In the discussion section, the quality of heart sounds reduction among different approaches is compared. Finally, the whole structure of central platform is summarized in the last section.

4.2 Adaptive Filter

4.2.1 Introduction to Adaptive Filtering

In the last thirty years, significant contributions have been made in the signal processing field. The advances in digital circuit design have been the key technological development that sparkled a growing interest in the field of digital signal processing. The resulting digital signal processing systems are attractive due to their reliability, accuracy, small physical sizes, and flexibility.

One example of a digital signal processing system is called filtering. Filtering is a signal processing operation whose objective is to process a signal in order to

manipulate the information contained in the signal. In other words, a filter is a device that maps its input signal in another output signal facilitating the extraction of the desired information contained in the input signal. A digital filter is the one that processes discrete-time signals represented in digital format. For time-invariant filters the internal parameters and the structure of the filter are fixed, and if the filter is linear the output signal is a linear function of the input signal. Once prescribed specifications are given, the design of time invariant linear filters entails three basic steps, namely: the approximation of the specifications by a rational transfer function, the choice of an appropriate structure defining the algorithm, and the choice of the form of implementation for the algorithm.

An adaptive filter [6] is required when either the fixed specifications are unknown or the specifications cannot be satisfied by time-invariant filters. Strictly speaking an adaptive filter is a nonlinear filter since its characteristics are dependent on the input signal and consequently the homogeneity and additivity conditions are not satisfied. However, if we freeze the filter parameters at a given instant of time, the adaptive filter considered in this text is linear in the sense that its output signal is a linear function of its input signal.

The adaptive filters are time-varying since their parameters are continually changing in order to meet a performance requirement. In this sense, we can interpret an adaptive filter as a filter that performs the approximation step-on-line. Usually the definition of the performance criterion requires the existence of a reference signal that is usually hidden in the approximation step of fixed-filter design. This discussion brings the concept that in the design of fixed (nonadaptive) filters, a complete characterization of the input and reference signals is required in order to design the most appropriate filter that meets a prescribed performance. Unfortunately, this is not the usual situation encountered in practice, where the environment is not well defined. The signals that compose the environment are the input and the reference signals, and in cases where any of them is not well defined, the design procedure could be costly and difficult to implement on-line. The solution to this problem is to employ an adaptive filter that performs on-line updating of its parameters through a rather simple algorithm, using only the information available in the environment. In other words, the adaptive filter performs a data-driven approximation step.

4.2.2 Least-Mean-Square (LMS) Algorithm

The basic objective of the adaptive filter is to set its parameter in such way that its output tries to minimize a meaningful objective function involving the reference signal. The least-mean-square (LMS) [7] is a search algorithm in which a simplification of the gradient vector computation is made possible by appropriately modifying the objective function. The LMS algorithm is widely used in various applications of adaptive filtering due to its computational simplicity. The convergence characteristics of the LMS algorithm are examined in order to establish a range for the convergence factor that will guarantee stability. The convergence speed of the LMS is shown to be dependent of the eigenvalue spread of the input-signal correlation matrix. The LMS algorithm is so far the most widely used algorithm in adaptive filtering for several reasons. The main features that attracted the use of the LMS algorithm are low computational complexity, proof of convergence in stationary environment, unbiased convergence to the Wiener solution, and stable behavior when implemented with finite-precision arithmetic.

In this brief section, the LMS algorithm as it is applied to the adaptation of time-varying finite-duration impulse response (FIR) filters is described. For the adaptive FIR system the transfer function (4.1) is described by

$$y(n) = \sum_{q=0}^{Q-1} b_q(k)x(n-q) \tag{4.1}$$

where *b(k)* indicates the time-varying coefficients of the filter, Q represents the length of filter, q represents the q^{th} component within the length of Q, y(n) indicates the component of output value, and x(n-q) represents the component of input signal. With FIR filter the mean-squared error performance surface in the multidimensional space of the filter coefficients is a quadratic function and has a single minimum mean-square error (MMSE). The coefficient values at the optimal solution are called the MMSE solution. The goal of the adaptive process is to adjust the filter coefficients in such a way that they move from their current position toward the MMSE solution. If the input signal changes with time, the adaptive system must continually adjust the coefficients to follow the MMSE solution. In practice, the MMSE solution is often never reached.

The LMS algorithm updates the filter coefficients based on the method of steepest descent. This can be described in vector notation (4.2) as follows:

$$\mathbf{B}_{k+1} = \mathbf{B}_k - \mu\nabla_k \tag{4.2}$$

where $\mathbf{B}_k$ is the coefficient column vector, μ is a parameter that controls the rate of convergence, and the gradient (4.3) is approximated as

$$\nabla_k = \frac{\partial E\left[\varepsilon_k^2\right]}{\partial \mathbf{B}_k} \cong -2\varepsilon_k \mathbf{X}_k \tag{4.3}$$

where $\mathbf{X}_k$ is the LECG signal column vector and ε_k is the error signal as shown in Figure 4.1. Thus, the basic LMS algorithm (4.4) and (4.5) can be written as

$$\mathbf{B}_{k+1} = \mathbf{B}_k + 2\mu\varepsilon_k \mathbf{X}_k \tag{4.4}$$

$$\varepsilon_k = d_k - 2\mathbf{X}_K^T \mathbf{B}_k \tag{4.5}$$

where d_k is the raw acoustic sounds as shown in Figure 4.1. The selection of the convergence parameter must be done carefully because if it is too small the coefficient vector will adapt very slowly and may not react to changes in the input signal. If the convergence parameter is too large, the system will adapt to noise in the signal and may never converge to the MMSE solution.

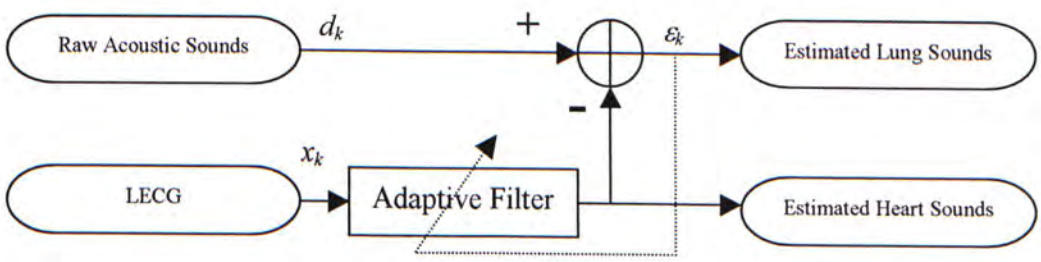

Fig. 4.1. Signal enhancement block diagram of heart sound reduction

4.2.3 Applications

In this section, we discuss some possible choices for the input and desired signals and how these choices are related to the applications. Some of the classical

applications of adaptive filtering are system identification, channel equalization, prediction, and signal enhancement.

In the system identification application, the desired signal is the output of the unknown system when excited by a broadband signal, in most cases a white noise signal. The broadband signal is also used as input for the adaptive filter as illustrated in Figure 4.2. When the output mean-square error (MSE) is minimized, the adaptive filter represents a model for the unknown system.

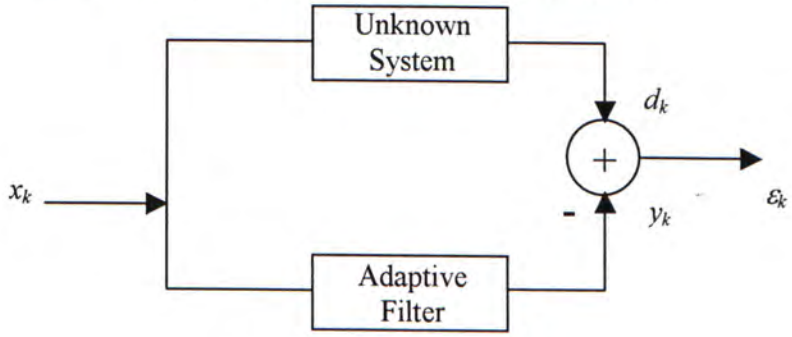

Fig. 4.2. System identification

The channel equalization scheme consists of applying the originally transmitted signal distorted by the channel as the input signal to an adaptive filter, whereas the desired signal is a delayed version of the original signal as depicted in Figure 4.3. This delayed version of the input signal is in general available at the receiver in a form of standard training signal. The minimization of the MSE indicates that the adaptive filter represents an inverse model (equalizer) of the channel.

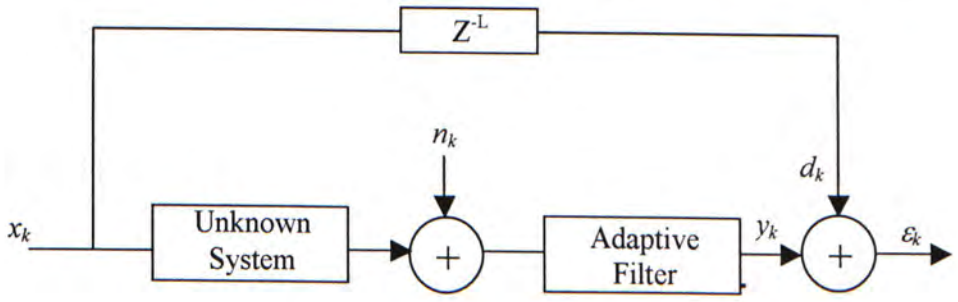

Fig. 4.3. Channel equalization

In the prediction case the desired signal is a forward (or eventually a backward) version of the adaptive filter input signal as shown in Figure 4.4. After convergence, the adaptive filter represents a model for the input signal. It can be used as a predictor model for the input signal.

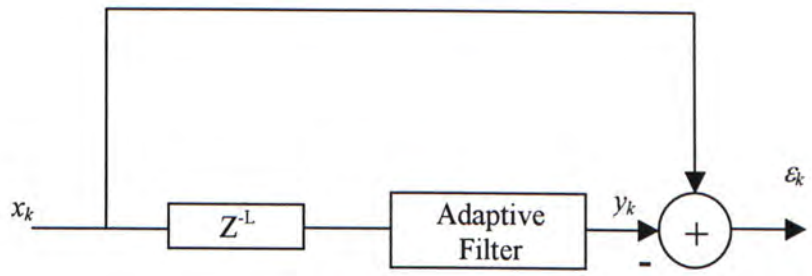

Fig. 4.4. Signal prediction

Finally, in the signal enhancement case [8], which is also our approach, lung sounds are mixed by heart sounds to form the signal d_k, and the signal x_k, which is LECG, correlated to the heart sounds. If x_k is used as an input to the adaptive filter with the lung sounds corrupted by heart sounds playing the role of the desired signal, after convergence the output error will be an enhanced version of the lung sounds (heart sounds depressed). Figure 4.5 illustrates a block diagram in this configuration.

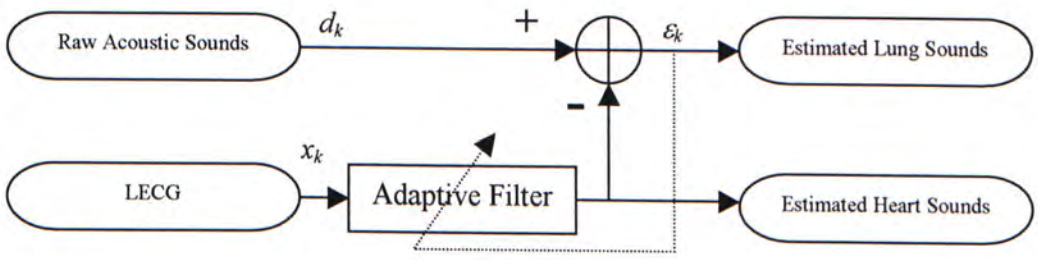

Fig. 4.5. Signal enhancement block diagram of heart sound reduction

4.3 Offline Processing

The concept of adaptive algorithm is introduced in the previous section. In this section, details of implementation of adaptive algorithm in a central platform are discussed. First of all, we used WINDAQ to acquire the biosignal (raw acoustic sounds and LECG) from the chest. All main algorithms were constructed in MATLAB to process the signal intelligently to remove heart sounds from lung sounds. Experimentally recorded and related experimental results pointed out that the success of our new approach [9]. Moreover, another new acoustic waveform based

algorithm was evaluated and examined. Results show that heart sounds can be removed even more effectively.

4.3.1 WINDAQ and MATLAB

WinDAQ is a PC based acquisition device to collect analog signals and convert them to a 12-bits digital format. Up to 16 input channels are multiplexed in a single parallel channel to make the program acquire different analog signals in different channels at the same time. In this case, LECG and raw acoustic sound are needed to be collected at the same time (Fig. 4.6). 3kHz sampling frequency in each channel is assigned for anti-aliasing (the highest frequency in normal breath sounds is around 1kHz). Data is in DAT format, which is compatible with other program such as EXCEL and MATLAB.

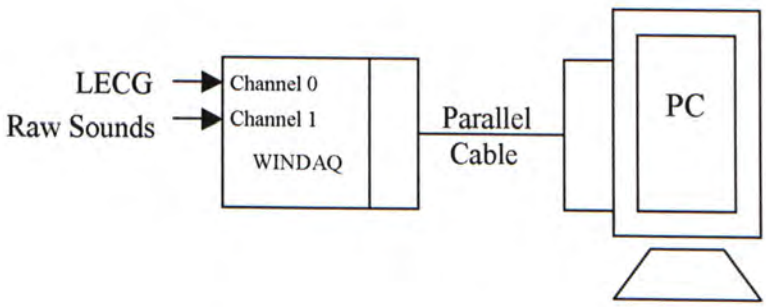

Fig. 4.6. Illustration of WINDAQ connection with PC

MATLAB is a technical computing environment for high-performance numeric computation and visualization. MATLAB integrates numerical analysis, matrix computation, signal processing, and graphics in an easy-to-use environment where problems and solutions are expressed just as they are written mathematically, without traditional programming. MATLAB also features a family of application-specific solutions that we call toolboxes, which are comprehensive collections of MATLAB environment in order to solve particular classes of problems. Areas in which toolboxes are available include signal processing, control systems design, dynamic systems simulation, systems identification, neural networks, and others. In our testing platform, MATLAB programming (Fig. 4.7) was composed for an offline central platform of adaptive filtering implementation.

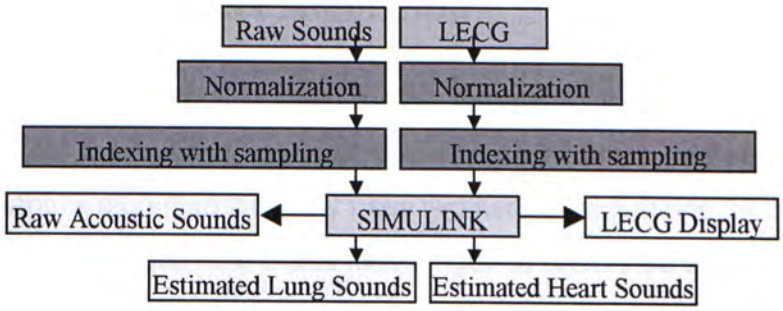

Fig. 4.7. Signal conditioning block diagram of MATLAB command mode

In the case of visualization, we constructed a SIMULINK program (Fig. 4.8) to present the function of adaptive filtering. SIMULINK is a program for simulating dynamic systems. As an extension to MATLAB, SIMULINK adds many features specific to dynamic systems while retaining all of MATLAB's general purpose functionality. To facilitate model definition, SIMULINK added a new class of windows called block diagram windows. In these windows, models were created and edited principally by mouse driven commands. After the signal conditioning in MATLAB command mode, LECG and raw acoustic signal were put in SIMULINK for the main core adaptive algorithm. Their source codes are mentioned in the chapter of Appendix A.3

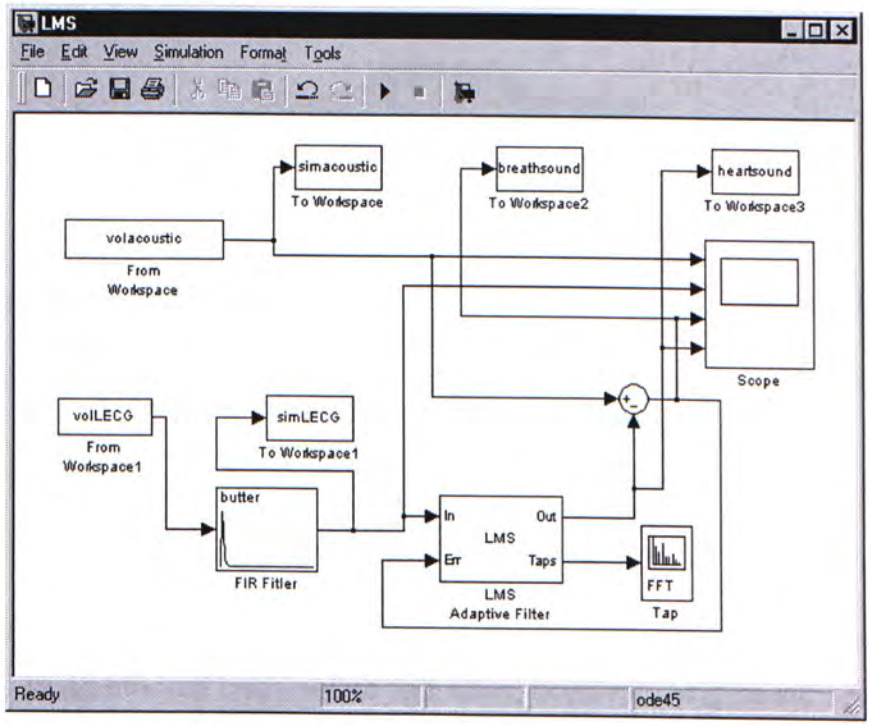

Fig. 4.8. Adaptive filtering block diagram of MATLAB SIMULINK mode

4.3.2 Direct Reference Algorithm

In this approach, LECG is directly used for the reference signal in adaptive filtering as shown in Figure 4.1. Thus, we call this approach direct reference algorithm (DRA). The adaptive algorithm basically uses two iterated equations, (4.5) and (4.6). A suitable value of unit step size μ and filter length $\mathbf{B}_k$ should be determined before a proper use of DRA approach

However, it is difficult to acquire pure lung sounds from human body due to the non-stop heartbeat. However, pure lung sounds is the necessary information to estimate the step size and filter length in LMS filter. To solve the problem, experimentally recorded lung sounds and experimentally recorded heart sounds can be used. The basic principle is that mixture of experimentally recorded lung sounds and experimentally recorded heart sounds represents raw acoustic signal. The corresponding LECG signal represents reference signal.

Experimentally recorded heart sounds and corresponding LECG were collected at left chest from human body by new stethoscope in holding breath. Besides, experimentally recorded lung sounds were collected at the bottom of the right chest in breathing normally. At this location, heart sounds are minimized. Acquisition locations are shown in Figure 4.9.

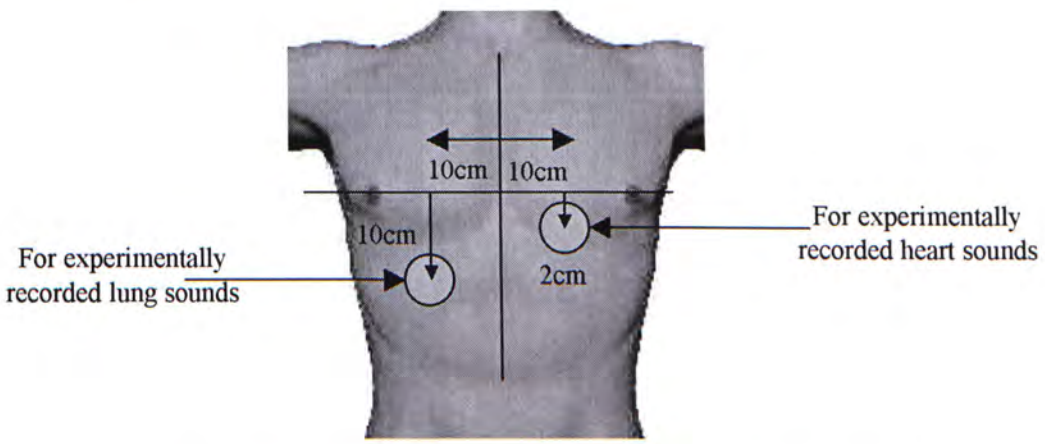

Fig. 4.9. Auscultatory locations of experimentally recorded signals

A parameter, step size -- μ, is needed in adaptive algorithm. A large unit step size leads to an efficient heart sound reduction; however, lung sound spectrum will be distorted. On the other hand, a small unit step size will restore lung sound

spectrum with an insignificant heart sound reduction. Thus, an optimum value of unit step size is needed to determine.

Based on the LMS algorithm implemented on SIMULINK mentioned in last sub-section, different estimated heart sounds and lung sounds by LMS algorithm were obtained by using different unit step sizes. According to this scheme, two cross-correlation coefficient (CC) (4.6) values are obtained corresponding to different unit step sizes. The equation of CC is defined as follow:

$$CC_{xy} = \frac{\sum xy}{\sqrt{\sum x^2 \sum y^2}} \tag{4.6}$$

where x is the component of the first signal and y is the component of the second signal. The first CC value is between experimentally recorded heart sounds and estimated heart sounds by adaptive filtering. The second CC value is between experimentally recorded lung sounds and estimated lung sounds. All values are plotted in Figure 4.10 with different step sizes and filter lengths to help us determine a suitable step size.

(a)

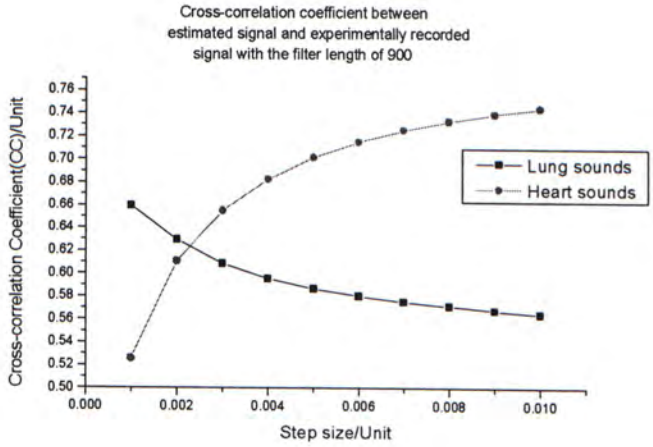

(b)

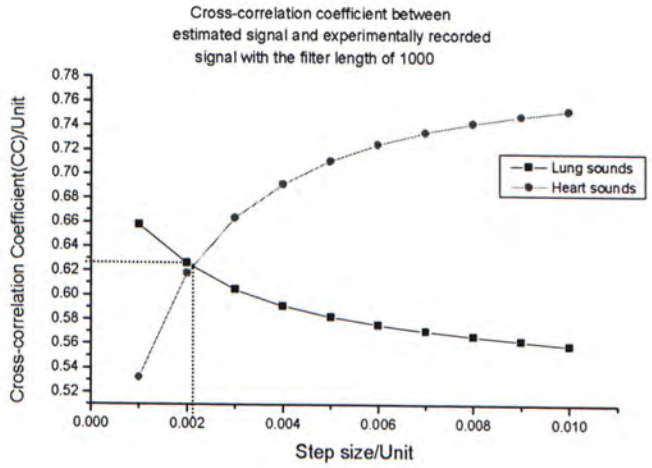

(c)

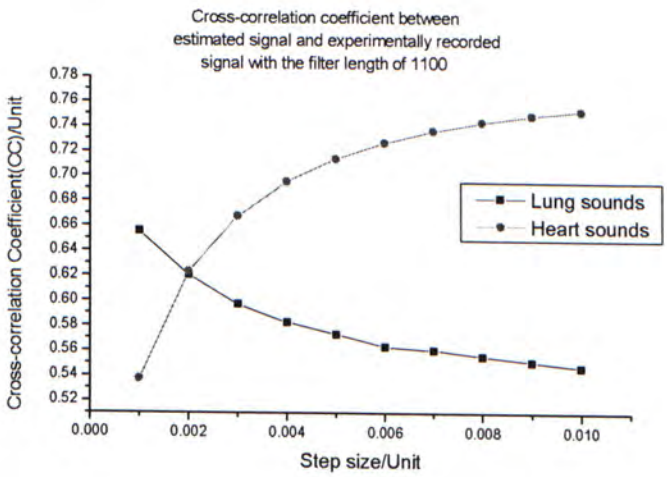

Fig. 4.10. (a) CC values in different step sizes with the filter length of 900. (b) CC values in different step sizes with the filter length of 1000. (c) CC values in different step sizes with the filter length of 1100.

Based on the same sample data, a conditional experiment of heart sound reduction scheme by using digital band pass filter was setup to compare the result with DRA approach (Fig. 4.11).

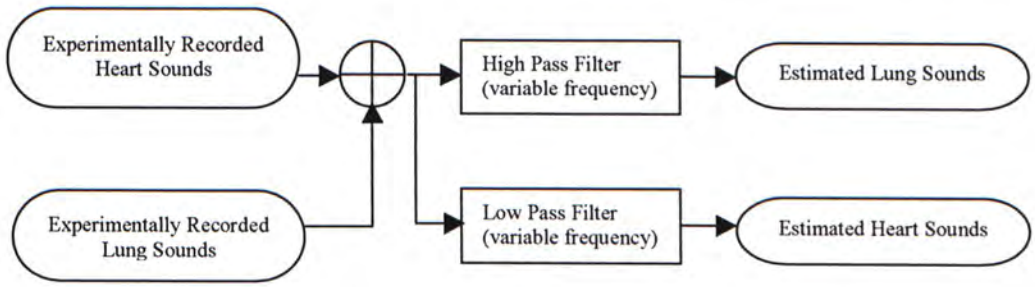

Fig. 4.11. Heart Sound Reduction by Digital Filter

Different estimated heart sounds and lung sounds by digital filter were obtained by using different cutoff frequency in high pass filter and low pass filter. All CC values are plotted in Figure 4.12.

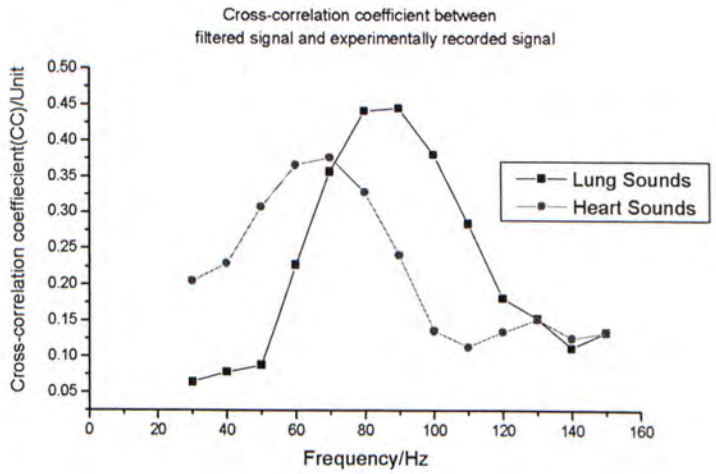

Fig. 4.12. CC values in different cutoff frequencies by using digital filter approach

Another parameter, filter length, should be decided in adaptive algorithm. If filter length is too short, desired signal will be truncated. If filter length is too long, many unwanted noise will be added into the desired signal. Thus, a suitable filter length should be determined to match the system requirement. Just like determining of step size, different estimated heart sounds and lung sounds by LMS algorithm can be obtained by using different filter lengths. Therefore, two cross-correlation coefficient (CC) values were obtained in each filter length as before. All values are plotted in Figure 4.13 with different values of filter lengths and unit step sizes.

(a)

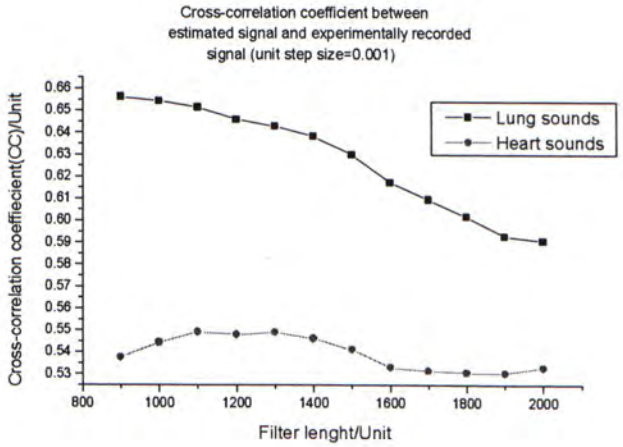

(b)

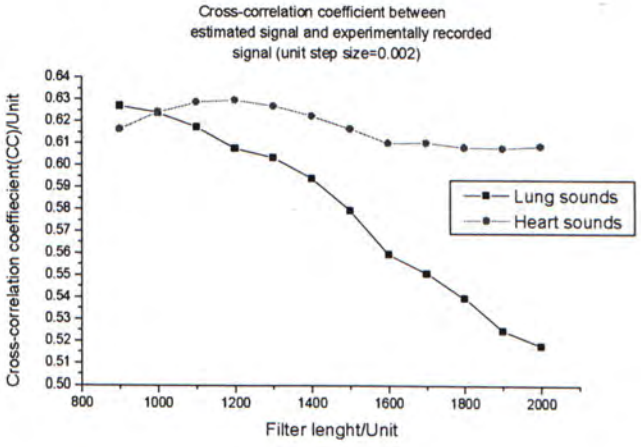

(c)

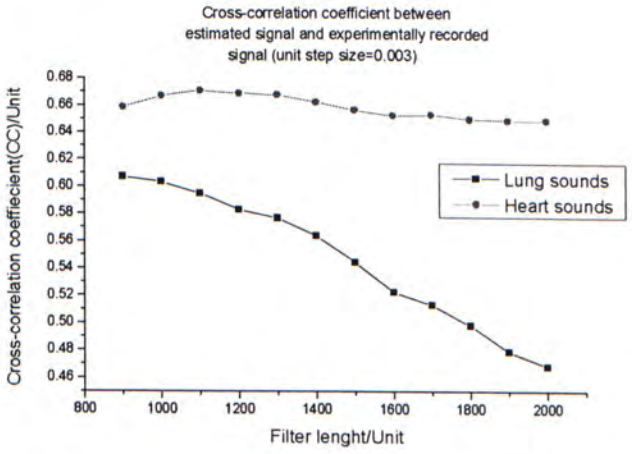

Fig. 4.13. (a) CC values in different filter lengths with the unit step size of 0.001. (b) CC values in different filter lengths with the unit step size of 0.002. (c) CC values in different filter lengths with the unit step size of 0.003.

4.3.3 Determination of Parameters in DRA

As shown in Figure 4.10, unit step size crossing points between two CC lines in different filter lengths are all around 0.002. At this optimum point, the CC values of heart sounds and lung sounds are around 0.62. In an experiment, we found that the maximum CC value of lung sounds approached to 0.70. With this in consideration, if unit step size 0.002 is chosen for optimum unit step, more than half of heart sounds will be reduced without significant lung sound distortion. Sample signals in different unit step sizes are displayed in Figure 4.14 and Figure 4.15.

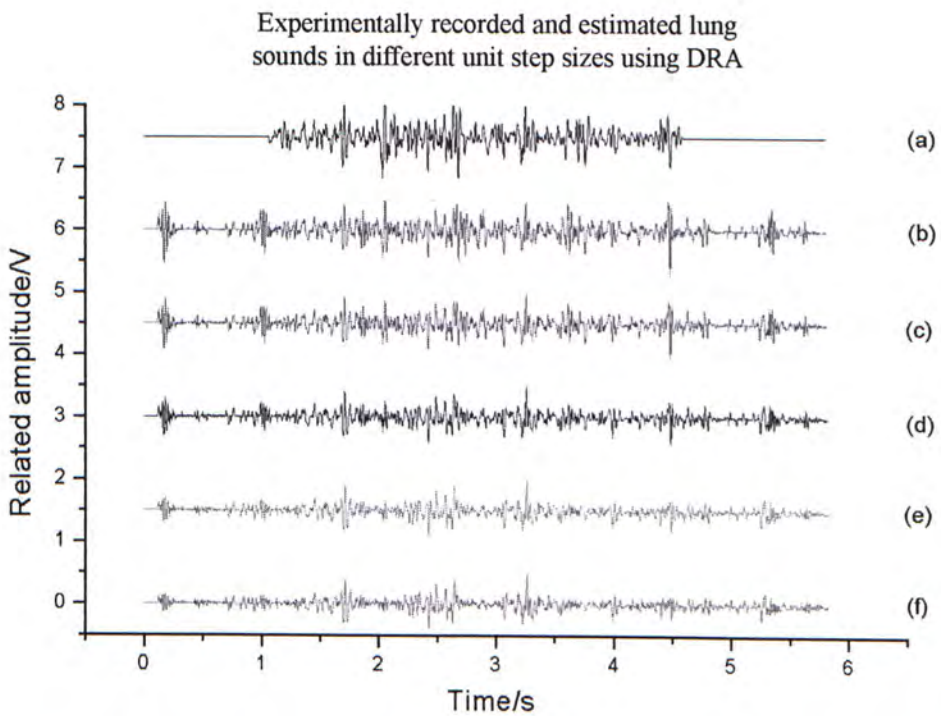

Fig. 4.14. Experimentally recorded and estimated lung sounds: (a) experimentally recorded lung sounds, (b) estimated lung sounds with the step size of 0.001, (c) estimated lung sounds with the step size of 0.002, (d) estimated lung sounds with the step size of 0.004, (e) estimated lung sounds with the step size of 0.007, and (f) estimated lung sounds with the step size of 0.01.

As shown in Fig. 4.14, we can see that most heart sounds are suppressed mostly in estimated lung sounds with the step size of 0.01. However, lung sound spectrum is distorted heavily compared with experimentally recorded reference signal.

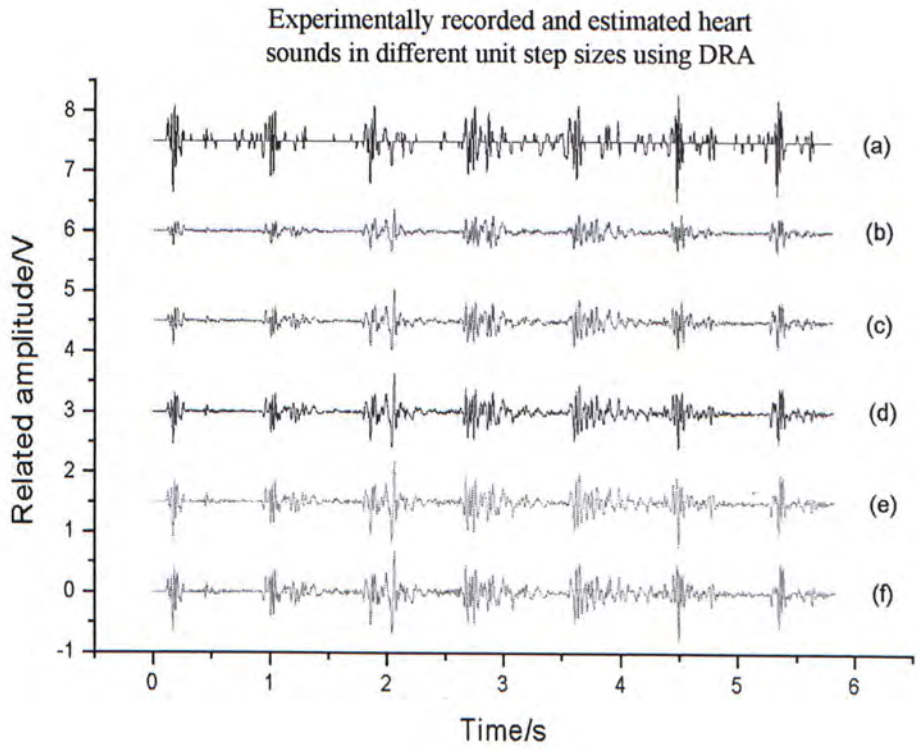

Fig. 4.15. Experimentally recorded and estimated heart sounds: (a) experimentally recorded heart sounds, (b) estimated heart sounds with the step size of 0.001, (c) estimated heart sounds with the step size of 0.002, (d) estimated heart sounds with the step size of 0.004, (e) estimated heart sounds with the step size of 0.007, and (f) estimated heart sounds with the step size of 0.01.

As shown in Fig. 4.15, when we look carefully in estimated heart sounds with the step size of 0.01, some continuous signals exist followed by the main heart sound but they are absent in experimentally recorded heart sounds. All these kinds of signals are resorted to the lung sounds spectrum. This adverse effect will be minimized if a small size of unit step is chosen.

On the other hand, as shown in Figure 4.12, the optimum frequency to separate heart sounds and lung sounds by using digital filter is around 70Hz. The CC value in digital filter scheme is around 0.38, which is much lower than in DRA scheme. It is no doubt that heart sounds and lung sounds cannot be separated by digital filter effectively.

According to Figure 4.13, when we compare the effect of unit step size on CC value and the effect of filter length on CC value, it is not difficult to notice that the unit step size is a dominant factor. However, we still can observe the trend of CC values in different length of filter lengths. Increasing filter length will decrease CC values between experimentally recorded lung sounds and estimated lung sounds, which implies that several unwanted noise, heart sounds, are added to sound channel. However, increasing filter length will slightly increase CC values within heart sounds until the filter length up to 1300 taps. Therefore, we consider the CC crossing point (Fig. 4.13 (b)) a suitable filter length, i.e. 1000.

Another factor is that LECG signal has only one spike, just like R wave in ECG. However, normally two heart sounds occur that correspond to the different valves contraction. Thus, a large LMS FIR filter is used to eliminate both heart sounds effectively. For reference, the time between two main heart sounds is almost equal to 300ms [2] (900 taps in 3kHz sampling frequency). For safety reason, a slightly longer filter length is determined.

Furthermore, filter length is directly proportional to the number of multiplifications per iteration as shown in Figure 4.16. A large taps size in adaptive filter consumes a great calculation power to make it difficult to be implemented on real time processing platform. Filter length should be determined as short as possible.

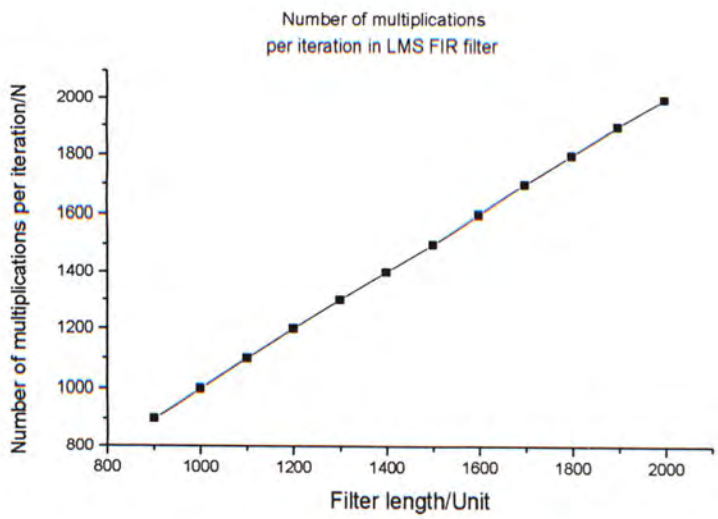

Fig. 4.16. Relationship between filter length and number of multiplications

Sample signals in different filter lengths are displayed in Figure 4.17 and Figure 4.18.

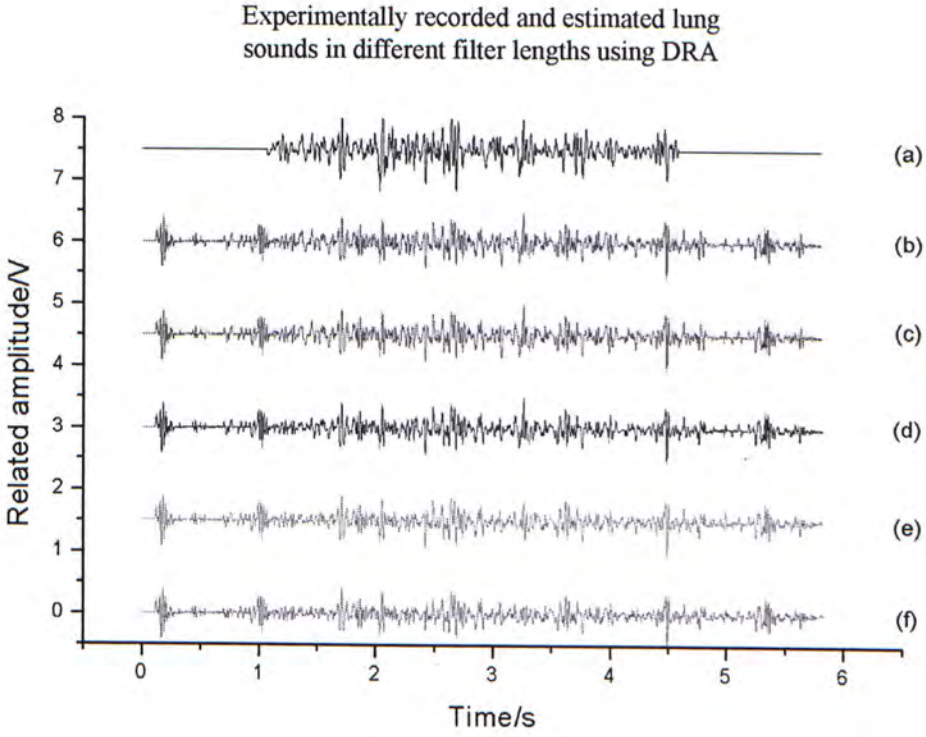

Fig. 4.17. Experimentally recorded and estimated lung sounds: (a) experimentally recorded lung sounds, (b) estimated lung sounds with the filter length of 900, (c) estimated lung sounds with the filter length of 1000, (d) estimated lung sounds with the filter length of 1300, (e) estimated lung sounds with the filter length of 1700, and (f) estimated lung sounds with the filter length of 2000.

As shown in Figure 4.17, distortion occurs when a long filter length, such as 2000, is applied in the adaptive filter. However, the influence is not as heavy as by unit step size effect.

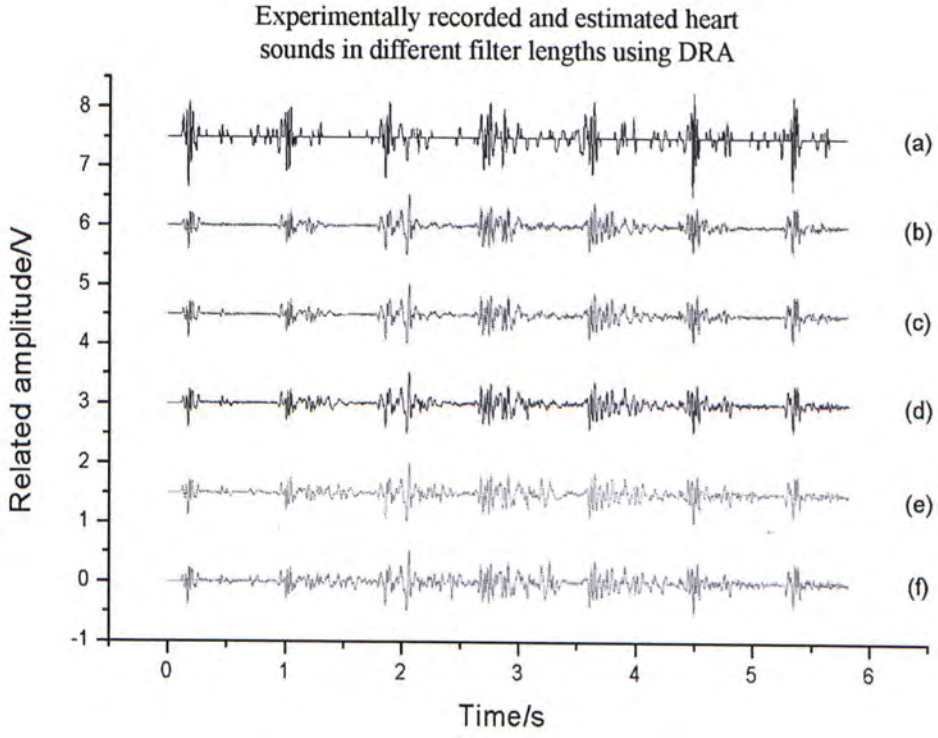

Fig. 4.18. Experimentally recorded and estimated heart sounds: (a) experimentally recorded heart sounds, (b) estimated heart sounds with the filter length of 900, (c) estimated heart sounds with the filter length of 1000, (d) estimated heart sounds with the filter length of 1300, (e) estimated heart sounds with the filter length of 1700, and (f) estimated heart sounds with the filter length of 2000.

As shown in Figure 4.18, when a long filter length is applied, some continuous signals exist followed by the main heart sound, but they are absent in experimentally recorded heart sounds. All these kinds of signals are minimized when a short filter length is chosen.

To sum up, we find that a suitable step size is around 0.002 and a suitable filter length is around 1000. Experimentally recorded result based on those requirements is shown in Figure 4.19.

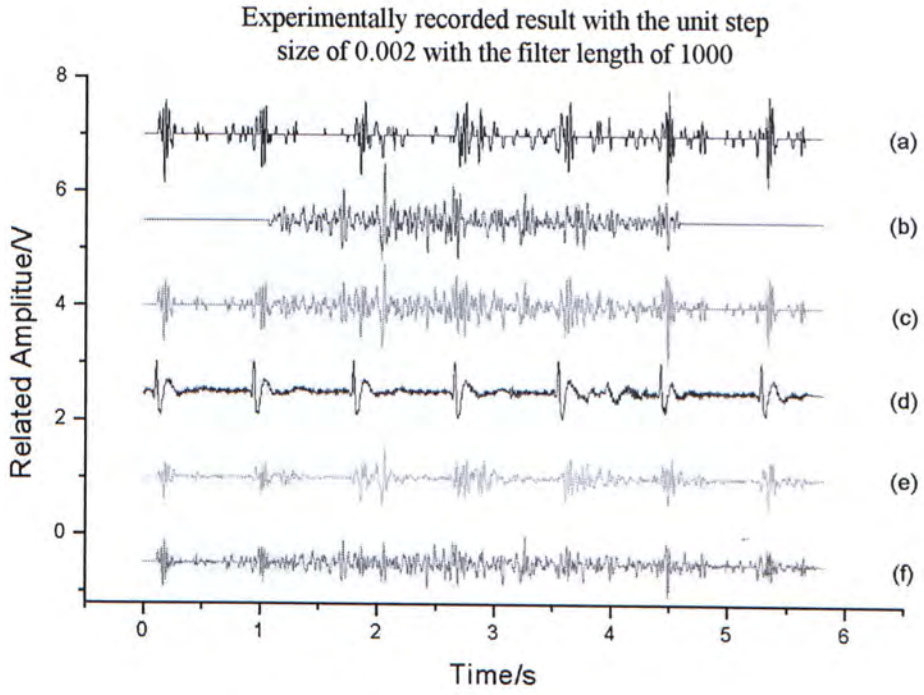

Fig. 4.19. Experimentally recorded result: (a) experimentally recorded heart sounds, (b) experimentally recorded lung sounds, (c) mixed acoustic sounds, (d) experimentally recorded LECG, (e) estimated heart sounds, and (f) estimated lung sounds.

4.3.4 Experimental Results of DRA

All experimental results (estimated lung sounds and heart sounds) were displayed at the block diagram of "scope", which is a SIMULINK block set mentioned in section 4.3.1. Moreover, the results were forced back to MATLAB command mode for further analysis. The energy of estimated heart sounds could be calculated to estimate the effective of a new algorithm. On the other hand, it was possible to form a "wave" file for speaker to playback. Thus we could listen the estimated lung sounds to decide whether heart sounds were reduced or not subjectively. Sample signals are shown in Figure 4.20.

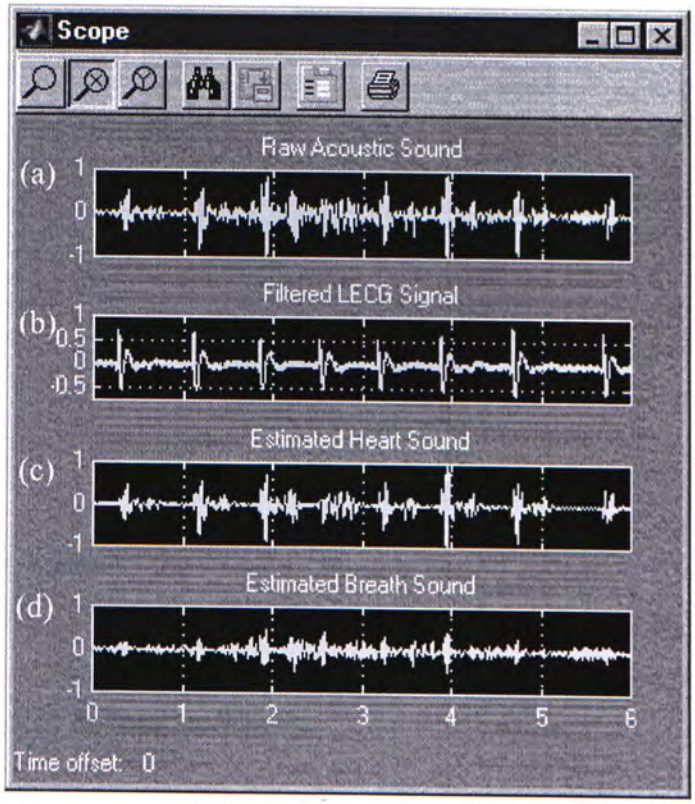

Fig. 4.20. Examples of signals processed by DRA approach: (a) raw acoustic sounds, (b) filtered LECG signal, (c) estimated heart sounds, and (d) estimated breath sounds

Six different locations of three young and healthy subjects were chosen. These locations included top left, middle left, low left, top right, middle right, and low right of the front chest (Fig. 4.21). Collected signals with the length of 6 seconds were processed using this algorithm. The estimated breath and heart sounds are given in Figure 4.20(c) and (d). The spike in estimated breath sounds was eliminated. Moreover, when we played back the signal, the heart sounds were reduced. However, the measurement of improvement in signal to noise cannot be reached directly because it is impossible to collect pure lung sounds. Thus, heart sound energy reduction is used to account for this problem. Using this approach, we should assume that the heart sounds does not change significantly in breathing normally.

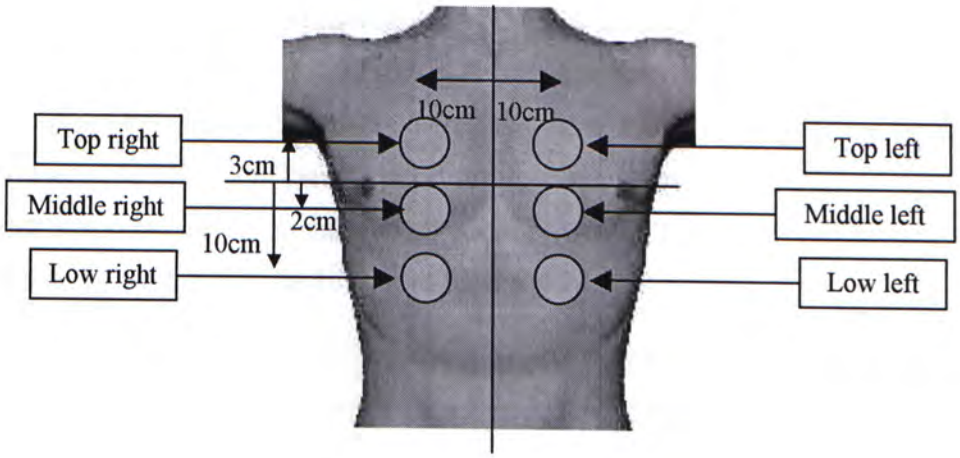

Fig. 4.21. Auscultatory locations

We cannot examine the quality of heart sound reduction directly due to the non-stop heartbeat. Therefore, an indirect approach, heart sound energy reduction (HSER), widely accepted by previous other researches, is used to examine DRA objectively. HSER is defined as follows:

$$100\% - \left(\frac{\sum y^2 - \sum x^2}{\sum y^2} \times 100\% \right) \tag{4.7}$$

where y is the component of raw mixed sounds and x is the component of estimated heart sounds. However, as shown in Figure 4.22, we have both totally different waveforms with a high HSER result. To solve this problem, a point-to-point heart sound energy reduction (PPHSER) is proposed as the second objective parameter to examine DRA.

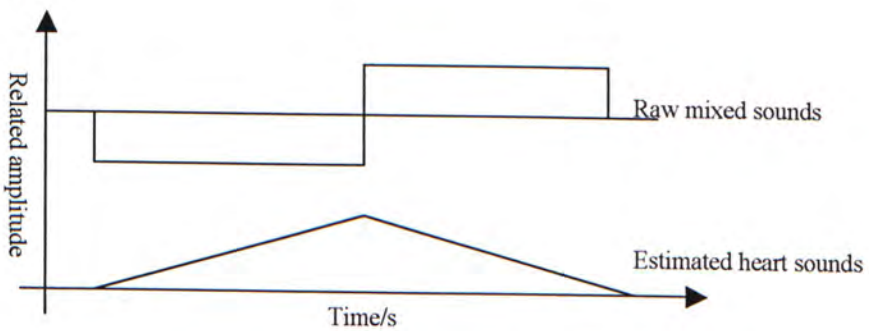

Fig. 4.22. Examples of different waveforms with same HSER

PPHSER is defines as follows:

$$100\% - \left(\frac{\sum (y - x)^2}{\sum y^2} \times 100\% \right) \tag{4.8}$$

where *y* is the component of raw mixed sounds and *x* is the component of estimated heart sounds. Using Figure 4.22 as an example, obviously, PPHSER is much more smaller than HSER. In this case, PPHSER is a more appropriated approach to justify the performance of heart sound energy reduction. The results of mean value (m) and standard deviation (std) in six locations over 3 subjects are summarized in Table 4.1, Table 4.2, Figure 4.23, and Figure 4.24.

Table 4.1. Experimental result of HSER using DRA

Location	m (normal)	std (normal)	m (holding)	std (holding)
Top left	70%	±3.51%	78%	±5.68%
Middle left	58%	±8.19%	68%	±7.02%
Low left	50%	±4.58%	55%	±4.73%
Top right	42%	±8.39%	63%	±7.02%
Middle right	24%	±6.00%	45%	±13.80%
Low right	24%	±10.22%	32%	±10.41%

Table 4.2. Experimental result of PPHSER using DRA

Location	m (normal)	std (normal)	m (holding)	std (holding)
Top left	72%	±3.51%	84%	±3.61%
Middle left	60%	±7.51%	73%	±5.00%
Low left	53%	±6.24%	60%	±5.00%
Top right	44%	±7.81%	68%	±8.50%
Middle right	26%	±6.03%	50%	±11.36%
Low right	27%	±10.41%	37%	±8.62%

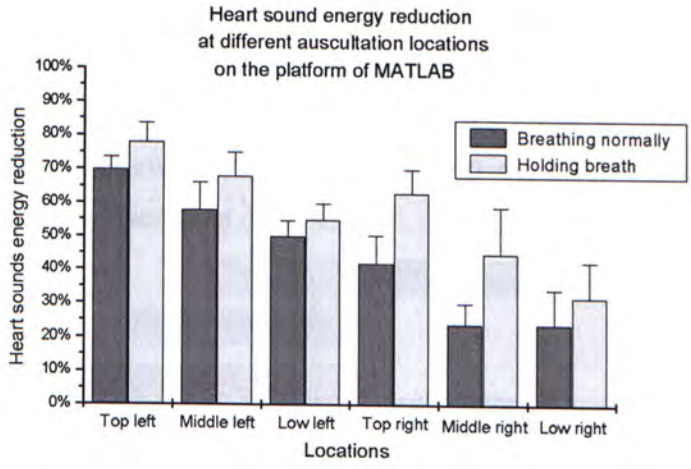

Fig. 4.23. Experimental results of HSER using DRA

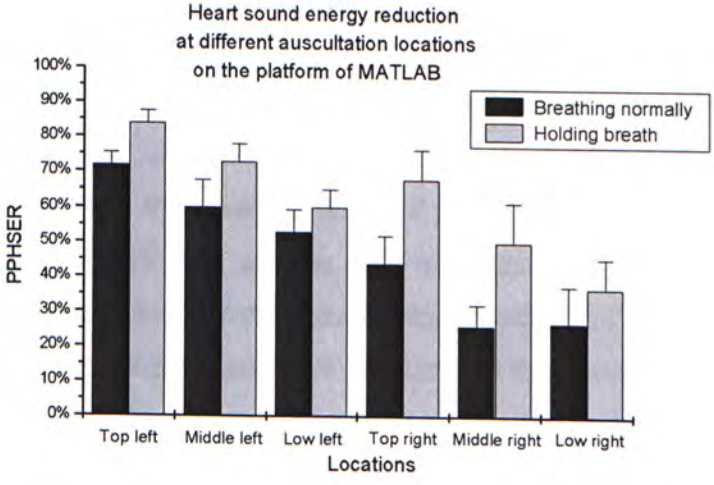

Fig. 4.24. Experimental results of PPHSER using DRA

We can notice that the overall performance, using HSER or PPHSER, of left chest is better than right chest. The reason is that the LECG signal at right chest is very weak. Among the six testing locations, the low right position is the worst case in LECG acquisition. Only 24% heart artifact reduction is achieved. The standard deviations of the results in right chest are higher than in left chest. The conditional experiments of each subject under holding breath are summarized in the same table for reference. The overall performance of subject in holding breath is better than in breathing normally.

4.3.5 Acoustic Waveform Based Algorithm

Another approach, named acoustic waveform based algorithm (AWBA) is proposed to reduce heart sounds from lung sound recording more effectively. In this case, a reference signal in adaptive filtering is not the LECG signal. We constructed another signal processing program in MATLAB command mode to estimate the peak of LECG location in each heartbeat (Fig. 4.25).

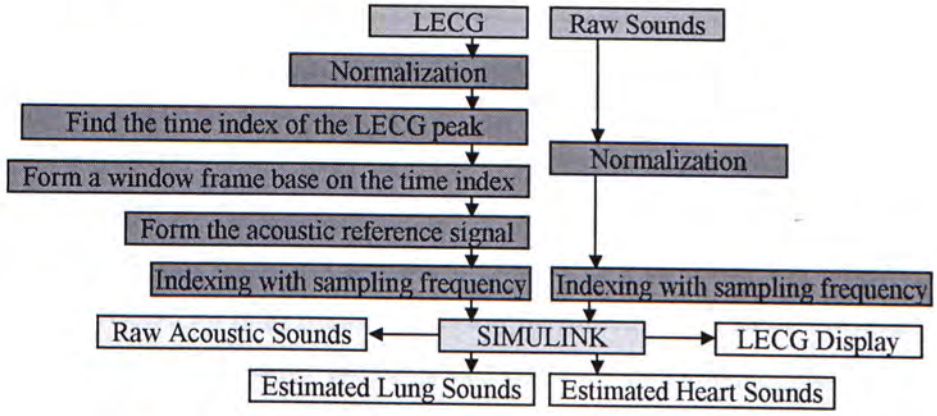

Fig. 4.25. Block diagram of AWBA in MATLAB command mode

A window frame is formed in each heartbeat by the peak location of LECG; the size of window frame is 300 samples (from 50 data before the peak location of LECG to 249 data after the peak location of LECT). According to the setting of sampling frequency, totally 0.1s sample data is in this window frame. This window frame is used to capture the sample data in raw sound channel. As a result, partial of heart sound in raw sound channel is captured in the window frame (Fig. 4.26). Therefore, a new reference signal for adaptive filtering is formed based on this frame. Source code of AWBA is attached in Appendix A.4.

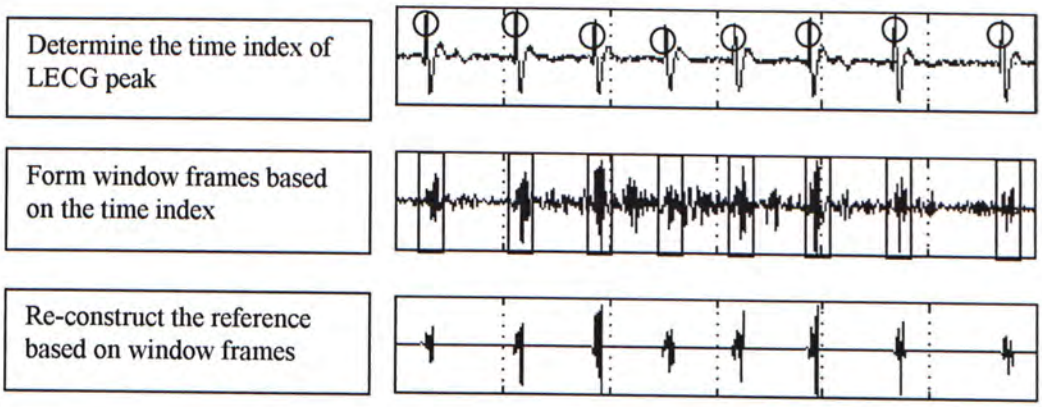

Fig. 4.26. Principle of estimated acoustic reference by LECG

The principle of this approach is to use raw acoustic sounds signal itself as the reference point at adaptive filter. LECG is just used for the heat sounds location estimation. In this case, the correlation coefficient between the desired signal and reference should be high (higher than the correlation coefficient between LECG and heart sounds). The same set of data, used in DRA, was used to evaluate the performance of AWBA. Similarly, two cross-correlation coefficient (CC) values were obtained. All values, compared with DRA results, are plotted in Figure 4.27 and Figure 4.28 with different values of filter lengths and unit step sizes.

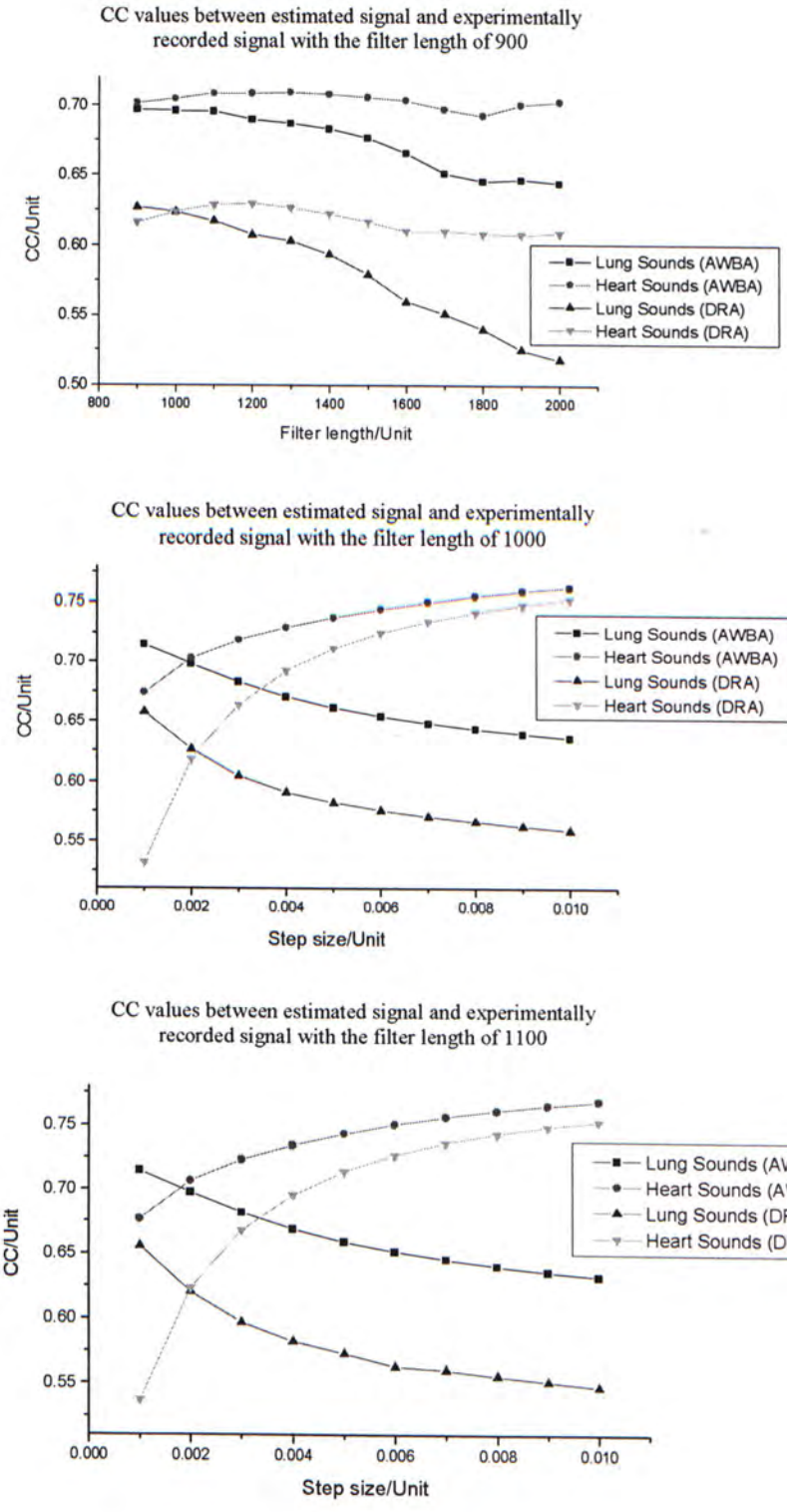

Fig. 4.27. (a) CC values of different approaches in different step sizes with the filter length of 900. (b) CC values of different approaches in different step sizes with the filter length of 1000. (c) CC values of different approaches in different step sizes with the filter length of 1100.

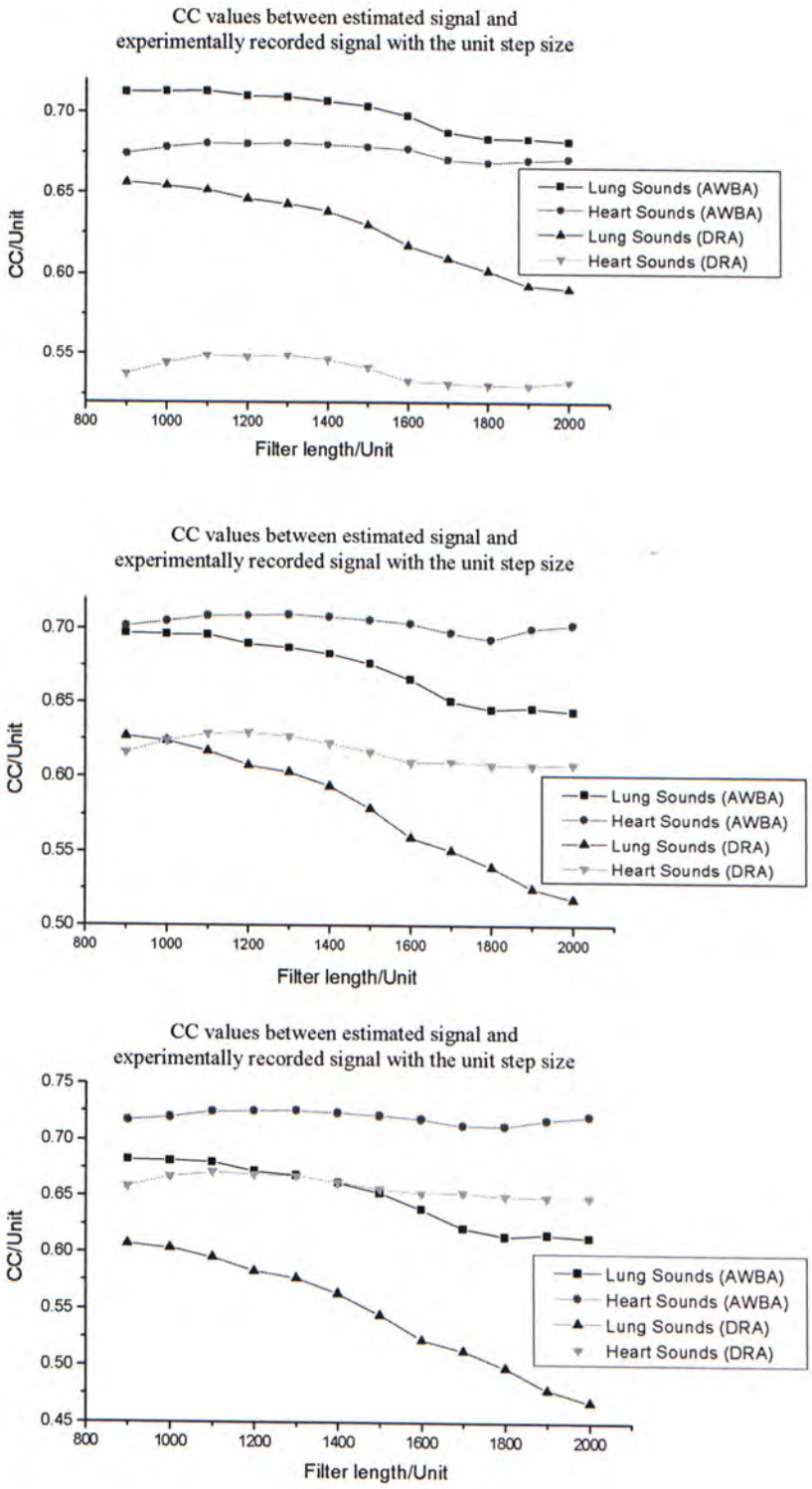

Fig. 4.28. (a) CC values of different approaches in different filter lengths with the step size of 0.001. (b) CC values of different approaches in different filter lengths with the step size of 0.002. (c) CC values of different approaches in different filter lengths with the step size of 0.003.

As shown in Figure 4.27 and Figure 4.28, AWBA approach has a higher CC value than DRA approach with the same unit step sizes, and filter lengths. The optimum unit step size and filter length of AWBA is closed to DRA. Parameters in AWBA were set the same as in DRA for comparison. Samples signal, compared with the signal processed by DRA, are plotted in Figure 4.29, Figure 4.30, Figure 4.31, and Figure 4.32.

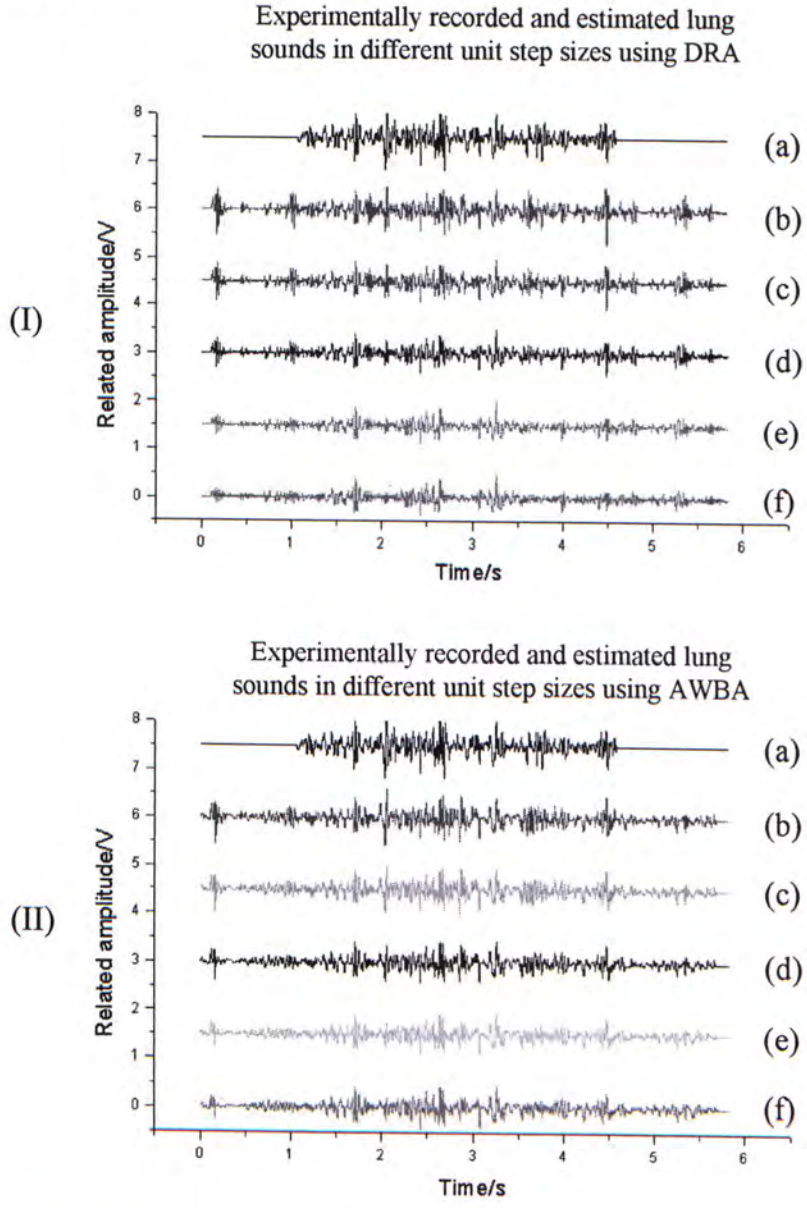

Fig. 4.29. Experimentally recorded and estimated lung sounds: (a) experimentally recorded lung sounds (I) DRA (II) AWBA, (b) estimated lung sounds with the step size of 0.001 (I) DRA (II) AWBA, (c) estimated lung sounds with the step size of 0.002 (I) DRA (II) AWBA, (d) estimated lung sounds with the step size of 0.004 (I) DRA (II) AWBA, (e) estimated lung sounds with the step size of 0.007 (I) DRA (II) AWBA, and (f) estimated lung sounds with the step size of 0.01. (I) DRA (II) AWBA

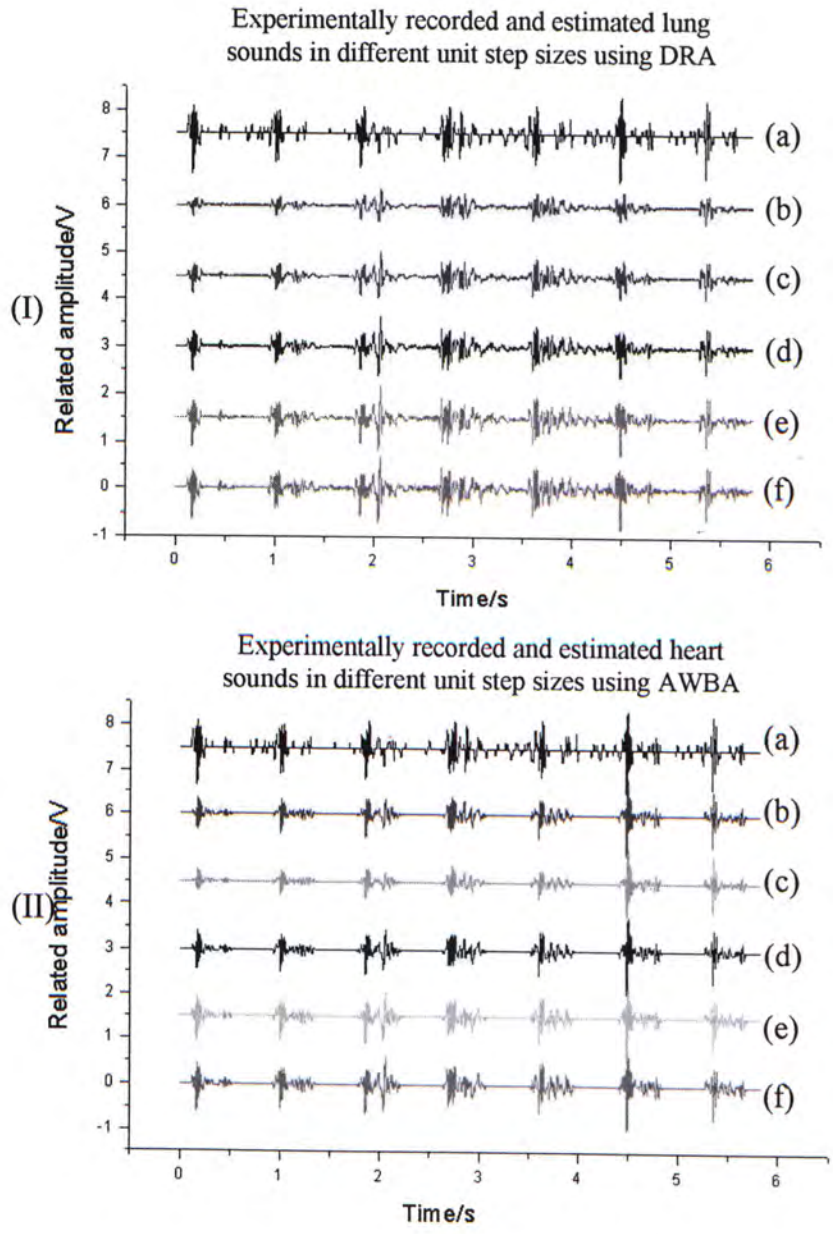

Fig. 4.30. Experimentally recorded and estimated heart sounds: (a) experimentally recorded heart sounds (I) DRA (II) AWBA, (b) estimated heart sounds with the step size of 0.001 (I) DRA (II) AWBA, (c) estimated heart sounds with the step size of 0.002 (I) DRA (II) AWBA, (d) estimated heart sounds with the step size of 0.004 (I) DRA (II) AWBA, (e) estimated heart sounds with the step size of 0.007 (I) DRA (II) AWBA, and (f) estimated heart sounds with the step size of 0.01. (I) DRA (II) AWBA

As shown in Figure 4.29, lung sounds are distorted slightly by using AWBA rather than by using DRA. As shown in Figure 4.30, heart sounds are estimated correctly by using AWBA instead of by using DRA.

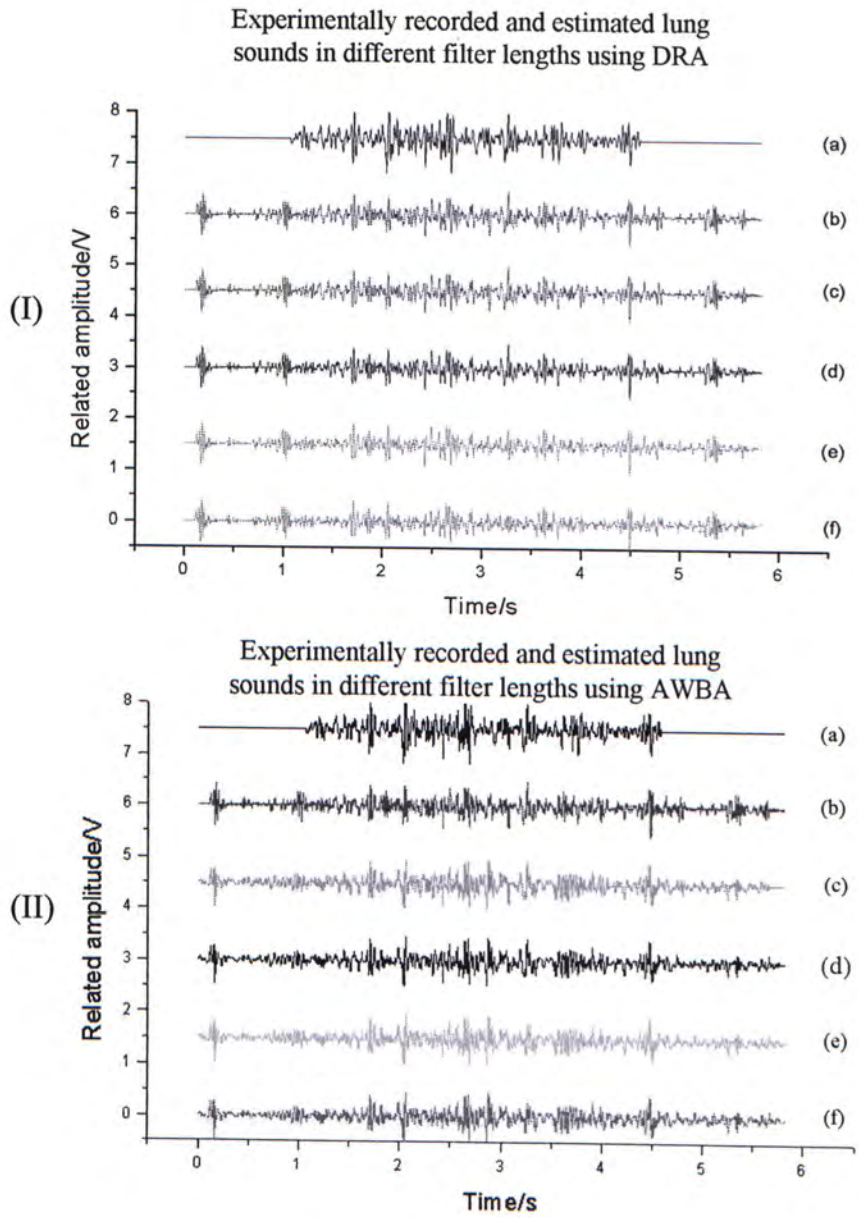

Fig. 4.31. Experimentally recorded and estimated lung sounds: (a) experimentally recorded lung sounds (I) DRA (II) AWBA, (b) estimated lung sounds with the filter length of 900 (I) DRA (II) AWBA, (c) estimated lung sounds with the filter length of 1000 (I) DRA (II) AWBA, (d) estimated lung sounds with the filter length of 1300 (I) DRA (II) AWBA, (e) estimated lung sounds with the filter length of 1700 (I) DRA (II) AWBA, and (f) estimated lung sounds with the filter length of 2000 (I) DRA (II) AWBA.

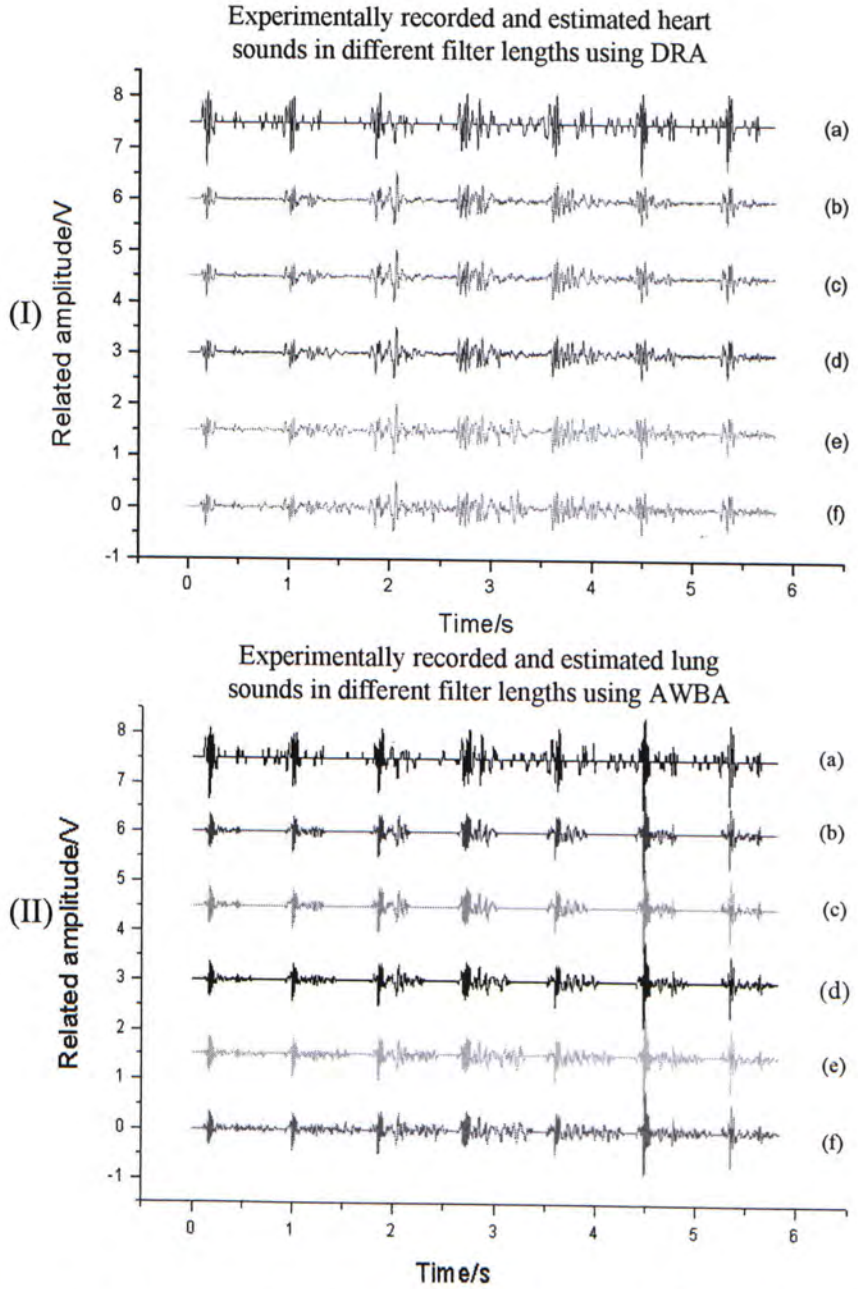

Fig. 4.32. Experimentally recorded and estimated heart sounds: (a) experimentally recorded heart sounds (I) DRA (II) AWBA, (b) estimated heart sounds with the filter length of 900 (I) DRA (II) AWBA, (c) estimated heart sounds with the filter length of 1000 (I) DRA (II) AWBA, (d) estimated heart sounds with the filter length of 1300 (I) DRA (II) AWBA, (e) estimated heart sounds with the filter length of 1700 (I) DRA (II) AWBA, and (f) estimated heart sounds with the filter length of 2000 (I) DRA (II) AWBA.

As shown in Figure 4.31 and Figure 4.32, it is not too difficult to observe that estimated lung sounds and estimated heart sounds processed by AWBA are more similar to experimentally recorded signal than by DRA.

To sum up, same parameters with DRA, unit step size = 0.002 and filter length = 1000, were used to process the experimentally recorded signal. Sample signal, compared with the signal processed by DRA and, based on those requirements is shown in Figure 4.33.

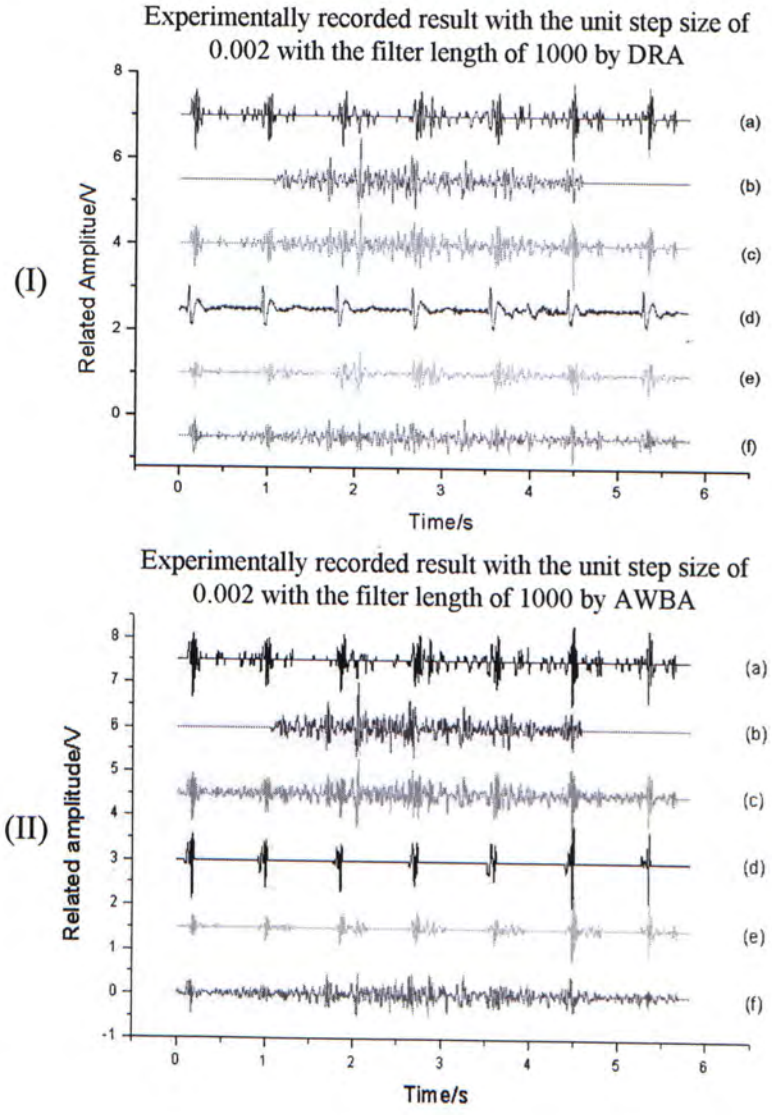

Fig. 4.33. Experimentally recorded results: (a) experimentally recorded heart sounds (I) DRA (II) AWBA, (b) experimentally recorded lung sounds (I) DRA (II) AWBA, (c) mixed acoustic sounds (I) DRA (II) AWBA, (d) experimentally recorded LECG (I) DRA (II) AWBA, (e) estimated heart sounds, and (f) estimated lung sounds (I) DRA (II) AWBA.

As shown in Figure 4.33, lung sounds and heart sounds estimated by AWBA are more effectively than by DRA.

4.3.6 Experimental Results of AWBA

The same set of sample data used in DRA was processed again by using AWBA approach. The same justification methods were used to compare the performance between DRA and AWBA. Sample signals calculated by AWBA are shown in Figure 4.34.

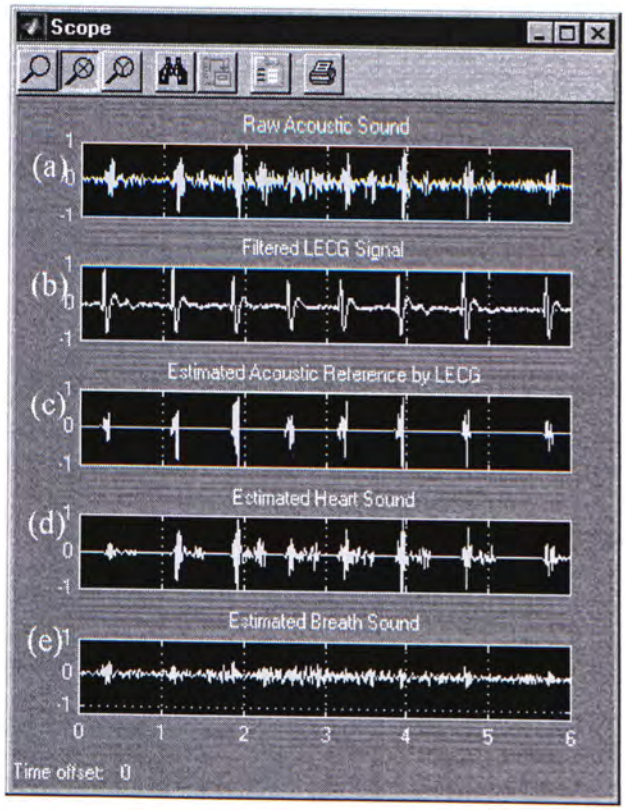

Fig. 4.34. Examples of signals processed by AWBA approach: (a) raw acoustic sound, (b) filtered LECG signal, (c) estimated acoustic reference by LECG (d) estimated heart sounds, and (e) estimated breath sounds

The results of HSER and PPHSER in both approaches, DRA and AWBA, are summarized in Table 4.3 and Table 4.4. The average results of CC on 3 subjects between pure heart sounds and estimated heart sounds of both approaches in the subject holding breath on different auscultation locations are summarized in the Table 4.5 for reference.

Table 4.3. Experimental result of HSER on the platform of MATLAB

Location	DRA, m (normal)	DRA, std (normal)	AWBA, m (normal)	AWBA, std (normal)	DRA, m (holding)	DRA, std (holding)	AWBA, m (holding)	AWBA, std (holding)
Top left	70%	±3.51%	72%	±3.06%	78%	±5.68%	88%	±6.56%
Middle left	58%	±8.19%	76%	±7.94%	68%	±7.02%	80%	±5.00%
Low left	50%	±4.58%	81%	±3.46%	55%	±4.73%	88%	±4.35%
Top right	42%	±8.39%	62%	±6.56%	63%	±7.02%	72%	±7.64%
Middle right	24%	±6.00%	38%	±9.07%	45%	±13.80%	50%	±9.29%
Low right	24%	±10.22%	34%	±15.50%	32%	±10.41%	38%	±17.50%

Table 4.4. Experimental result of PPHSER on the platform of MATLAB

Location	DRA, m (normal)	DRA, std (normal)	AWBA, m (normal)	AWBA, std (normal)	DRA, m (holding)	DRA, std (holding)	AWBA, m (holding)	AWBA, std (holding)
Top left	72%	±3.51%	74%	±2.65%	84%	±3.61%	91%	±3.79%
Middle left	60%	±7.51%	77%	±7.77%	73%	±5.00%	84%	±3.61%
Low left	53%	±6.24%	83%	±4.16%	60%	±5.00%	90%	±2.65%
Top right	44%	±7.81%	64%	±6.11%	68%	±8.50%	75%	±7.51%
Middle right	26%	±6.03%	40%	±8.89%	50%	±11.36%	58%	±7.57%
Low right	27%	±10.41%	36%	±16.29%	37%	±8.62%	44%	±17.01%

Table 4.5. Experimental result of CC on the platform of MATLAB in holding breath

Location	DRA, m	DRA, std	AWBA, m	AWBA, std
Top left	0.88	±0.032	0.91	±0.033
Middle left	0.82	±0.041	0.83	±0.038
Low left	0.76	±0.031	0.90	±0.032
Top right	0.75	±0.051	0.79	±0.067
Middle right	0.64	±0.062	0.69	±0.1
Low right	0.49	±0.071	0.56	±0.09

Also, according to Table 4.3, Table 4.4, and Table 4.5, all results are summarized in Figure 4.35, Figure 4.36 and Figure 4.37.

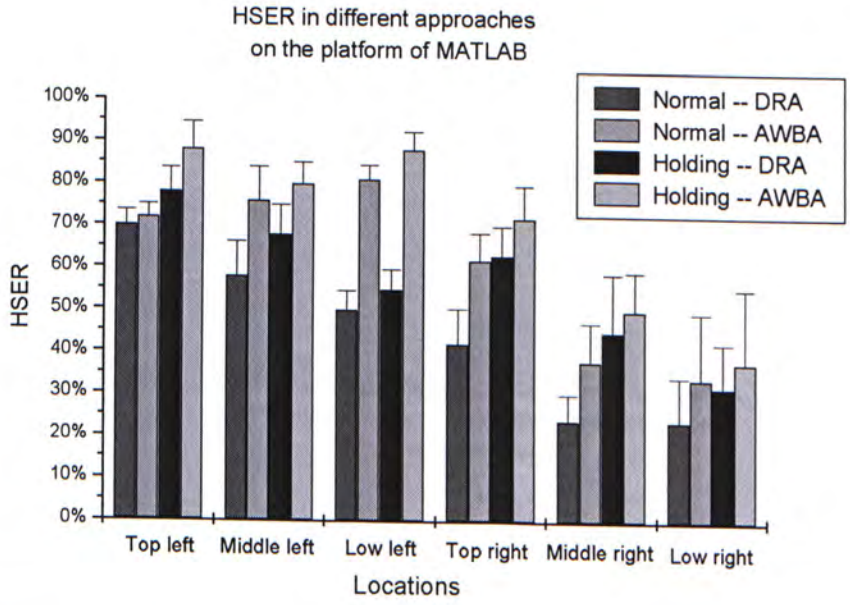

Fig. 4.35. Experimental result of HSER on the platform of MATLAB

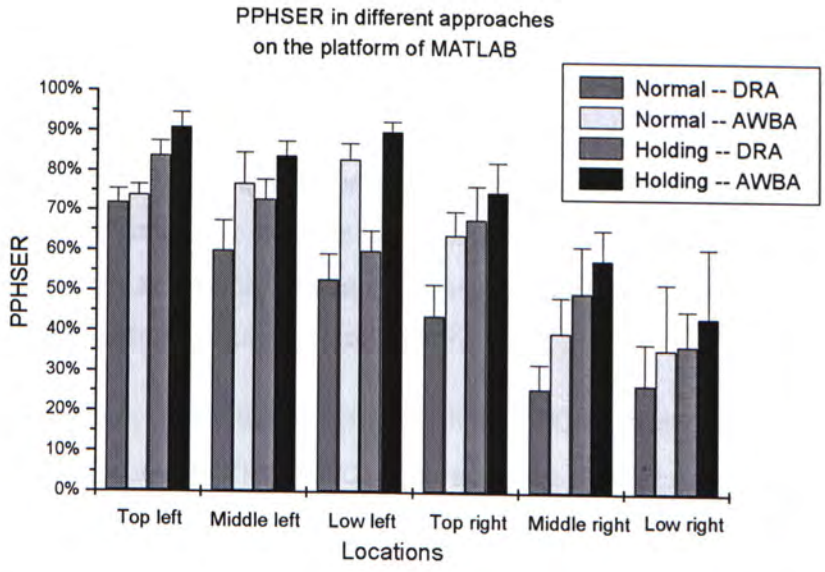

Fig. 4.36. Experimental result of PPHSER on the platform of MATLAB

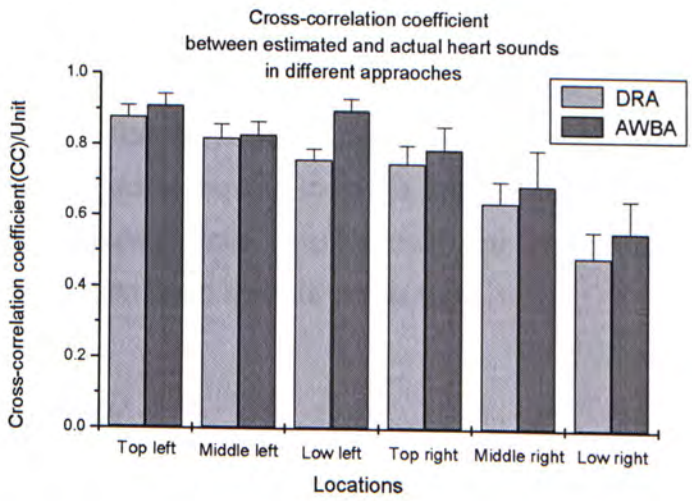

Fig. 4.37. Experimental result of CC on the platform of MATLAB in holding breath

According to those comparison charts, we believe that the overall performance of AWBA approach is better than the result of using DRA approach. A higher correlation coefficient in AWBA implies a better heart sound estimation from adaptive filtering. As a result, lung sounds with less distortion are estimated by using AWBA approach. However, an unsatisfactory heart sounds reduction in right chest urges us to develop another advanced algorithm, which is discussed in the following section.

4.4 Online Processing

Offline adaptive canceling the heart sounds from lung sound recordings are discussed in the section 4.3. Satisfactory result indicates that an adaptive algorithm is a suitable method to reduce heart sounds intelligently. For backend signal analysis, offline adaptive algorithm is enough. However, physicians will not like to analyze the patients' acoustic sounds in one day after. They need real time diagnosis. Thus, a new approach, online processing, has been developed to cancel the heart sounds immediately during auscultation.

For adaptive filter calculation consideration, 100ns multiplying duration in microprocessor is assumed. The 1000 taps adaptive filter totally needs 100μs (100ns × 1000) in each sample. By 3000Hz sampling frequency, the processing time is 0.3s in one-second signal. It is enough for real time auscultation. Besides, we want to implement all the circuit, calculation, and algorithm in an integrated platform. Thus, a signal processing program, named LABVIEW, will be a central platform to implement our heart sounds reduction algorithm.

In this sub-section, a program structure and data flow of LABVIEW program we constructed are discussed. A new approach, automated gain control (AGC) algorithm, will be explained on how to increase the heart sounds reduction in right chest. Finally, related experimental result shows that this central platform has a satisfactory result to reduce heart sounds in real time.

4.4.1 LABVIEW

LABVIEW is a program development environment, much like modern C or BASIC development environments. However, LABVIEW is different from those applications in one important aspect. Other programming systems use text-based languages to create lines of code, while LABVIEW uses a graphical programming language, G, to create programs in block diagram form. LABVIEW includes libraries for data acquisition, data analysis, data presentation, and data storage. And, that is the main reason why we chose LABVIEW for the development tool in a central platform to acquire biosignal from signal pre-processing unit and then process it (Fig. 4.38 and Fig. 4.39). Source code is attached in the chapter of Appendix A.5.

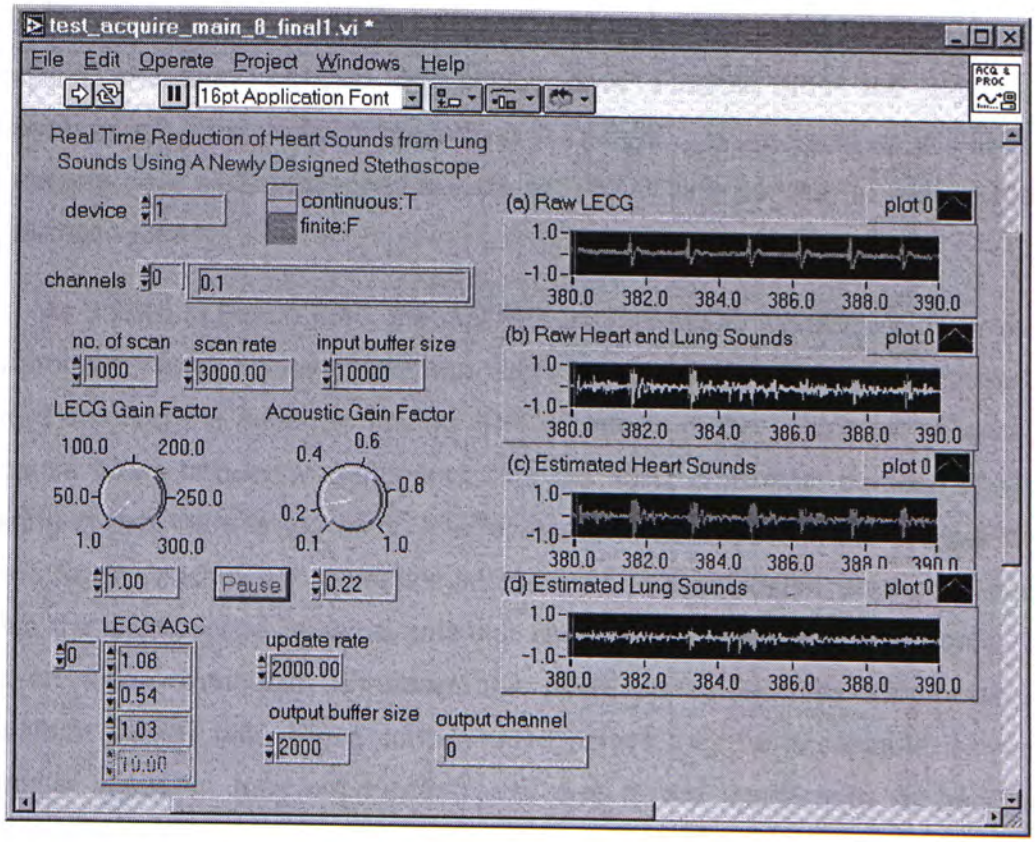

Fig. 4.38. Central platform implemented on LABVIEW display mode

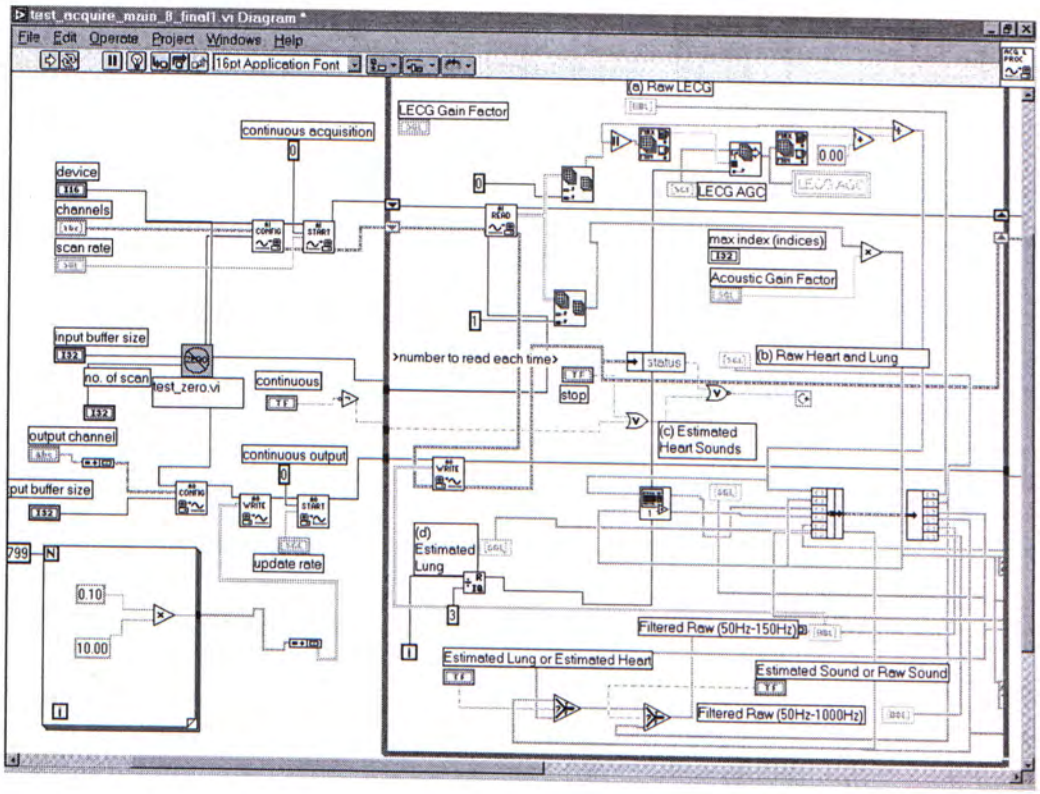

Fig. 4.39. Central platform implemented on LABVIEW circuit mode

In this real time algorithm, a LABVIEW acquisition card in 12bits at 3kHz sampling frequency digitized the analog data acquired from the signal pre-processing unit. The configuration setting in LABVIEW is the same as in WINDAQ. All sample data were processed in data set (1000 data per set) to reduce the IO initialization time.

As shown in Figure 4.40, the digitized original LECG signals are displayed at the program panel; however, they are filtered by the 40Hz 2nd order low pass filter before entering the adaptive filtering. The waveform of the LECG will be distorted because it has frequency component over the 40Hz. The main purpose of LECG filtering is that there is too much interference and harmonics in the original signal above 50Hz, which is the power line interference. In auscultation, physicians cannot press the stethoscope towards patients' chest in an absolutely even force. This uneven force distribution enhances the 50Hz artifact and its harmonics. For waveform display only, those contaminated noises may be acceptable. However, adaptive algorithm may not function well due to the interference embedded in reference signal.

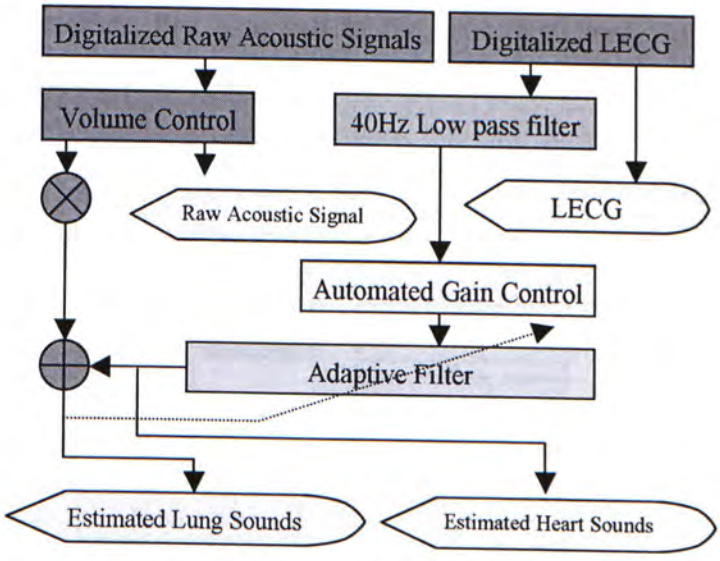

Fig. 4.40. Block diagram of the algorithm in LABVIEW

Actually, the performance of low pass filtered LECG waveform is no better than the original LECG waveform without interference. However, it is better to use a distorted LECG waveform for an adaptive reference rather than a fluctuated LECG waveform with interference.

4.4.2 Automated Gain Control

The processed LECG can be used as a reference signal in adaptive filtering method. To make estimate accurately the heart sounds, the amplitude of the LECG signals should be kept constant from beat to beat at different locations. However, the strength of LECG signal in the human body is different from the left chest to the right chest. The acquisition at the left chest may be 10 times larger than that at the right side. The fluctuated heart sounds reduction on different auscultation locations in the offline approach, in the last section, indicates the needs of a stable LECG signal.

Another problem in the LECG signal is over-amplification. It is difficult to adjust the gain factor manually in the LECG signal due to the amplitude variation in different chest locations. The over-amplified LECG signal will saturate the adaptive filter. As a result, the LMS algorithm may never converge to the minimum-mean-square error (MMSE).

Automated gain control (AGC) algorithm (Fig. 4.41) amplifies the LECG signal in different scale according to the amplitude of the signal itself. The algorithm finds a maximum value among the data set to be a denominator. To make the signal smooth, up to 3 denominators in 3 different data sets (present data set, last data set, and the data set before the last one) were founded and stored in an array. The maximum value in the denominator array was a final denominator. All data in the present data set were divided by this value.

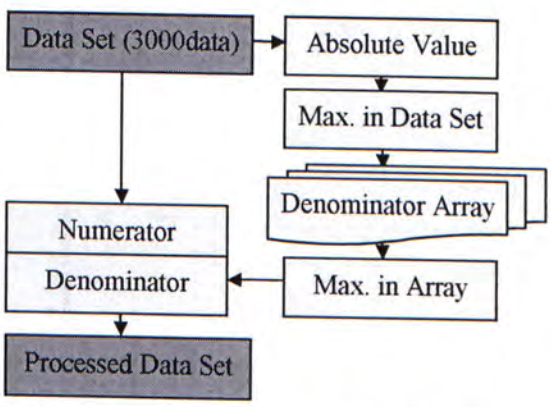

Fig. 4.41. Block diagram of automated gain control (AGC)

After the automated gain control algorithm, the data set in different auscultation locations could be adjusted to a proper amplitude level as shown in Figure 4.42 and Figure 4.43.

Fig. 4.42. Example of adjusted LECG signal at the left chest

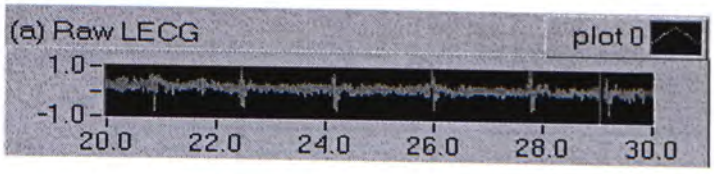

Fig. 4.43. Example of adjusted LECG signal at the right chest

4.4.3 Implementation of LMS adaptive filter

After the AGC algorithm, the main program passed the data set (1000 data) to LMS subprogram. The time-varying FIR filter of LMS algorithm has previously been introduced (please refer to the section of 4.2). In this section, we implement that in LABVIEW program as shown in Figure 4.44 and Figure 4.45 [10]; all variable are defined the same as the equations (4.4) and (4.5).

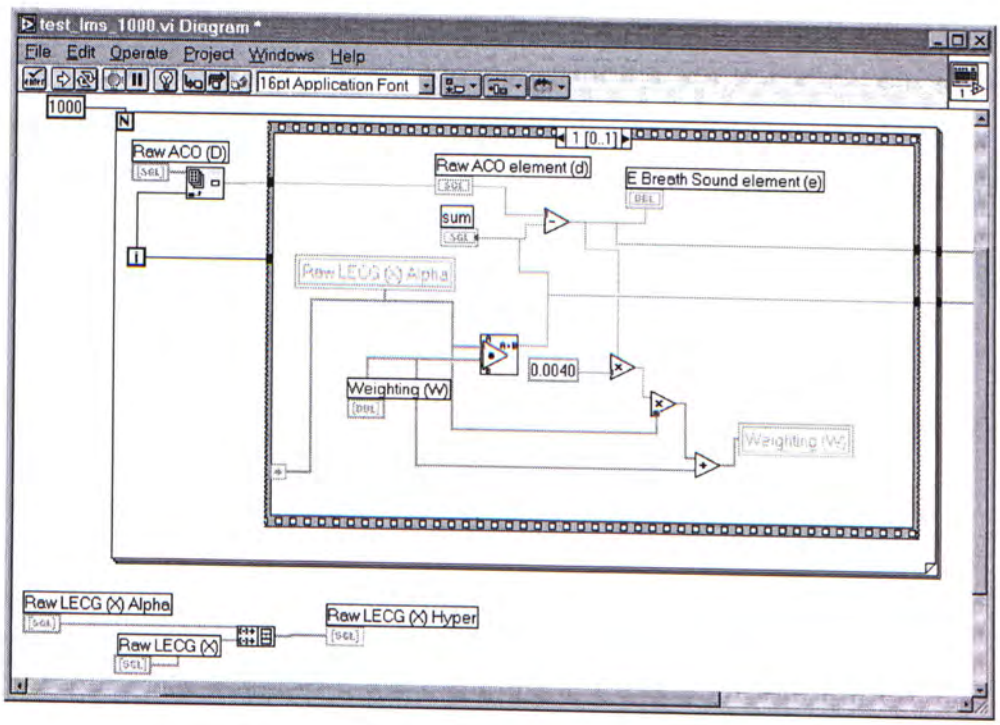

Fig. 4.44. LMS algorithm implemented on LABVIEW circuit mode

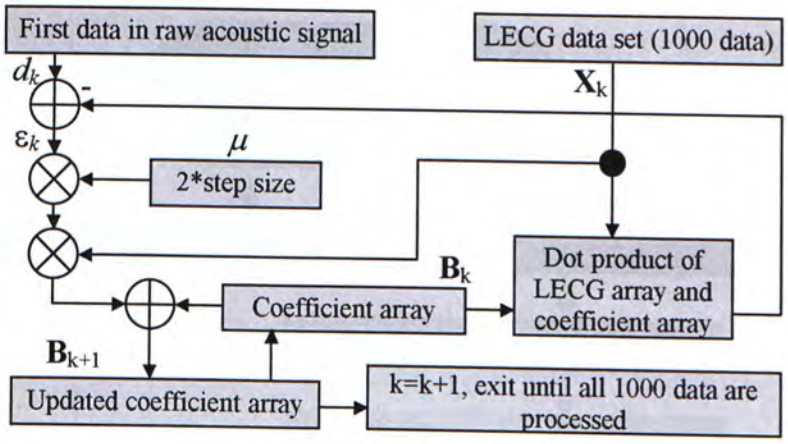

Fig. 4.45. LMS data flow diagram

According to Figure 4.45, the dot product of LECG array and coefficient array, $\mathbf{X}_k^T \bullet \mathbf{B}_k$, form a single value. The difference between *d* and this single value is an error signal ε_k, which realizes the equation (4.5). The sum of error signal ε_k, unit step size μ, and previous coefficient array $\mathbf{B}_k$, is the updated coefficient array $\mathbf{B}_{k+1}$, which fulfills the requirement of equation (4.4). The LMS loop implemented on LABVIEW processes the whole data set (1000) to calculate the estimated lung sounds ε_k and estimated heart sounds $\mathbf{X}_k^T \bullet \mathbf{B}_k$. In each loop, a parameter *k* is added by an increment of 1. LMS loop exits after the completion of both estimated lung sound data set (1000) and estimated heart sound data set (1000). After that, the LMS subprogram passes the handle back to main program to analyze another data set. An overall data flow diagram is shown in Figure 4.46.

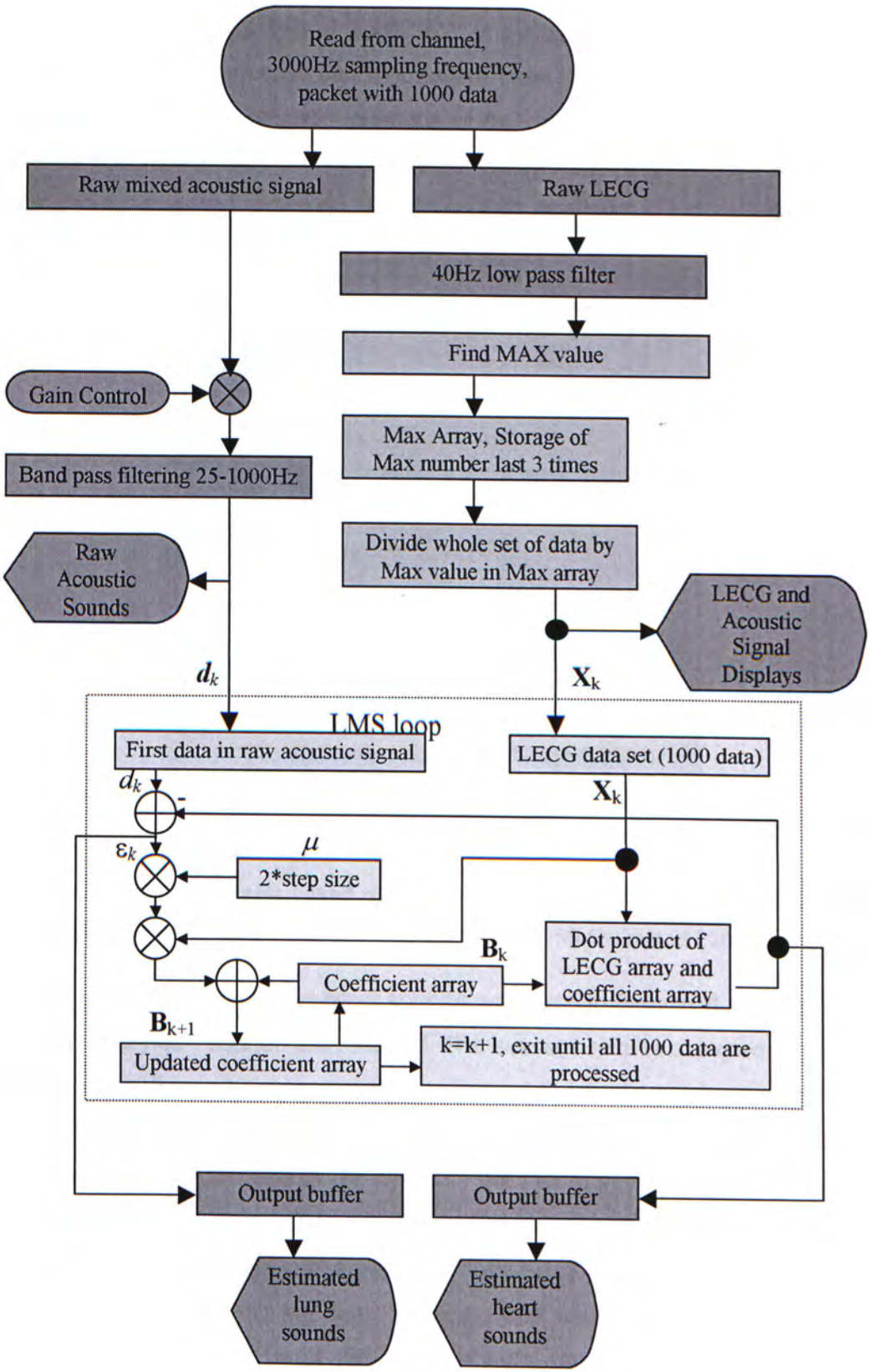

Fig. 4.46. Data operation diagram in the central platform

4.4.4 Experimental Results of Online-AGC

The configuration of LMS filter in LABVIEW is the same as DRA, a FIR filter with 1000-taps and a unit step size with 0.002 were used to cover the time separation in both sounds. Same auscultation locations of five male and healthy subjects were chosen for the experiments. Each collected signal with the length of 10 seconds was recorded to examine the reduction of heart sounds as shown in Figure 4.47.

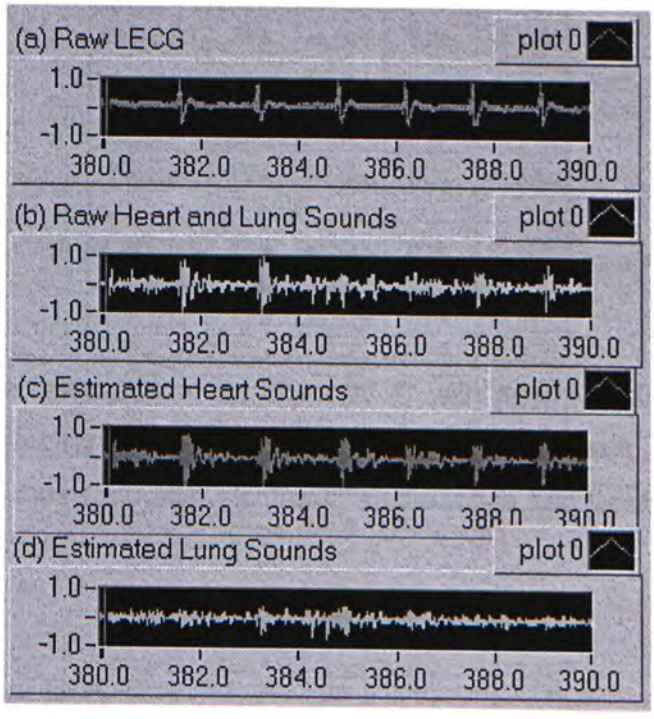

Fig. 4.47. Examples of signals based on online central platform: (a) Raw LECG, (b) Raw Heart and Lung Sounds, (c) Estimated Heart Sounds, and (d) Estimated Lung Sounds.

The estimated breath and heart sounds are given in Figures 4.47(c) and (d). It is clear that the heart sounds are reduced. The average results of experiments at six locations on the five subjects are shown in Table 4.6. Heart sound reduction is from 75% to 83%. Only about 30% reduction of heart sounds at right chest was achieved early without the AGC algorithm [9], because the LECG signal from right chest was very weak. The heart sound reduction level is now similar at different locations after introducing AGC and adaptive algorithms. Among the six testing locations, the middle right position is still the worst case in heart sounds reduction; even in this worst case, over 75% of heart artifacts reduction can be reached. The average experimental results of the five subjects under the condition of holding breath are

summarized in the same table for reference. In this case, only HSER is used for the justification because PPHSER is difficult to be implanted in on-line platform.

Table 4.6. Experimental result of HSER using online-AGC

Location	m (normal)	std (normal)	m (holding)	std (holding)
Top left	83%	±5.76%	85%	±4.74%
Middle left	78%	±9.04%	82%	±4.74%
Low left	81%	±6.50%	85%	±7.01%
Top right	78%	±4.44%	81%	±5.03%
Middle right	75%	±5.83%	80%	±3.96%
Low right	76%	±6.53%	82%	±4.88%

For real-time auscultation, an online-AGC with adaptive algorithm has been implemented for electronic stethoscopes application. As a result, a convenient and effective heart sounds reduction electronic stethoscope has been proposed in this work.

4.5 Discussion

In the section of offline processing, both HSER and PPHSER indicate that the overall performance of DRA and AWBA of subject in holding breath is better than in breathing normally. The main reason is that lung sounds present the error signal in heart sound estimation when the subject breathing normally. However, in holding breath, this lung artifact is minimized. Another reason is the inherent problem of heart sound energy reduction approach, both in HSER and in PPHSER. In breathing normally, lung sounds embedded in raw acoustic signal. If we use this raw acoustic signal for the reference to calculate the heart sound energy reduction, (4.7) and (4.8), an underestimated result will be obtained.

The standard deviation of HSER and PPHSER obtained in right chest is higher than in left chest on the offline platform. The primary reason is the effect of unstable LECG in right chest. Using online-AGC platform has solved this kind of problem.

The overall performance of AWBA approach is better than the result of using DRA approach. However, there are three primary disadvantages on AWBA approach. The first one is that this technique sacrifices the time for LECG peak estimation. A whole heartbeat cycle is needed to estimate the peak of LECG and then to form a window frame for reference. The duration of a whole heartbeat is around 1s, adding the duration of 1000 taps of adaptive filter, totally 1.33s delay occurs on this approach. It is not a big problem on signal play back offline analysis in computer. However, physicians do not like to listen a delayed version of lung sounds over 1 second.

The second problem is the embedded lung sounds in raw acoustic sounds. The main purpose of this thesis is proposed a new reference signal. However, lung sounds and heart sounds are mixed together in human normal breathing. Based on AWBA approach, a small portion of raw acoustic signal acts as the reference signal in adaptive filtering. If the size of window frame is too small, heart signal will be removed ineffectively even though the chance of lung signal occurring is small. However, if the size of window frame is too large, embedded lung signal in reference will distort the adaptive algorithm leading to the defeated spectrum of estimated lung sounds.

The third problem is the wrong estimation of heart peak location. Basically, AWBA should have good enough HSER in right chest due to the new reference signal. However, according to Figure 4.35, the overall performance of HSER by using AWBA is around 45% only, slightly better than by using DRA. The main reason is the wrong estimation of heart peak location due to the relatively weak LECG signal on right chest.

A new parameter, cross-correlation coefficient (CC) value is chosen for another indicator. A comparison of CC value of actual heart sounds and estimated heart sounds between DRA and AWBA in holding breath indicates an advantage of AWBA approach. However, it is difficult to acquire pure lung sounds because of the non-stop heartbeat. A comparison of CC value between pure lung sounds and estimated lung sounds among different approaches becomes impossible.

Even for this reason, in other previous works [2], [4], [5], HSER was used to evaluate the performance of their approaches. Thus, we used this scheme to compare those approaches with ours. In this chapter, totally three approaches (two

offline and one online) are evaluated and tested. In this section, a comparison of HSER among three approaches together with previous other works (refer to the section of introduction) are summarized Figure 4.48, and Figure 4.49. The overall performance of heart sounds reduction using LECG approach with online-AGC is similar as using forth-order statistics approach; however, less calculation is required.

Actually, based on HSER comparison and computation power consideration, on-line AGC is the most suitable approach to reduce unwanted heart sounds from lung sounds. However, all parameters we used in online-AGC were basically used in DRA. Thus, a further analysis of online-AGC is needed.

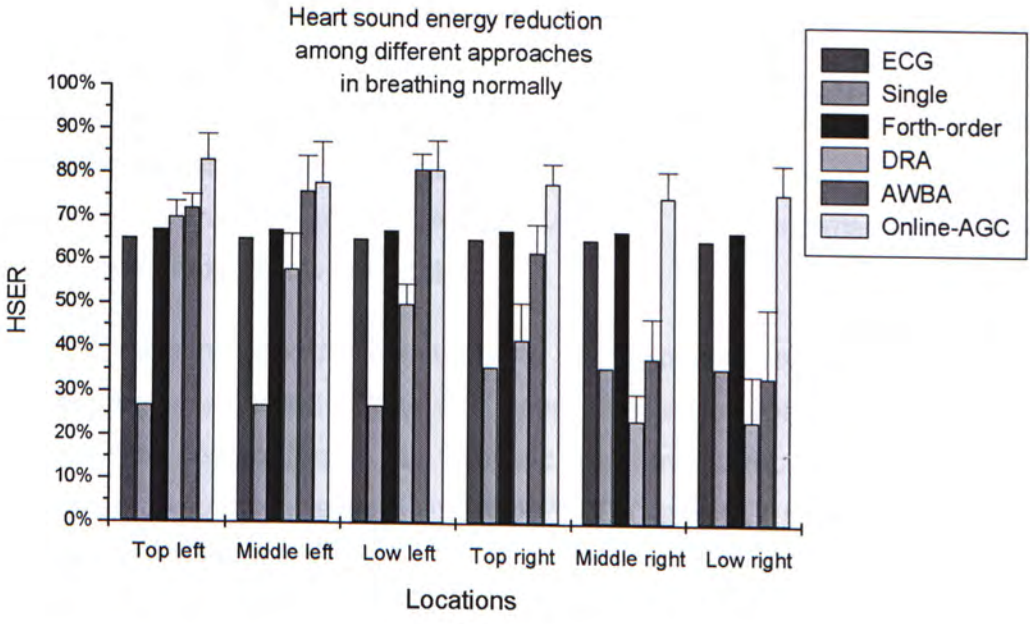

Fig. 4.48. Comparison among different approaches in breathing normally

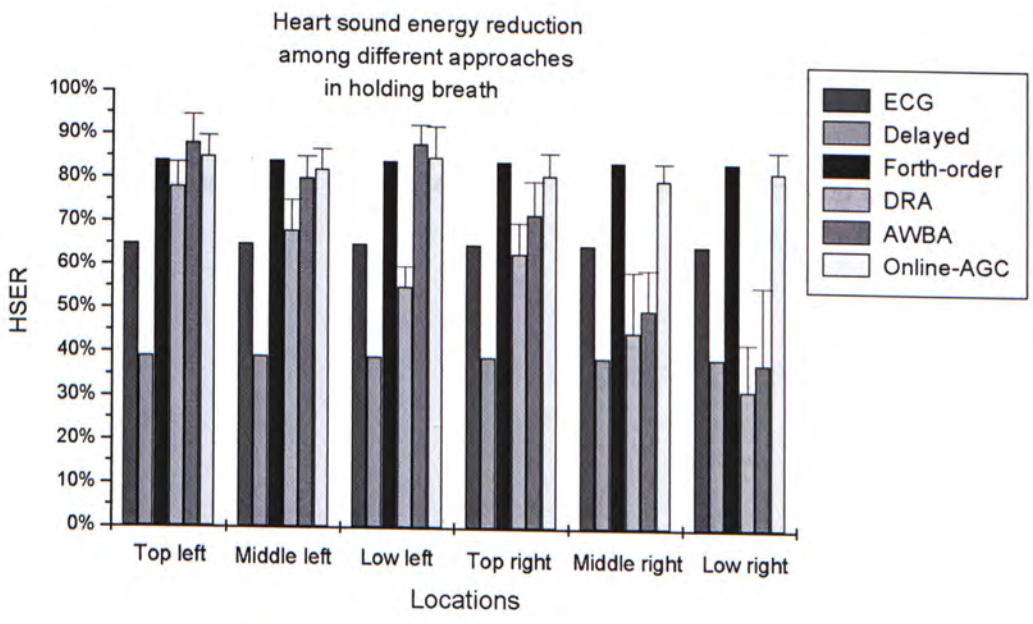

Fig. 4.49. Comparison among different approaches in holding breath

4.6 Section Summary

In this chapter, a brief history of development in adaptive filtering to remove heart sounds from lung sounds has been introduced. After introducing the principle of adaptive filtering signal enhancement system and determination of adaptive parameters including unit step size and filter length, DRA approach has been developed on the platform of WINDAQ and MATLAB. The performance shows that the heart sound reduction is acceptable.

To minimize the distortion effect on lung sound spectrum after adaptive filtering, a new approach, so-called AWBA has been invented to set a window frame to capture a small portion data in raw acoustic waveform to rebuild a new reference signal. Three comparison factors, HSER, PPHSER, and CC, have been examined to compare the correlation between the recorded heart sounds in holding breath and estimated heart sounds. A higher CC value of AWBA implies a satisfactory result in this algorithm to minimize the adaptive noise.

After that, an online central platform, on LABVIEW, has been developed to process all signals come from signal pre-processing unit in real time. A new approach, named AGC, has been invented to condition the amplitude of LECG signal automatically. A satisfactory result in right chest heart sound reduction indicates the success of this approach. Finally, after comparison among different approaches with other researches, it is concluded that the online-AGC approach is the most suitable approach to reduce heart sounds from lung sound recordings.

References

[1] B. Widrow, J. R. Glover, J. M. McGool, J. Kaunitz, C. S. Williams, R. H. Hearn, J. R. Zeidler, E. Dong, and R. C. Goodlin, "Adaptive Noise Canceling: Principles and Applications," in Proc. IEEE, 1692-716, 1975.

[2] V. K. IYER, P. A. Ramamoorthy, H. Fan, and Y. Ploysongsang, "Reduction of Heart Sounds from Lung Sounds by Adaptive Filtering," *IEEE Trans. on BME*, vol. 33, pp. 1141-8, 1986.

[3] Y. Ploysongsang, V. K. Iyer, and P. A. Ramamoorthy, "Characteristics of normal lung sounds after adaptive filtering," *Amer. Rev. Respir. Dis.*, pp. 951-6, 1989.

[4] M. Kompis and E. Russi, "Adaptive Heart-noise Reduction of Lung Sounds Recorded by a Single Microhphone," in Proc. 14th Annu. Int. Conf. IEEE. Eng. Med. Biol. Soc., 691-2, 1992.

[5] L. J. Hadjileontiadis and S. M. Panas, "Adaptive Reduction of Heart Sounds from Lung Sounds Using Fourth-Order Statistics," *IEEE Trans. on BME*, vol. 44, pp. 642-8, 1997.

[6] P. S. R. Diniz, "Introduction to Adaptive Filtering," in *Adaptive Filtering, Algorithms and Practical Implementation*. London: Lluwer Academic, 1997.

[7] P. S. R. Diniz, "The Least-Mean-Square (LMS) Algorithm," in *Adaptive Filtering, Algorithms and Practical Implementation*. London: Lluwer Academic, 1997, pp. 71-4.

[8] S. B. Patel, T. F. Callahan, M. G. Callahan, J. T. Johnes, G. P. Graber, K. S. Foster, K. Glifort, and G. R. Wodicka, "An adaptive noise reduction stethoscope for auscultation in high noise," *the Acoustical Society of America*, vol. 103, pp. 2483-91, 1998.

[9] L. Yip and Y. T. Zhang, "Real-Time Adaptive Reduction of Heart Sounds from Lung Recordings Using a New Electronic Stethoscope," in Proc. IEEE-EMBS, APBME, 2000.

[10] P. M. Embree and D. Danieli, "Digital Signal Processing Fundamentals," in *C++ Algorithms for Digital Signal Processing*. London: Prentice-Hall International (UK) Limited, 1999.

Chapter 5

Conclusion and Further Development

5.1 Conclusion of the Main Contribution

- **A New Scheme:** Based on the adverse effect of contaminated heart sounds in lung sound recordings, a heart sound reduction scheme is needed to depress such kind of noise. An unsatisfactory result in past studies is the motivation to urge us to develop a new advanced scheme. In this thesis, an adaptive filtering scheme with the reference signal of LECG has been developed. Two approaches DRA and AWBA have been designed in offline platform for preliminary analysis. Meanwhile, an optimum unit step size and a suitable filter length have been determined. However, unsatisfactory results in heart sound reduction at right chest compared with a previous forth-order statistics approach indicated the need of further improvement of LECG approach. Therefore, a new concept, online-AGC, has been invented and implemented on the LABVIEW platform to adjust the amplitude of LECG signal automatically. Finally, a new approach has been developed to reduce heart sounds from lung sound recordings not only in offline processing, but also in real time.

- **Comparison among different approaches:** A pure lung signal is difficult to be collected due to the co-existence of non-stop heartbeat. Direct approach to evaluate heart sound reduction becomes impossible. In this thesis, three indirect approaches: HSER, PPHSER, and cross-correlation coefficient (CC) have been introduced to evaluate the performance of these schemes indirectly. When we compare those results, it is not too difficult to observe that the performance of online-AGC is comparable with a forth-order

statistics approach. However, as mentioned before, a fewer calculation step in adaptive filtering in the new approach compared to the forth-order approach indicates that our new scheme is a preferable method for heart sounds reduction in real time.

- **A New Electronic Stethoscope:** A newly designed stethoscope's head comprising of original stethoscope's head, conductive rubber, acoustic-electric transducer, and silver epoxy has been developed and tested to successfully acquire both electronic LECG signal and raw acoustic signal. Then, a signal pre-processing unit processed collected raw signals before entering a central platform. Thus, lung sounds, from which over 75% of the heart sounds have been eliminated, are calculated. Three these modules, including the newly designed stethoscope's head, the signal pre-processing unit, and the central platform unit have formed a new integrated device (Fig. 5.1) to help physicians in auscultation diagnosis. The new electronic stethoscope has similar acoustic performance compared with the market product, named SimulScope. Moreover, we have proved that the new product has high quality of heart sound energy reduction. Therefore, a new electronic stethoscope scheme, including the function of better lung sound quality, acoustic waveform display (on LABVIEW), and LECG display (on LABVIEW) has been developed.

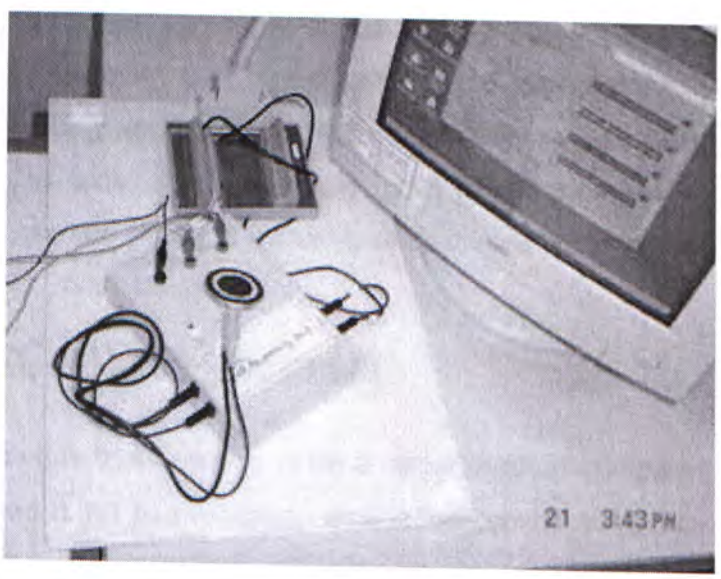

Fig. 5.1. Hardware of new electronic stethoscope

5.2 Future Works

5.2.1 Modification of the Head of Stethoscope

LECG signal is difficult to collect stably due to the interference of power line and the uneven pressing force towards patient's chest. Even if some schemes were used to accommodate such problem, such as AGC and 40Hz low pass filter, the quality of LECG is still not good enough. Thus, it is suggested to mount the signal pre-processing circuit behind the head of stethoscope. The effect of interference of power line will be minimized. Moreover, a 100MΩ input impedance, or above, circuit is suggested to pre-process LECG signal in order to reduce the motion artifact. All these methods are aimed to achieve the stable LECG signal.

5.2.2 Validation of Abnormal Breath

The new algorithm will be tested in subject breathing abnormally, such as "deep breathing" and "relaxation". Patients with heart diseases or pulmonary disorders will be examined by using the new electronic stethoscope to test its performance.

5.2.3 Low Frequency Analysis

Sub-audio frequency, below 25Hz, in acoustic signal had not drawn much interest in past researches. However, such signal can be analyzed in computer by visualized waveform. There may exist pathological information in sub-audio signal that we haven't known. In order to convert sub-audio frequency from acoustic signal to electrical signal, a more powerful acoustic-electric transducer is needed.

5.2.4 AGC-AWBA Approach

AWBA approach has been proved to be a better method compared with DRA. The problem of wrong heart peak location estimation can be solved by AGC algorithm mentioned in the online-platform. Finally, an advanced algorithm is needed to reduce the heart peak searching time.

5.2.5 Standalone Device

In this thesis, a central platform of adaptive filtering has been built on the platform of LABVIEW. For further development, a central processing unit will be built in a micro-controller device (MCU) rather than in the platform of LABVIEW to form a standalone device. Several features will be added to make it more powerful.

a) Adjustable Volume Control

An electronic circuit consisting of an operational amplifier and several passive components will be designed to control volume with the adjustable gain from 1 to 10.

b) Diaphragm Mode Control

Different from mechanical stethoscope, electronic stethoscope can be calibrated to amplify signals within a certain frequency range. The new design will modify the stethoscope's head that has one diaphragm channel only. The diaphragm can act in the bell mode or the diaphragm mode. With the new stethoscope, the user could simply press one button to switch the operation mode.

c) LCD Panel

A LCD display allows the user to see the features extracted from bio-acoustic signals.

d) Wireless Transmission

Wireless transmission between the stethoscope's head and headpieces [1] will allow several users to examine the same patient at the same time, which is not possible in the conventional mechanical stethoscope. This function is very useful for training and for INTERNET applications.

e) Slow Play-Back

This function allows the user to re-exam patients with either the normal speed or a slow speed of the play-back.

f) Computer Interface

Communication between the stethoscope and Personal Computer (PC) becomes an important issue in telemedicine [2], [3]. Software development tools in PC can store the patient's record for advanced feature extraction and auto-diagnosis [4].

g) Pre-diagnosis Algorithm

After digitalizing the patient's signals, certain feature extraction and medical expert algorithm can be built in the device for pre-diagnosis [5], [6], [7].

h) Conclusion

As a result, an acoustic-sensor-based wireless multifunction stethoscope is proposed. A hardware block diagram of the proposed micro-controller based system is shown in Figure 5.2:

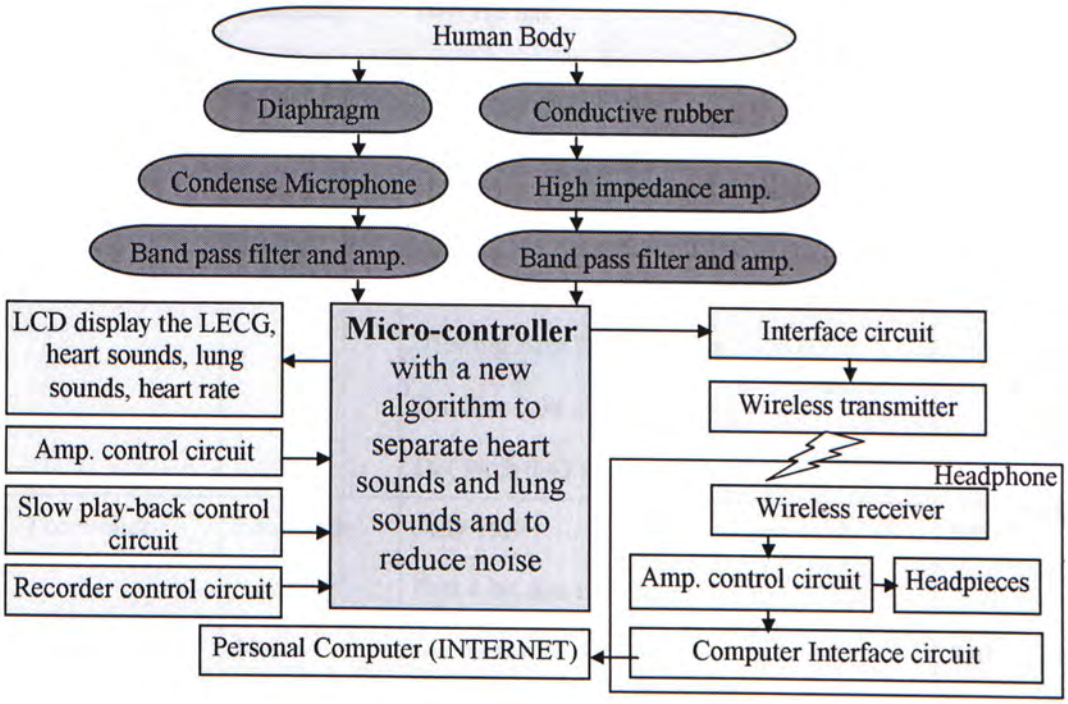

Fig. 5.2. Hardware block diagram

The estimated cost of the hardware standalone system is given in Table 5.1.

Table 5.1. The cost estimation of a hardware standalone system

Devices	**Company**	**Description**	**Unit Price $(HK)**
Micro-controller Unit (MCU)	Texas Instrument	TMS320VC5416 160 64k on boards RAM 32k on boards ROM	$195
Dots LCD module	Data Modul	BT 100032 Viewing Area 46 × 18.4 mm Dot Size 0.38 × 0.43 mm Dot Pitch 0.43 × 0.48 mm	$110
LCD controller	Data Modul	SED 1520 Fast 8-bit data interface	$40
RS232	Max	Interface with computer	$10
Wireless Devices	Bluetooth	Spread spectrum scheme with hoping frequency PS: $20 HK in the 2 year later	$100
Development System	**Company**	**Description**	**Unit Price $(HK)**
MCU Development Kit	Texas Instrument	TMS320C5416 evaluation module	$31000
Bluetooth Development Kit	Ericsson	Development bundle	$100000

The software block diagram in Figure 5.3 describes the data flow and operation in the Micro-controller (MCU).

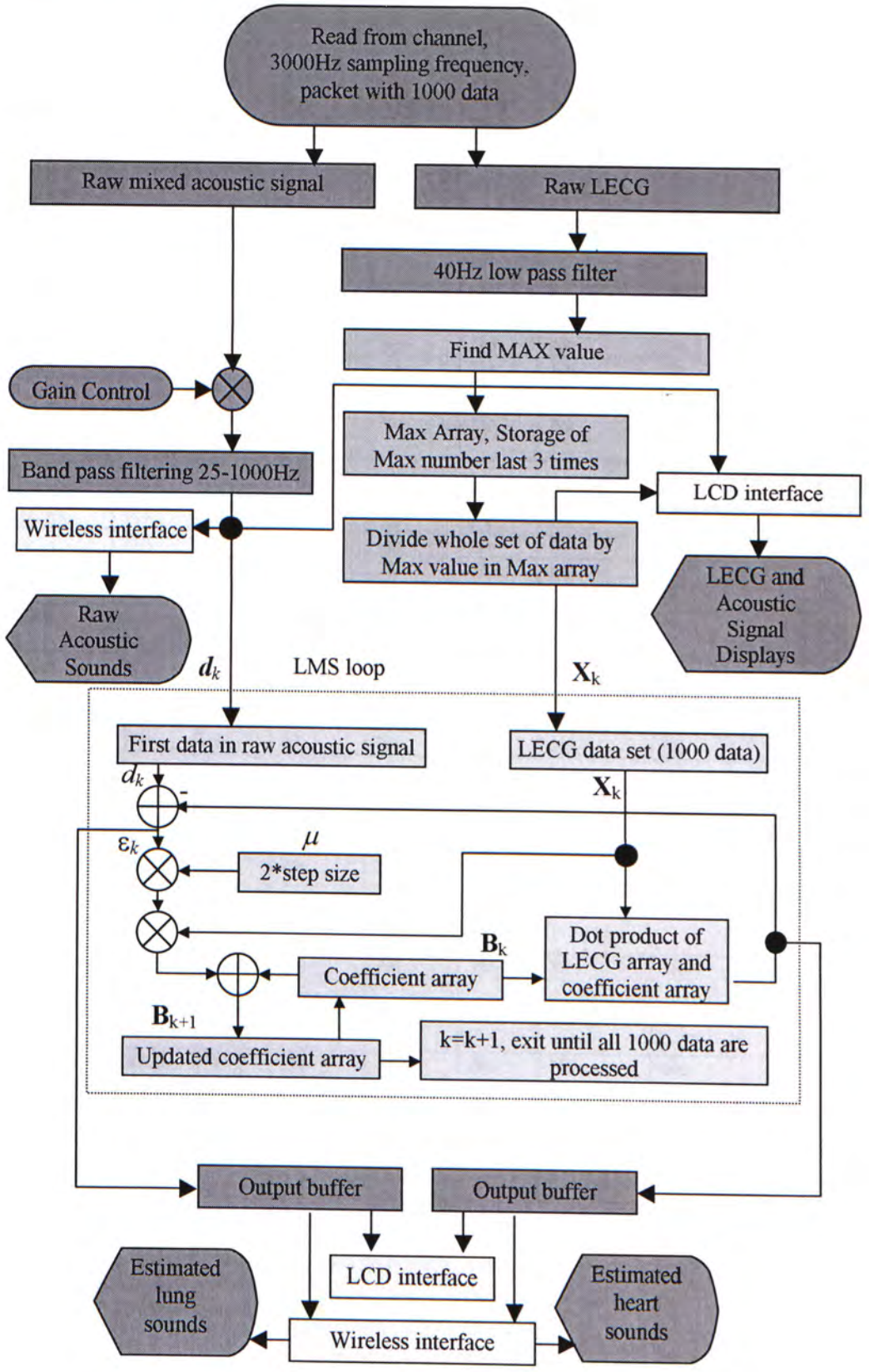

Fig. 5.3. Proposed data operation in the micro-controller (MCU)

A comparison among different stethoscopes on the market is summarized in Table 5.2.

Table 5.2. Comparison among typical stethoscopes

Items	Freq. Range (Hz)	Amp. 1	Wire-less Option 2	LCD Display 3	Slow Play Back 4	Auto-mated Gain Control 5	Reduction of Heart sounds and Lung sounds	Price in HK$
Monaural Stethoscope								
Laennec's	NA	No	No	No	No	No	No	NA
2-piece monaural	NA	<1	No	No	No	No	No	NA
Ebony stethoscope	NA	<1	No	No	No	No	No	NA
Ebony 2-piece	NA	<1	No	No	No	No	No	NA
Aluminum	NA	<1	No	No	No	No	No	NA
Three pieces	NA	<1	No	No	No	No	No	NA
French monaural	NA	<1	No	No	No	No	No	NA
Binaural Stethoscope								
Cammann's	NA	<1	No	No	No	No	No	NA
Davis's	NA	<1	No	No	No	No	No	NA
Ford's Bell	NA	<1	No	No	No	No	No	NA
SHEPPARD'S	NA	<1	No	No	No	No	No	NA
LYNCH'S model	NA	<1	No	No	No	No	No	NA
Jefferson's model	NA	<1	No	No	No	No	No	NA
G. Pilling	NA	1	No	No	No	No	No	NA
Rieger-Bowles	NA	1	No	No	No	No	No	NA
Mechanical Stethoscope								
Master Cardiology	30-1k	1	No	No	No	No	No	$1520
Welch Allyn Tycos	30-1k	1	No	No	No	No	No	$1210
Electronic Stethoscope								
Hewlett-Packard	45-20k	1~14	No	No	No	**Yes**	No	$2100
Welch Analyzer	30-1k	1~5	No	No	No	No	No	$3510
Welch Distributor	30-1k	1~5	No	No	No	No	No	$3900
SimulScope	30-2k	1~5	**Yes**	No	No	No	No	$31200
Wireless Multifunction Stethoscope	25-1k	1~10	**Yes**	**Yes**	**Yes**	**Yes**	**Yes**	$4000 Estimated

1 Amplification level of acoustic signal compared to neutral diaphragm amplification
2 Wireless transmission between the stethoscope's head and the stethoscope's body
3 Standalone LCD display the signal waveform graphically
4 Replay the signal in slow playing format
5 Adjust the signal volume automatically to prevent saturation

5.2.6 Demand on Stethoscope

As mentioned previously, auscultation is normally the first step for physicians to check patients' status especially for diseases related to heart and the respiratory systems. It is no doubt that every physician (Table 5.3) should have at least one stethoscope. There is always a demand for stethoscope because clinicians have to replace the old with a new one every now and then. Besides, hundreds of thousands of medical graduates enter the profession every year around the world, which implies stethoscope is in great demand.

Table 5.3. Number of physician and registered nurse in China and the USA

	China*	USA**
Number of physician	1.4 millions	0.6 millions
Number of registered nurse	1.0 million	1.9 millions

* Estimated based on the information on web page www.chinatoday.com [8]

** From the United States census report 1990 [9]

Assuming that clinicians replace their stethoscopes within 5 years, based on the above figures, demand on stethoscope in both countries will reach almost 1 million units per year. Clearly, stethoscope is indispensable in the medical field.

Stethoscope is a useful device for clinician. However, if it becomes accepted as a home care device, we can imagine the market will grow even bigger. The new stethoscope system could transmit the data from the stethoscope's head to the clinician's office through the INTERNET. Under an interactive computer program, a remote diagnosis will be possible through standard telephone network.

The total population in China and the USA are around 1500 millions in 2001. Assuming that there are totally 500 millions families in the world, the demand for new stethoscope system is around 50 millions if one out of ten families buys the device for home care and telemedicine. Assuming that the device is durable for five years, the demand for new stethoscope will be 10 millions per year for home health care applications.

References

[1] B. Hok, V. Bythell, and M. Bengtsson, "Development of a wireless stethoscope for auscultatory monitoring during anaesthesia," *Med. & Biol. Eng. & Comput.*, vol. 26, pp. 317-20, 1988.

[2] H. Murakami, K. Shimizu, K. Yamamoto, T. Mikami, N. Hoshimiya, and K. Kondo, "Telemidicine Using Mobile Sateliite Communication," *IEEE Trans. on BME*, vol. 41, pp. 1994, 1994.

[3] G. Williams, P. J. King, A. M. Capper, K. Doughty, H. Boom, C. Robinson, W. Rutten, M. Neuman, and H. Wijkstra, "The Electronic Doctor (TED)-a home telecare system," in Proc. 18th Annu. Int. Conf. IEEE. EMBS., NY, USA., 53-4, 1996.

[4] L. J. Hadjileontiadis and S. M.Panas, "Separation of Discontinuous Adventitious Sounds from Vesicular Sounds Using a Wavelet-Based Filter," *IEEE Trans. on BME*, vol. 44, pp. 1269-81, 1997.

[5] M. Ono, K. Arakawa, M. Mori, T. Sugimoto, and H. Harashima, "Separation of Fine Crackles from Vesicular Sounds by a Nonlinear Digital Filter," *IEEE Trans. on BME*, vol. 36, pp. 286-91, 1989.

[6] K. E. Forkheim, D. Scuse, and H. Pasterkamp, "A Comparison of Neural Network Models for Wheeze Detection," in Proc. IEEE WESCANES, pp. 214-9, 1995.

[7] R. Grieve, P. A. Parker, B. Hudgins, and K. Englehart, "Nonlinear Adaptive Filtering of Stimulus Artifact," *IEEE Trans. on BME*, vol. 47, pp. 389-95, 2000.

[8] China Today home page, "http://www.chinatoday.com"

[9] United States census report, 1990.

Appendix

A.1 Determination of parameters in VCVS High Pass Filter

Voltage control voltage source high pass filter employs the infinite gain VCVS concept associated with the operational amplifier and the circuit offers external gain adjustment via components R_4 and R_3. This type of filter structure, employing the non-inverting (positive gain) operational amplifier, exhibits a high Q-factor sensitivity with the circuit gain *K*:

$$K = 1 + (R_4 / R_3) \tag{A.1.1}$$

Because of this high sensitivity, the configuration is restricted to low Q and low gain values with a trade-off being a wide frequency bandwidth. The filter transfer functions are summarized in the following equations:

$$\frac{V_0}{V_i}(j\omega) = \frac{-\omega^2 C_1 C_2 (1 + R_4 / R_3)}{\left(j\omega C_2 + \frac{1}{R_1}\right)\left(j\omega C_1 + j\omega C_2 + \frac{1}{R_2}\right) + \omega^2 C_2^2 - \frac{j\omega C_2}{R_2}\left(1 + \frac{R_4}{R_3}\right)}$$

which on simplification becomes

$$\frac{V_0}{V_i}(j\omega) = \frac{-\omega^2 K}{-\omega^2 + j\omega\left(\frac{1}{C_1 R_1} + \frac{1}{C_2 R_1} + \frac{(1-K)}{C_1 R_2}\right) + \frac{1}{C_1 C_2 R_1 R_2}} \tag{A.1.2}$$

Then, we may obtain the standard form for a second-order low-pass filter:

$$\frac{V_0}{V_i}(j\omega) = \frac{-\omega^2 K}{-\omega^2 + j\omega\omega_0 B_1 + B_0 \omega_0^2} \tag{A.1.3}$$

where ω_0 is the cutoff frequency for the Butterworth filter, B_0 and B_1 are the high pass coefficients, noting that

$$B_0\omega_0^2 = \frac{1}{C_1C_2R_1R_2} \tag{A.1.4}$$

$$B_1\omega_0 = \frac{(1-K)}{C_1R_2} + \frac{1}{C_1R_1} + \frac{1}{C_2R_1} \tag{A.1.5}$$

For the normalization of ω_0, C_1, and C_2, $\omega_0 = 1$ rad/s, $C_1 = C_2 = 1$F, Therefore,

$$B_0 = \frac{1}{R_1R_2} \tag{A.1.6}$$

$$B_1 = \frac{(1-K)}{R_2} + 2B_0R_2 \tag{A.1.7}$$

from which is obtained

$$R_2 = \frac{\left[-B_1 \pm \left(B_1^2 - 8B_0(1-K)\right)^{0.5}\right]}{4B_0} \tag{A.1.8}$$

In the signal pre-processing unit, two VCVS high pass filters are used to filter out the low frequency background noise in LECG signal and raw acoustic signal separately. High pass cutoff frequency ω_0 are set to 5Hz in LECG and 25Hz in raw mixed sounds with both voltage gain factors of 2.

In the case of LECG amplification, by the above requirement, the value of all resistors and capacitors are decided. Considering the calculation, the value of C_1 and C_2 are pre-determined firstly. A good choice of capacitors value is made using the formula $C \leq (10/f_0)\mu F$. Here $f_0 = 5$Hz giving C_1 and $C_2 \leq 2\mu F$. In this case, the proper capacitors $2\mu F$ are used. The value of Butterworth coefficients for second order filter B_0 and B_1 are 1 and 0.707 separately, hence (by equation (A.1.8))

$$R_2 = \frac{\left[-0.707 \pm \left((0.707)^2 - 8(1-2)\right)^{0.5}\right]}{4}$$

$R_2 = 0.552$ (neglect the negative one)

$$R_1 = \frac{1}{b_0R_2} = 1.812$$

The values of the gain resistors R_3 and R_4 are decided for the good circuit design condition of minimum dc offset. However, these values are not unique. In this case, we choose

$$R_3 = R_4 = 2\times(R_1 + R_2) = 2\times(1.812 + 0.552) = 4.728$$

Scaling factors:

$$k_f = \frac{\omega_0}{\omega_n} = \frac{2\pi \times 5}{1} = 10\pi$$

$$k_m k_f = \frac{C_n}{C_0} \quad giving \quad k_m = \frac{1}{10\pi \times 2\times 10^{-6}} = 1.592\times 10^4$$

where k_m is the scaling factor of cutoff frequency, k_f is the scaling factor of the value of resistor, ω_n is the normalized frequency, C_n is the normalized value of the capacitor, and C_0 is the actual value of capacitor. After multiplying by the scaling factor, we obtain the scaled values in Table A.1.1:

Table A.1.1. Scaled values of component in VCVS LECG channel

Components	Calculation	Values
R_1	$1.812\times 1.592\times 10^4$	$28.85k\Omega$
R_2	$0.552\times 1.592\times 10^4$	$8.79k\Omega$
R_3	$4.728\times 1.592\times 10^4$	$75.27k\Omega$
R_4	$4.728\times 1.592\times 10^4$	$75.27k\Omega$
C_1	Nil	$2\mu F$
C_2	Nil	$2\mu F$

The value of gain factor is evaluated by the equation (A.1.1) and the above figures:

$$K = 1 + \left(\frac{R_4}{R_3}\right) = 1 + \left(\frac{75.27 \times 10^3}{75.27 \times 10^3}\right)$$

$$K = 2$$

The value of high pass filter cutoff frequency f_0 is proved by equation (A.1.4) and the above figures:

$$(2\pi f_0)^2 = \frac{1}{C_1 C_2 R_1 R_2} = \frac{1}{2 \times 10^{-6} \times 2 \times 10^{-6} \times 28.85 \times 10^3 \times 8.79 \times 10^3}$$

$$f_0 = 4.997Hz$$

In the case of raw acoustic sound channel, the calculation method is as similar as in LECG channel. However, 25Hz high pass cutoff frequency rather than 5Hz cutoff frequency is used in the circuit. The revised values including resistors, capacitors, gain factor, and cutoff frequency are listed in Table A.1.2:

Table A.1.2. Scaled values of component in VCVS raw acoustic sound channel

Components	Calculation	Values
R_1	$1.812 \times 1.592 \times 10^4$	$28.85k\Omega$
R_2	$0.552 \times 1.592 \times 10^4$	$8.79k\Omega$
R_3	$4.728 \times 1.592 \times 10^4$	$75.27k\Omega$
R_4	$4.728 \times 1.592 \times 10^4$	$75.27k\Omega$
C_1	Nil	$0.4\mu F$
C_2	Nil	$0.4\mu F$
K	Same as in LECG channel	2
f_0	Same as in LECG channel	24.956Hz

A.2 Determination of parameters in MFB Low Pass Filter

Different from the VCVS circuit, a gain factor *K* in MFB circuit is changed to

$$K = R_2 / R_1 \tag{A.2.1}$$

The transfer function of MFB filter is introduced as follows:

$$\frac{V_0}{V_i}(j\omega) = \frac{-\frac{1}{R_1 R_3}}{j\omega C_2\left(\frac{1}{R_1}+\frac{1}{R_3}+\frac{1}{R_2}+j\omega C_1\right)+\frac{1}{R_3 R_2}}$$

which after manipulation becomes

$$\frac{V_0}{V_i}(j\omega) = \frac{\frac{1}{R_1 R_3 C_1 C_2}}{-\omega^2+\frac{j\omega}{C_1}\left(\frac{1}{R_1}+\frac{1}{R_3}+\frac{1}{R_2}\right)+\frac{1}{C_1 C_2 R_3 R_2}} \tag{A.2.2}$$

Then, the second order MFB standard equation will be obtained as follows

$$\frac{V_0}{V_i}(j\omega) = \frac{-Kb_0\omega_0^2}{-\omega^2 + jb_1\omega\omega_0 + \omega_0^2} \tag{A.2.3}$$

where ω_0 is the cutoff frequency for the Butterworth filter, b_0 and b_1 are the low pass coefficients. The gain and phase responses have the same shape as for the VCVS filter but it should be noted that the MFB filter provides an extra phase shift of 180^0 because of the input signal being applied to the inverting terminal. Comparing equation (A.2.2) and equation (A.2.3) yields

$$Kb_0\omega_0^2 = \frac{1}{R_1 R_3 C_1 C_2} \tag{A.2.4}$$

$$b_0\omega_0^2 = \frac{1}{R_2 R_3 C_1 C_2} \tag{A.2.5}$$

$$b_1\omega_0 = \frac{1}{C_1}\left(\frac{1}{R_1}+\frac{1}{R_2}+\frac{1}{R_3}\right) \tag{A.2.6}$$

let ω_0 = 1 rad/s, C_1 = 1F for normalization, therefore, equations (A.2.4), (A.2.5), and (A.2.6) reduce to

$$\frac{1}{R_1} = Kb_0R_3C_2 = \frac{K}{R_2} \tag{A.2.7}$$

$$\frac{1}{R_3} = b_0R_2C_2 \tag{A.2.8}$$

$$b_1 = \left(\frac{1}{R_1}+\frac{1}{R_2}+\frac{1}{R_3}\right) \tag{A.2.9}$$

which on substituting for equation (A.2.7) and equation (A.2.8) gives the quadratic expression

$$b_0R_2^2 = \frac{b_1R_2}{C_2}+\frac{(1+K)}{C_2} = 0 \tag{A.2.10}$$

which has a solution

$$R_2 = \frac{\frac{b_1}{C_2} \pm \left(\left(\frac{b_1}{C_2}\right)^2 - \frac{4(1+K)b_0}{C_2}\right)^{0.5}}{2b_0} \tag{A.2.11}$$

For R_2 to be real and positive, the following condition for C_2 must prevail;

$$\left(\frac{b_1}{C_2}\right)^2 \geq \frac{4(1+K)b_0}{C_2}$$

$$b_1^2 \geq 4(1+K)\ C_2b_0$$

$$C_2 \leq \frac{b_1^2}{4(1+K)b_0} \tag{A.2.12}$$

In the signal pre-processing unit, two second-order MFB low pass filters are used to filter out the high frequency white noise in LECG signal and raw acoustic

signal separately. Low pass cutoff frequency ω_0 are set to 500Hz in LECG and 1kHz in raw mixed sounds with the voltage gain factors of 10 and 20 separately.

Considering the calculation in LECG channel, The value of Butterworth coefficients for second order filter b_0 and b_1 are 1 and 1.414 separately, the normalized value of C_1 = 1F and ω_0 = 1 rad/s is chosen to obtain C_2 by equation (A.2.12):

$$C_2 \leq \frac{1.414^2}{4(1+10)} = 0.045F$$

The normalized appropriate value of C_2 is chosen by 0.01F. Then, the value of R_2 can be calculated by equation (A.2.11):

$$R_2 = \frac{\frac{1.414}{0.01} \pm \left(\left(\frac{1.414}{0.01} \right)^2 - \frac{4(1+10)}{0.01} \right)^{0.5}}{2}$$

This yields R_2 = 133Ω or 8.3Ω, giving

$$R_1 = \frac{R_2}{K} = 0.83\,\Omega \text{ (neglect the larger one)}$$

$$R_3 = \frac{1}{b_0 R_2 C_2} = 12.12\,\Omega$$

Select $C_1 = \frac{10}{f_0}\mu F = \frac{10}{500} = 20nF$, the calculation of scaling factor is as follows:

$$k_f = \frac{2\pi \times 500}{1} = 1 \times 10^3 \pi$$

$$k_m = \frac{1}{1 \times 10^3 \pi \times 20 \times 10^{-9}} = 1.592 \times 10^4$$

Then, we obtain the scaled values and summarized in Table 3.3:

Table A.2.1. Scaled values of component in MFB LECG channel

Components	Calculation	Values
R_1	$0.83 \times 1.592 \times 10^4$	$13.21k\Omega$
R_2	$8.3 \times 1.592 \times 10^4$	$132.14k\Omega$
R_3	$12.12 \times 1.592 \times 10^4$	$192.95k\Omega$
C_1	Nil	$2\eta F$
C_2	$\frac{0.01}{1 \times 10^3 \pi \times 1.592 \times 10^4}$	$200\rho F$

A value of gain factor is evaluated by the equation (A.2.1) and the above figures:

$$K = \frac{R_2}{R_1} = \left(\frac{132.14 \times 10^3}{13.21 \times 10^3} \right)$$

$$K = 10$$

A value of low pass filter cutoff frequency f_0 is proved by equation (A.2.4) and the above figures:

$$(2\pi f_0)^2 = \frac{1}{C_1 C_2 R_2 R_3} = \frac{1}{20 \times 10^{-9} \times 200 \times 10^{-12} \times 132.14 \times 10^3 \times 192.95 \times 10^3}$$

$$f_0 = 498.369Hz$$

In the case of raw acoustic sounds channel, the calculation method is as similar as in LECG channel. However, 1000Hz low pass cutoff frequency rather than 500Hz cutoff frequency is used in the circuit. A gain value of 20 instead of 10 is used in sounds channel. The revised values including resistors, capacitors, gain factor, and cutoff frequency are listed in Table 3.4:

Table A.2.2. Scaled values of component in MFB raw acoustic sound channel

Components	Calculation	Values
R_1	$8.4 \times 1.592 \times 10^4$	$134.13k\Omega$
R_2	$16.85 \times 1.592 \times 10^4$	$268.25k\Omega$
R_3	$5.93 \times 1.592 \times 10^4$	$94.48k\Omega$
C_1	Nil	$10\eta F$
C_2	$\frac{0.01}{2 \times 10^3 \pi \times 1.592 \times 10^4}$	$100\rho F$
K	Same as in LECG channel	20
f_0	Same as in LECG channel	999.72Hz

A.3 Source code of DRA (MATLAB)

MATLAB Main Program

```
clear all


%File I/O
%inf column and 2 row
%the first column is acoustic
%the second column is LECG


%Deciding auscultatory location
%fid = fopen('Righlowy1.dat','r');
%fid = fopen('Righlown1.dat','r');
%fid = fopen('Righmidn1.dat','r');
%fid = fopen('Righmidy1.dat','r');
%fid = fopen('Rightopn1.dat','r');
%fid = fopen('Rightopy1.dat','r');
```

```
%fid = fopen('Lefttopy1.dat','r');

%fid = fopen('Lefttopn1.dat','r');

fid = fopen('Leftmidn1.dat','r');

%fid = fopen('Leftmidy1.dat','r');

%fid = fopen('Leftlowy1.dat','r');

%fid = fopen('Leftlown1.dat','r');


volraw = fscanf(fid,'%f',[2,inf]);


fclose(fid);

volraw = volraw';


%%normalization

%[max_num, max_index] = max (abs(volraw));

%volfirst(:,1) = volraw(:,1)/max_num(1);

%volfirst(:,2) = volraw(:,2)/max_num(2);

%%zero offset

%volfirst(:,1) = volfirst(:,1) - mean(volfirst(:,1));

%volfirst(:,2) = volfirst(:,2) - mean(volfirst(:,2));


%zero offset

volfirst(:,1) = volraw(:,1) - mean(volraw(:,1));

volfirst(:,2) = volraw(:,2) - mean(volraw(:,2));

%normalization

[max_num, max_index] = max (abs(volfirst));

volfirst(:,1) = volfirst(:,1)/max_num(1);

volfirst(:,2) = volfirst(:,2)/max_num(2);


%adding index


for i = 1:length(volfirst)

        volfirst(i,3) = i/3000;

end


%Acoustic signal
```

```
volacoustic(:,1) = volfirst(:,3);
volacoustic(:,2) = volfirst(:,1);

%LECG signal
volLECG(:,1) = volfirst(:,3);
volLECG(:,2) = volfirst(:,2);

%for neural network consideration
%net = newff([0 2;-2 2], [15,1], {'tansig', 'purelin'}, 'traingdm');
%net.trainparam.show = 100;
%net.trainparam.ir=0.01;
%net.trainparam.mc=0.5;
%net.trainparam.epochs = 20000;
%net.trainparam.goal = 1e-4;
%net = train(net,x,t);

%y = sim(net,x)
```

SIMULINK LMS Filtering

```
Model {
  Name               "lms"
  Version            3.00
  SimParamPage               "Solver"
  SampleTimeColors           off
  InvariantConstants off
  WideVectorLines    off
  ShowLineWidths     off
  ShowPortDataTypes          off
  StartTime                  "0"
  StopTime                   "6"
  SolverMode                 "Auto"
  Solver             "ode45"
  RelTol             "1e-3"
  AbsTol             "auto"
  Refine             "1"
```

```
MaxStep                 "auto"
InitialStep             "auto"
FixedStep               "auto"
MaxOrder                5
OutputOption            "RefineOutputTimes"
OutputTimes             "[]"
LoadExternalInput   off
ExternalInput           "[t, u]"
SaveTime                on
TimeSaveName            "tout"
SaveState               off
StateSaveName           "xout"
SaveOutput              on
OutputSaveName  "yout"
LoadInitialState    off
InitialState            "xInitial"
SaveFinalState  off
FinalStateName  "xFinal"
SaveFormat              "Matrix"
LimitMaxRows            off
MaxRows                 "1000"
Decimation              "1"
AlgebraicLoopMsg  "warning"
MinStepSizeMsg  "warning"
UnconnectedInputMsg     "warning"
UnconnectedOutputMsg    "warning"
UnconnectedLineMsg      "warning"
InheritedTsInSrcMsg     "warning"
IntegerOverflowMsg      "warning"
UnnecessaryDatatypeConvMsg "none"
Int32ToFloatConvMsg     "warning"
SignalLabelMismatchMsg  "none"
ConsistencyChecking     "off"
ZeroCross               on
SimulationMode  "normal"
```

```
BlockDataTips                   on
BlockParametersDataTip  on
BlockAttributesDataTip  off
BlockPortWidthsDataTip  off
BlockDescriptionStringDataTip           off
BlockMaskParametersDataTip off
ToolBar                 on
StatusBar                       on
BrowserShowLibraryLinks off
BrowserLookUnderMasks   off
OptimizeBlockIOStorage  on
BufferReuse                     on
BooleanDataType  off
RTWSystemTargetFile             "grt.tlc"
RTWInlineParameters             off
RTWRetainRTWFile                off
RTWTemplateMakefile             "grt_default_tmf"
RTWMakeCommand                  "make_rtw"
RTWGenerateCodeOnly             off
ExtModeMexFile   "ext_comm"
ExtModeBatchMode                off
ExtModeTrigType  "manual"
ExtModeTrigMode  "oneshot"
ExtModeTrigPort  "1"
ExtModeTrigElement              "any"
ExtModeTrigDuration             1000
ExtModeTrigHoldOff              0
ExtModeTrigDelay  0
ExtModeTrigDirection            "rising"
ExtModeTrigLevel  0
ExtModeArchiveMode              "off"
ExtModeAutoIncOneShot   off
ExtModeIncDirWhenArm    off
ExtModeAddSuffixToVar   off
ExtModeWriteAllDataToWs off
```

```
ExtModeArmWhenConnect   off
Created         "Wed May 10 16:43:26 2000"
UpdateHistory           "UpdateHistoryNever"
ModifiedByFormat  "%<Auto>"
LastModifiedBy    "lyip"
ModifiedDateFormat      "%<Auto>"
LastModifiedDate  "Tue Jun 26 18:44:22 2001"
ModelVersionFormat      "1.%<AutoIncrement:26>"
ConfigurationManager    "none"
BlockDefaults {
 Orientation            "right"
 ForegroundColor  "black"
 BackgroundColor  "white"
 DropShadow             off
 NamePlacement    "normal"
 FontName               "Helvetica"
 FontSize               10
 FontWeight             "normal"
 FontAngle              "normal"
 ShowName               on
}
AnnotationDefaults {
 HorizontalAlignment    "center"
 VerticalAlignment  "middle"
 ForegroundColor  "black"
 BackgroundColor  "white"
 DropShadow             off
 FontName               "Helvetica"
 FontSize               10
 FontWeight             "normal"
 FontAngle              "normal"
}
LineDefaults {
 FontName               "Helvetica"
 FontSize               9
```

```
  FontWeight              "normal"
  FontAngle               "normal"
}
System {
  Name                    "lms"
  Location                [415, 228, 1102, 696]
  Open                    on
  ModelBrowserVisibility  off
  ModelBrowserWidth       200
  ScreenColor             "automatic"
  PaperOrientation        "landscape"
  PaperPositionMode       "auto"
  PaperType               "usletter"
  PaperUnits              "inches"
  ZoomFactor              "100"
  AutoZoom                on
  ReportName              "simulink-default.rpt"
  Block {
    BlockType               Reference
    Name                    "FIR Fitler"
    Ports                   [1, 1, 0, 0, 0]
    Position                [140, 252, 210, 308]
    SourceBlock             "dspddes2/Digital IIR\nFilter Design"
    SourceType              "Digital IIR Filter Design"
    method                  "Butterworth"
    filttype                "Bandpass"
    N                       "4"
    Wlo                     "0.001"
    Whi                     "0.03"
    Rp                      "2"
    Rs                      "20"
    frame                   off
    numCHANS                "1"
  }
  Block {
```

```
  BlockType                 FromWorkspace
  Name                      "From\nWorkspace"
  Position                  [35, 72, 145, 98]
  VariableName              "volacoustic"
  SampleTime                "3.3334e-4"
  Interpolate               off
  HoldFinalValue            off
}
Block {
  BlockType                 FromWorkspace
  Name                      "From\nWorkspace1"
  Position                  [30, 193, 95, 217]
  VariableName              "volLECG"
  SampleTime                "3.3334e-4"
  Interpolate               off
  HoldFinalValue            off
}
Block {
  BlockType                 FromWorkspace
  Name                      "From\nWorkspace2"
  Position                  [150, 112, 260, 138]
  VariableName              "simu_heart"
  SampleTime                "3.3334e-4"
  Interpolate               off
  HoldFinalValue            off
}
Block {
  BlockType                 FromWorkspace
  Name                      "From\nWorkspace3"
  Position                  [40, 137, 150, 163]
  VariableName              "simu_lung"
  SampleTime                "3.3334e-4"
  Interpolate               off
  HoldFinalValue            off
}
```

```
Block {
  BlockType              Reference
  Name                   "LMS\nAdaptive Filter"
  Ports                  [2, 2, 0, 0, 0]
  Position               [295, 256, 380, 314]
  SourceBlock            "dspadpt2/LMS\nAdaptive Filter"
  SourceType             "LMS Adaptive Filter"
  n                      "1000"
  mu        "0.0021"
  ic        "0.0"
  normalized             off
  Adapt                  off
}
Block {
  BlockType              Scope
  Name                   "Scope"
  Ports                  [6, 0, 0, 0, 0]
  Position               [600, 84, 675, 171]
  Floating               off
  Location               [470, 198, 823, 676]
  Open                   off
  NumInputPorts          "6"
  TickLabels             "OneTimeTick"
  ZoomMode               "xonly"
  List {
    ListType             AxesTitles
    axes1                "Raw Acoustic Sound"
    axes2                "Filtered LECG Signal"
    axes3                "Estimated Heart Sound"
    axes4                "Estimated Breath Sound"
    axes5                "Simu_heart"
    axes6                "Simu_lung"
  }
  Grid                   "on"
  TimeRange              "6"
```

```
    YMin            "-1~-0.75~-1~-1~-1~-1"
    YMax            "1~1~1~1~1~1"
    SaveToWorkspace         off
    SaveName                "ScopeData"
    DataFormat      "StructureWithTime"
    LimitMaxRows    off
    MaxRows                 "15000"
    Decimation      "1"
    SampleInput     off
    SampleTime      "0"
  }
  Block {
    BlockType               Sum
    Name            "Sum"
    Ports           [2, 1, 0, 0, 0]
    Position                [420, 180, 440, 200]
    ShowName                off
    IconShape               "round"
    Inputs          "|+-"
    SaturateOnIntegerOverflow       on
  }
  Block {
    BlockType               ToWorkspace
    Name            "To Workspace"
    Position                [195, 20, 255, 50]
    VariableName    "simacoustic"
    Buffer          "17500"
    Decimation      "1"
    SampleTime      "-1"
    SaveFormat      "StructureWithTime"
  }
  Block {
    BlockType               ToWorkspace
    Name            "To Workspace1"
    Position                [175, 190, 235, 220]
```

```
    VariableName    "simLECG"
    Buffer          "17500"
    Decimation      "1"
    SampleTime      "-1"
    SaveFormat      "StructureWithTime"
  }
  Block {
    BlockType               ToWorkspace
    Name            "To Workspace2"
    Position                [335, 20, 395, 50]
    VariableName    "breathsound"
    Buffer          "17500"
    Decimation      "1"
    SampleTime      "-1"
    SaveFormat      "StructureWithTime"
  }
  Block {
    BlockType               ToWorkspace
    Name            "To Workspace3"
    Position                [485, 20, 545, 50]
    VariableName    "heartsound"
    Buffer          "17500"
    Decimation      "1"
    SampleTime      "-1"
    SaveFormat      "StructureWithTime"
  }
  Block {
    BlockType               ToWorkspace
    Name            "To Workspace4"
    Position                [590, 215, 650, 245]
    VariableName    "simu_heart"
    Buffer          "17500"
    Decimation      "1"
    SampleTime      "-1"
    SaveFormat      "StructureWithTime"
```

```
  }
  Block {
    BlockType                 ToWorkspace
    Name                      "To Workspace5"
    Position                  [550, 260, 610, 290]
    VariableName              "simu_lung"
    Buffer                    "17500"
    Decimation                "1"
    SampleTime                "-1"
    SaveFormat                "StructureWithTime"
  }
  Line {
    SrcBlock                  "From\nWorkspace"
    SrcPort                   1
    Points                    [30, 0]
    Branch {
      DstBlock                "To Workspace"
      DstPort                 1
    }
    Branch {
      Points                  [0, 10; 110, 0]
      Branch {
        Points                [295, 0]
        DstBlock              "Scope"
        DstPort               1
      }
      Branch {
        Points                [0, 95]
        DstBlock              "Sum"
        DstPort               1
      }
    }
  }
  Line {
    SrcBlock                  "Sum"
```

```
  SrcPort                  1
  Points           [15, 0]
  Branch {
    Points                 [30, 0; 0, 155; -235, 0; 0, -45]
    DstBlock         "LMS\nAdaptive Filter"
    DstPort                  2
  }
  Branch {
    Labels                 [1, 0]
    Points                 [0, -35]
    Branch {
      Points         [-150, 0; 0, -120]
      DstBlock       "To Workspace2"
      DstPort        1
    }
    Branch {
      Points         [125, 0]
      DstBlock       "Scope"
      DstPort        4
    }
  }
}
Line {
  SrcBlock               "LMS\nAdaptive Filter"
  SrcPort                1
  Points           [45, 0; 0, -20]
  Branch {
    DstBlock         "Sum"
    DstPort                  2
  }
  Branch {
    Points                 [20, 0; 0, -115]
    Branch {
      Points         [0, -100]
      DstBlock       "To Workspace3"
```

```
        DstPort         1
      }
      Branch {
        Points          [135, 0]
        DstBlock        "Scope"
        DstPort         3
      }
    }
  }
  Line {
    SrcBlock            "From\nWorkspace1"
    SrcPort             1
    Points              [5, 0; 0, 75]
    DstBlock            "FIR Fitler"
    DstPort             1
  }
  Line {
    SrcBlock            "FIR Fitler"
    SrcPort             1
    Points              [20, 0]
    Branch {
      Points                [35, 0; 0, -10]
      Branch {
        DstBlock        "LMS\nAdaptive Filter"
        DstPort         1
      }
      Branch {
        Points          [0, -165]
        DstBlock        "Scope"
        DstPort         2
      }
    }
    Branch {
      Points                [0, -40; -95, 0; 0, -35]
      DstBlock          "To Workspace1"
```

```
        DstPort                 1
      }
    }
    Line {
      SrcBlock                  "From\nWorkspace2"
      SrcPort                   1
      Points                    [95, 0; 0, 25; 205, 0]
      Branch {
        DstBlock                "Scope"
        DstPort                 5
      }
      Branch {
        Points                  [0, 80]
        DstBlock                "To Workspace4"
        DstPort                 1
      }
    }
    Line {
      SrcBlock                  "From\nWorkspace3"
      SrcPort                   1
      Points                    [0, 15; 370, 0]
      Branch {
        DstBlock                "Scope"
        DstPort                 6
      }
      Branch {
        Points                  [0, 110]
        DstBlock                "To Workspace5"
        DstPort                 1
      }
    }
  }
}
```

A.4 Source code of AWBA (MATLAB)

MATLAB Main Program

```
clear all
figure(1);
clf;

%File I/O
%inf column and 2 row
%the first column is acoustic
%the second column is LECG
lowerguard = 50;
upperguard = 250;

p = [];

how_seconds = 6;

how_seconds = how_seconds*3000;

%fid = fopen('Righlowy1.dat','r');
%fid = fopen('Righlown1.dat','r');
%fid = fopen('Righmidn1.dat','r');
%fid = fopen('Righmidy1.dat','r');
%fid = fopen('Rightopn1.dat','r');
%fid = fopen('Rightopy1.dat','r');
%fid = fopen('Lefttopy1.dat','r');
%fid = fopen('Lefttopn1.dat','r');
%fid = fopen('Leftmidn1.dat','r');
fid = fopen('Leftmidy1.dat','r');
%fid = fopen('Leftlowy1.dat','r');
%fid = fopen('Leftlown1.dat','r');
```

```
volraw = fscanf(fid,'%f',[2,inf]);
fclose(fid);
volraw = volraw';

%%normalization
%[max_num, max_index] = max (abs(volraw));
%volfirst(:,1) = volraw(:,1)/max_num(1);
%volfirst(:,2) = volraw(:,2)/max_num(2);
%%zero offset
%volfirst(:,1) = volfirst(:,1) - mean(volfirst(:,1));
%volfirst(:,2) = volfirst(:,2) - mean(volfirst(:,2));

%zero offset
volfirst(:,1) = volraw(:,1) - mean(volraw(:,1));
volfirst(:,2) = volraw(:,2) - mean(volraw(:,2));
%normalization
[max_num, max_index] = max (abs(volfirst));
volfirst(:,1) = volfirst(:,1)/max_num(1);
volfirst(:,2) = volfirst(:,2)/max_num(2);

%Acoustic signal
%volacoustic(:,1) = volfirst(:,3);
%volacoustic(:,2) = volfirst(:,1);
volacoustic(:,1) = volfirst(:,1);

%%
volacoustic= volacoustic(1:how_seconds,1);
%%

%LECG signal
%volLECG(:,1) = volfirst(:,3);
%volLECG(:,2) = volfirst(:,2);
volLECG(:,1) = volfirst(:,2);

%%
```

```
volLECG= volLECG(1:how_seconds,1);

%%

volLECG = volLECG(:,1)';


N = 2;

passband = [0.0133 0.99];

[Bb,Ab] = butter(N, passband, 'stop');

volLECG_bandpass = filter(Bb, Ab, volLECG);


%normalization

[max_num, max_index] = max (abs(volLECG_bandpass));

volLECG_bandpass = volLECG_bandpass/max_num;


LECGpeak = find(volLECG_bandpass>0.6);

%%for i=1:length(LECGpeak)

lengthofLECG = length(LECGpeak);


for i=1:lengthofLECG-1,

        if LECGpeak(i+1) - LECGpeak(i) ~= 1

    ONEpeak(i) = LECGpeak(i+1);

  end

end

a = find(ONEpeak~=0);

ONEpeak = [LECGpeak(1) ONEpeak(a)];


%%

REFvolacoustic = zeros(size(volacoustic));

for i=1:length(ONEpeak),

REFvolacoustic(ONEpeak(i)-lowerguard:ONEpeak(i)+upperguard) = volacoustic(ONEpeak(i)-
lowerguard:ONEpeak(i)+upperguard);

end


Fs = 3000;

S = fft(volLECG_bandpass, 3000);

w = (0:299)/3000*3000;

Sf = fft(volLECG, 3000);
```

```
AS = fft(volacoustic, 3000);

figure(1);
subplot(6,1,1);
plot (volLECG_bandpass);
axis ([0 how_seconds -1 1]);
subplot(6,1,2);
plot (volLECG);
axis ([0 how_seconds -1 1]);
subplot(6,1,3);
plot (w, abs(S(1:300)'));
subplot(6,1,4);
plot (w, abs(Sf(1:300)'));
subplot(6,1,5);
plot (volacoustic);
axis ([0 how_seconds -1 1]);
%subplot(6,1,6);
%plot (w, abs(AS(1:300)'));
subplot(6,1,6);
plot (REFvolacoustic);
axis ([0 how_seconds -1 1]);

%adding index

for i = 1:length(volacoustic)
        volref(i) = i/3000;
end

%Raw Acoustic signal

volref = volref';

A_volacoustic = zeros([18000,2]);

A_volacoustic(:,1) = volref(:,1);
```

```
A_volacoustic(:,2) = volacoustic(:,1);

%Adjusted Acoustic signal
A_adjvolacoustic = zeros([18000,2]);

A_adjvolacoustic(:,1) = volref(:,1);
A_adjvolacoustic(:,2) = REFvolacoustic(:,1);

%bandpass LECG
A_LECG_bandpass = zeros([18000,2]);

volLECG_bandpass = volLECG_bandpass';
A_LECG_bandpass(:,1) = volref(:,1);
A_LECG_bandpass(:,2) = volLECG_bandpass(:,1);

%Raw LECG
A_LECG = zeros([18000,2]);

volLECG = volLECG';
A_LECG(:,1) = volref(:,1);
A_LECG(:,2) = volLECG(:,1);

%%%%
%%p(1) = volLECG_bandpass(

%%for i = 1:inputlayer_no;

%%end
```

SIMULINK LMS Filtering – same as in DRA

A.5 Source code of online AGC (LABVIEW)

LAVIEW Main Program

<VI syntaxVersion=3 LVversion=5118001 revision=145 name="test_acquire_main_8.vi">

<TITLE><NO_TITLE name="test_acquire_main_8.vi"></TITLE>

<HELP_PATH></HELP_PATH>

<HELP_TAG></HELP_TAG>

<RTM_PATH type="default"></RTM_PATH>

<DESC>Acquire & Process N Scans acquires data from one or more analog input channels. This is a timed acquisition, meaning that a hardware clock is used to control the acquisition rate for fast and accurate timing. It is also a buffered acquisition, meaning that the data is stored in an intermediate memory buffer after it is acquired from the analog input channels. This VI retrieves the data from the memory buffer while the acquisition is in progress, allowing the data to be processed and displayed as it is being acquired. <CR>

<CR>

You will probably want to add more functions to the diagram to customize this VI for your application. A common reason to read data while the acquisition is in progress is to process and display the data in pseudo-real time. The acquisition rate you can achieve depends on how much processing and display the VI must do. Acquire & Process N Scans calls a subVI named My Data Processing. Add whatever processing you need to this subVI, or replace it with one of your own. The data processing subVI also demonstrates how to use error clusters in your own subVIs, so they can be included in the error data flow chain. The data you will be processing comes from AI Continuous Scan as a two-dimensional array; the first dimension is the scan number, the second is the channel.<CR>

<CR>

Before running this VI, set the values of the controls on the front panel. Select Show Help Window from the Help menu to see a description of each control. If the values you select for all the controls are values you will usually use, select Make Current Values Default from the Operate menu and save the VI. Or, you may save individual control's default values by popping up on the control, selecting Data Operations, then selecting Make Current Value Default, and saving the VI.<CRLF>

<LF>

The buffer size is the number of scans that will be held in the internal memory buffer, and is limited by the amount of memory available. If you are acquiring a small, finite amount of data and can keep it all in memory, set buffer size to the number of scans to acquire. More often, you want to acquire more data than you can hold in memory, and you set the buffer size to hold a subset of the data, at least several seconds worth. Experiment with the buffer size and the number of scans to read each time. If the buffer is too small or you are not reading data from it fast enough, your data will be overwritten by new data before you have a chance to read it (overwrite error). If the buffer is too big, you will run out of memory (out of memory error).<LF>

<LF>

When you run this VI, it displays the data from all the channels on the graph as they are retrieved from the buffer, while the acquisition is still going on. Press the Stop button to stop the acquisition at any time, or, if you have specified a finite number of scans, the VI will stop after the acquisition is complete.<LF>

</DESC>

<CONTENT>

<CONTROL ID=79 type="Boolean" name="continuous:T<CR>

finite:F">

<DESC>Set this switch TRUE (up) for continuous acquisition. Set it FALSE (down) to acquire a finite number of scans. In this case, you must also specify the number to acquire.</DESC>

<PARTS>

<PART ID=82 order=0 type="Caption"><LABEL><STEXT>continuous:T<CR>

finite:F</STEXT></LABEL></PART>

</PARTS>

</CONTROL>

<CONTROL ID=82 type="Array" name="channels">

<DESC>([abc]) channels: identifies the analog input channels on which you want to acquire data. The default input is onboard channel 0.</DESC>

<PARTS>

<PART ID=82 order=0 type="Caption"><LABEL><STEXT>channels</STEXT></LABEL></PART>

</PARTS>

<DEFAULT>

<ARRAY nElems=1>

<STRING>0,1</STRING>

</ARRAY>

</DEFAULT>

<CONTENT>

<CONTROL ID=81 type="String" name="channels">

<DESC>(abc) channels: identifies the analog input channels on which you want to acquire data. The default input is onboard channel 0.</DESC>

<PARTS>

<PART ID=11 order=0 type="Text"><LABEL><STEXT>0,1</STEXT></LABEL></PART>

</PARTS>

<DEFAULT><SAME_AS_LABEL></DEFAULT>

</CONTROL>

</CONTENT>

</CONTROL>

<CONTROL ID=80 type="Numeric" name="device">

<DESC>(I16) device: the device number you assigned to the plug-in DAQ board during configuration. The default input is 1.</DESC>

<PARTS>

<PART ID=82 order=0 type="Caption"><LABEL><STEXT>device</STEXT></LABEL></PART>

</PARTS>

</CONTROL>

<LABEL><STEXT><FONT predef=APPFONT color=0000FF>Real Time Reduction of Heart Sounds from Lung Sounds Using A Newly Designed Stethoscope</STEXT></LABEL>

<CONTROL ID=80 type="Numeric" name="scan rate">

<DESC>(SGL) scan rate: the number of scans per second to acquire. This is equivalent to the sampling rate per channel. The default input is 1000 scans/sec.</DESC>

<PARTS>

<PART ID=82 order=0 type="Caption"><LABEL><STEXT>scan rate</STEXT></LABEL></PART>

</PARTS>

</CONTROL>

<CONTROL ID=79 type="Boolean" name="stop">

<DESC>(TF) STOP: stop acquiring and generating data and clear the board resources for these operations.</DESC>

<PARTS>

<PART ID=22 order=0 type="Boolean Text"><MLABEL><FONT predef=SYSFONT color=FF0000><STRINGS><STRING>Pause</STRING><STRING>STOP</STRING><STRING>Pause</STRING><STRING>STOP</STRING></STRINGS></MLABEL></PART>

</PARTS>

</CONTROL>

<CONTROL ID=80 type="Numeric" name="no. of scan">

<DESC>(I32) number of scans to read at a time: the number of scans the VI retrieves from the acquisition buffer each time the loop iterates. The default input is 500.</DESC>

<PARTS>

<PART ID=82 order=0 type="Caption"><LABEL><STEXT>no. of scan</STEXT></LABEL></PART>

</PARTS>

</CONTROL>

<CONTROL ID=80 type="Numeric" name="input buffer size">

<DESC>(I32) input buffer size: the number of scans you want the buffer to hold. The default setting is 1000 scans.</DESC>

<PARTS>

<PART ID=82 order=0 type="Caption"><LABEL><STEXT>input buffer size</STEXT></LABEL></PART>

</PARTS>

</CONTROL>

<CONTROL ID=94 type="Waveform Chart" name="Estimated Heart Sounds">

<DESC>(cluster) transposed waveform graph: This waveform graph displays the data acquired on the specified channels. The transpose option is enabled for this graph so that the data is plotted correctly. Colors have been defined for the first four channels on the graph's legend.<LF>

<LF>

In this VI, this graph's data type is a cluster of three elements: initial X, X increment, and a 2D array of data.</DESC>

<PARTS>

<PART ID=82 order=0 type="Caption"><LABEL><STEXT>Estimated Heart Sounds</STEXT></LABEL></PART>

</PARTS>

<PRIV>

<PLOTS><STRING>plot 0</STRING></PLOTS></PRIV>

</CONTROL>

<CONTROL ID=94 type="Waveform Chart" name="Raw Heart and Lung Sounds">

<DESC>(cluster) transposed waveform graph: This waveform graph displays the data acquired on the specified channels. The transpose option is enabled for this graph so that the data is plotted correctly. Colors have been defined for the first four channels on the graph's legend.<LF>

<LF>

In this VI, this graph's data type is a cluster of three elements: initial X, X increment, and a 2D array of data.</DESC>

<PARTS>

<PART ID=82 order=0 type="Caption"><LABEL><STEXT>Raw Heart and Lung Sounds</STEXT></LABEL></PART>

</PARTS>

<PRIV>

<PLOTS><STRING>plot 0</STRING></PLOTS></PRIV>

</CONTROL>

<CONTROL ID=94 type="Waveform Chart" name="Raw LECG">

<DESC>(cluster) transposed waveform graph: This waveform graph displays the data acquired on the specified channels. The transpose option is enabled for this graph so that the data is plotted correctly. Colors have been defined for the first four channels on the graph's legend.<LF>

<LF>

In this VI, this graph's data type is a cluster of three elements: initial X, X increment, and a 2D array of data.</DESC>

<PARTS>

<PART ID=82 order=0 type="Caption"><LABEL><STEXT>Raw LECG</STEXT></LABEL></PART>

</PARTS>

<PRIV>

<PLOTS><STRING>plot 0</STRING></PLOTS></PRIV>

</CONTROL>

<CONTROL ID=94 type="Waveform Chart" name="Estimated Lung Sounds">

<DESC>(cluster) transposed waveform graph: This waveform graph displays the data acquired on the specified channels. The transpose option is enabled for this graph so that the data is plotted correctly. Colors have been defined for the first four channels on the graph's legend.<LF>

<LF>

In this VI, this graph's data type is a cluster of three elements: initial X, X increment, and a 2D array of data.</DESC>

<PARTS>

<PART ID=82 order=0 type="Caption"><LABEL><STEXT>Estimated Lung Sounds</STEXT></LABEL></PART>

</PARTS>

```
<PRIV>
  <PLOTS><STRING>plot 0</STRING></PLOTS></PRIV>
</CONTROL>
<CONTROL ID=89 type="Dial" name="LECG Gain Factor">
<DESC></DESC>
<PARTS>
  <PART ID=82 order=0 type="Caption"><LABEL><STEXT>LECG Gain Factor</STEXT></LABEL></PART>
</PARTS>
</CONTROL>
<CONTROL ID=89 type="Dial" name="Acoustic Gain Factor">
<DESC></DESC>
<PARTS>
  <PART ID=82 order=0 type="Caption"><LABEL><STEXT>Acoustic Gain Factor</STEXT></LABEL></PART>
</PARTS>
</CONTROL>
<CONTROL ID=82 type="Array" name="LECG AGC">
<DESC></DESC>
<PARTS>
  <PART ID=82 order=0 type="Caption"><LABEL><STEXT>LECG AGC</STEXT></LABEL></PART>
</PARTS>
<DEFAULT>
  <ARRAY nElems=3>
    <NON_STRING>
    <NON_STRING>
    <NON_STRING>
  </ARRAY>
</DEFAULT>
<CONTENT>
  <CONTROL ID=80 type="Numeric" name=" ">
    <DESC></DESC>
    <PARTS>
    </PARTS>
  </CONTROL>
</CONTENT>
```

```
</CONTROL>

<CONTROL ID=80 type="Numeric" name="update rate">

<DESC>(SGL) update rate: the number of updates to generate per second. The default input is 1000 updates/s.</DESC>

<PARTS>

  <PART ID=82 order=0 type="Caption"><LABEL><STEXT>update rate</STEXT></LABEL></PART>

</PARTS>

</CONTROL>

<CONTROL ID=81 type="String" name="output channel">

<DESC>(abc) output channel: identifies the analog output channel on which you want to generate voltage updates. The default output is onboard channel 0. This example only supports a single output channel.</DESC>

<PARTS>

  <PART ID=11 order=0 type="Text"><LABEL><STEXT>0</STEXT></LABEL></PART>

  <PART ID=82 order=0 type="Caption"><LABEL><STEXT>output channel</STEXT></LABEL></PART>

</PARTS>

<DEFAULT><SAME_AS_LABEL></DEFAULT>

</CONTROL>

<CONTROL ID=80 type="Numeric" name="output buffer size">

<DESC>(I32) output buffer size: the number of updates you want the buffer to hold. The default input is 1000 updates. Remember, an update is defined as one data point for each channel in the channels array.</DESC>

<PARTS>

  <PART ID=82 order=0 type="Caption"><LABEL><STEXT>output buffer size</STEXT></LABEL></PART>

</PARTS>

</CONTROL>

<CONTROL ID=79 type="Boolean" name="Estimated Sound or Raw Sound">

<DESC></DESC>

<PARTS>

  <PART ID=82 order=0 type="Caption"><LABEL><STEXT>Estimated Sound or Raw Sound</STEXT></LABEL></PART>

</PARTS>

</CONTROL>

<CONTROL ID=79 type="Boolean" name="Estimated Lung or Estimated Heart">

<DESC></DESC>

<PARTS>

  <PART ID=82 order=0 type="Caption"><LABEL><STEXT>Estimated Lung or Estimated Heart</STEXT></LABEL></PART>
```

```
</PARTS>

</CONTROL>

<CONTROL ID=80 type="Numeric" name="max index (indices)">

<DESC></DESC>

<PARTS>

  <PART ID=82 order=0 type="Caption"><LABEL><STEXT>max index (indices)</STEXT></LABEL></PART>

</PARTS>

</CONTROL>

<CONTROL ID=94 type="Waveform Chart" name="Pre-process LECG">

<DESC>(cluster) transposed waveform graph: This waveform graph displays the data acquired on the specified channels. The transpose option is enabled for this graph so that the data is plotted correctly. Colors have been defined for the first four channels on the graph's legend.<LF>
<LF>
In this VI, this graph's data type is a cluster of three elements: initial X, X increment, and a 2D array of data.</DESC>

<PARTS>

  <PART ID=82 order=0 type="Caption"><LABEL><STEXT>Pre-process LECG</STEXT></LABEL></PART>

</PARTS>

<PRIV>

  <PLOTS><STRING>plot 0</STRING></PLOTS></PRIV>

</CONTROL>

</CONTENT>

</VI>
```

LABVIEW LMS Sub-program

```
<VI syntaxVersion=3 LVversion=5118001 revision=86 name="test_lms_1000.vi">

<TITLE><NO_TITLE name="test_lms_1000.vi"></TITLE>

<HELP_PATH></HELP_PATH>

<HELP_TAG></HELP_TAG>

<RTM_PATH type="default"></RTM_PATH>

<DESC></DESC>

<CONTENT>

<CONTROL ID=82 type="Array" name="E Breath Sound (E)">

<DESC></DESC>

<PARTS>
```

```
<PART ID=82 order=0 type="Caption"><LABEL><STEXT>E Breath Sound (E)</STEXT></LABEL></PART>
</PARTS>
<DEFAULT>
<ARRAY nElems=1000>
<NON_STRING>
.
.---1000 elements
.
<NON_STRING>
</ARRAY>
</DEFAULT>
<CONTENT>
<CONTROL ID=80 type="Numeric" name=" ">
<DESC></DESC>
<PARTS>
</PARTS>
</CONTROL>
</CONTENT>
</CONTROL>
<CONTROL ID=82 type="Array" name="Raw LECG (X)">
<DESC></DESC>
<PARTS>
<PART ID=82 order=0 type="Caption"><LABEL><STEXT>Raw LECG (X)</STEXT></LABEL></PART>
</PARTS>
<DEFAULT>
<ARRAY nElems=1000>
<NON_STRING>
.
.---1000 elements
.
<NON_STRING>
</ARRAY>
</DEFAULT>
<CONTENT>
<CONTROL ID=80 type="Numeric" name=" ">
```

```
                <DESC></DESC>
                <PARTS>
                </PARTS>
    </CONTROL>
  </CONTENT>
  </CONTROL>
  <CONTROL ID=82 type="Array" name="Raw ACO (D)">
  <DESC></DESC>
  <PARTS>
    <PART ID=82 order=0 type="Caption"><LABEL><STEXT>Raw ACO (D)</STEXT></LABEL></PART>
  </PARTS>
  <DEFAULT>
    <ARRAY nElems=1000>
                <NON_STRING>
                .
                .---1000 element
                .
                <NON_STRING>
    </ARRAY>
  </DEFAULT>
  <CONTENT>
    <CONTROL ID=80 type="Numeric" name=" ">
                <DESC></DESC>
                <PARTS>
                </PARTS>
    </CONTROL>
  </CONTENT>
  </CONTROL>
  <CONTROL ID=80 type="Numeric" name="sum">
  <DESC></DESC>
  <PARTS>
    <PART ID=82 order=0 type="Caption"><LABEL><STEXT>sum</STEXT></LABEL></PART>
  </PARTS>
  </CONTROL>
  <CONTROL ID=82 type="Array" name="Weighting (W)">
```

```
<DESC></DESC>
<PARTS>
  <PART ID=82 order=0 type="Caption"><LABEL><STEXT>Weighting (W)</STEXT></LABEL></PART>
</PARTS>
<DEFAULT>
  <ARRAY nElems=1000>
        <NON_STRING>
        .
        .---1000 elements
        .
        <NON_STRING>
  </ARRAY>
</DEFAULT>
<CONTENT>
  <CONTROL ID=80 type="Numeric" name=" ">
        <DESC></DESC>
        <PARTS>
        </PARTS>
  </CONTROL>
</CONTENT>
</CONTROL>
<CONTROL ID=80 type="Numeric" name="Raw ACO element (d)">
<DESC></DESC>
<PARTS>
  <PART ID=82 order=0 type="Caption"><LABEL><STEXT>Raw ACO element
(d)</STEXT></LABEL></PART>
</PARTS>
</CONTROL>
<CONTROL ID=80 type="Numeric" name="E Breath Sound element (e)">
<DESC></DESC>
<PARTS>
  <PART ID=82 order=0 type="Caption"><LABEL><STEXT>E Breath Sound element
(e)</STEXT></LABEL></PART>
</PARTS>
</CONTROL>
<CONTROL ID=82 type="Array" name="Raw LECG (X) Hyper">
```

<DESC></DESC>

<PARTS>

<PART ID=82 order=0 type="Caption"><LABEL><STEXT>Raw LECG (X) Hyper</STEXT></LABEL></PART>

</PARTS>

<DEFAULT>

<ARRAY nElems=2000>

<NON_STRING>

.

.---2000 elements

.

<NON_STRING>

</ARRAY>

</DEFAULT>

<CONTENT>

<CONTROL ID=80 type="Numeric" name=" ">

<DESC></DESC>

<PARTS>

</PARTS>

</CONTROL>

</CONTENT>

</CONTROL>

<CONTROL ID=82 type="Array" name="Raw LECG (X) Alpha">

<DESC>X Vector. If the number of elements in X Vector is different from the number of elements in Y Vector, the VI computes the dot product based on the sequence that contains the fewest elements. If X Vector is an empty array, the dot product is NaN.<LF>

</DESC>

<PARTS>

<PART ID=82 order=0 type="Caption"><LABEL><STEXT>Raw LECG (X) Alpha</STEXT></LABEL></PART>

</PARTS>

<DEFAULT>

<ARRAY nElems=1000>

<NON_STRING>

.

.---1000 elements

.

```
            <NON_STRING>
    </ARRAY>
  </DEFAULT>
  <CONTENT>
    <CONTROL ID=80 type="Numeric" name=" ">
            <DESC></DESC>
            <PARTS>
            </PARTS>
    </CONTROL>
  </CONTENT>
  </CONTROL>
  <CONTROL ID=80 type="Numeric" name="Iteration">
  <DESC></DESC>
  <PARTS>
    <PART ID=82 order=0 type="Caption"><LABEL><STEXT>Iteration</STEXT></LABEL></PART>
  </PARTS>
  </CONTROL>
  <CONTROL ID=82 type="Array" name="E Heart Sound (H)">
  <DESC></DESC>
  <PARTS>
    <PART ID=82 order=0 type="Caption"><LABEL><STEXT>E Heart Sound
(H)</STEXT></LABEL></PART>
  </PARTS>
  <DEFAULT>
    <ARRAY nElems=1000>
            <NON_STRING>
            .
            .---1000 elements
            .
            <NON_STRING>
    </ARRAY>
  </DEFAULT>
  <CONTENT>
    <CONTROL ID=80 type="Numeric" name=" ">
            <DESC></DESC>
            <PARTS>
```

```
                </PARTS>
            </CONTROL>
        </CONTENT>
        </CONTROL>
</CONTENT>
</VI>
```